NATIONAL ADVISORY COMMITTEE FOR AERONAUTICS

TECHNICAL NOTE

No. 1472

THE CALCULATION OF THE HEAT REQUIRED FOR WING THERMAL ICE PREVENTION IN SPECIFIED ICING CONDITIONS

By Carr B. Neel, Jr., Norman R. Bergrun, David Jukoff, and Bernard A. Schlaff

Ames Aeronautical Laboratory
Moffett Field, Calif.

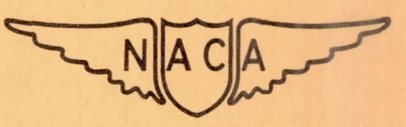

Washington
December 1947

NATIONAL ADVISORY COMMITTEE FOR AERONAUTICS

TECHNICAL NOTE NO. 1472

THE CALCULATION OF THE HEAT REQUIRED FOR WING THERMAL ICE PREVENTION IN SPECIFIED ICING CONDITIONS

By Carr B. Neel, Jr., Norman R. Bergrun, David Jukoff, and Bernard A. Schlaff

SUMMARY

As a result of a fundamental investigation of the meteorological conditions conducive to the formation of ice on aircraft and a study of the process of airfoil thermal ice prevention, previously derived equations for calculating the rate of heat transfer from airfoils in icing conditions were verified. Knowledge of the manner in which water is deposited on and evaporated from the surface of a heated airfoil was expanded sufficiently to allow reasonably accurate calculations of airfoil heat requirements. The research consisted of flight tests in natural-icing conditions with two 8-foot-chord heated airfoils of different sections. Measurements of the meteorological variables conducive to ice formation were made simultaneously with the procurement of airfoil thermal data.

It was concluded that the extent of knowledge on the meteorology of icing, the impingement of water drops on airfoil surfaces, and the processes of heat transfer and evaporation from a wetted airfoil surface has been increased to a point where the design of heated wings on a fundamental, wet-air basis now can be undertaken with reasonable certainty.

INTRODUCTION

For a period of several years, the National Advisory Committee for Aeronautics has conducted research on the prevention of ice formation on aircraft through the use of heat. During this time, research of a fundamental nature on the problem of thermal ice prevention was retarded by the more urgent need for development of ice-prevention systems for specific airplanes in military service. Satisfactory wing- and tail-surface thermal ice-prevention systems for a Lockheed 12-A, Consolidated B-24, Boeing B-17, and

Curtiss-Wright C-46 airplanes (references 1, 2, 3, and 4, respectively) were designed, fabricated, and tested in natural-icing conditions. Windshield thermal ice-prevention systems which proved adequate in the icing conditions encountered were provided for the 12-A, B-24, and C-46 airplanes. Each wing- and tail-surface design was based on establishing, for flight in clear-air conditions, a surface-temperature rise above free-stream temperature which experience in simulated- and natural-icing conditions had shown to be adequate for ice prevention. This empirical method, while proving satisfactory for the airplanes tested, was limited, since it was not established on a fundamental basis, and a more basic procedure founded on designing for the conditions existing in icing clouds was needed.

The NACA at present is engaged in an investigation to provide a fundamental understanding of the process of thermal ice prevention in order (1) to establish a basis for the extrapolation of present limited data on heat requirements to meteorological and flight conditions for which test data are not available, (2) to provide data for improving the efficiency of thermal ice-prevention equipment, and (3) to provide a wet-air, or meteorological, basis for the preparation of design specifications for thermal ice-prevention equipment. The research consists of an investigation of the meteorological factors conducive to icing, and a study of the heat-transfer processes which govern the operation of thermal ice-prevention equipment for airfoils and for windshield configurations.

The airfoil heat-transfer phase of this investigation consisted of the measurement of the factors affecting the transfer of heat from airfoil surfaces during flight in natural-icing conditions. These data are correlated with the simultaneous measurements of the meteorological parameters which influence the heat-transfer process, and are analyzed for the purpose of establishing a wet-air ice-prevention design basis for airfoils.

The first approach to the icing heat-transfer problem on a fundamental basis was made in England by Hardy and Mann prior to 1942. In this study, a method for the calculation of heat transfer from a heated surface subjected to icing conditions was presented and substantiated by measurements in an icing tunnel. Later work by Hardy in which these heat-transfer equations were modified for general application is presented in references 5 and 6. Reference 5 contains information on the protection of all aircraft components against ice accretion. Reference 6, prepared during a period of active participation by Mr. Hardy in the NACA icing research program, presents an analysis of the dissipation of heat in conditions of icing from a section of the heated wing of the C-46 airplane (reference 4).

Other research in the present NACA investigation has been reported in references 7, 8, and 9. Reference 7 gives the first measurements in this program of the liquid-water concentration in clouds. References 8 and 9 deal with the meteorological aspects of icing conditions in stratus clouds and in precipitation areas of the warm-front type.

Research on the problem of heat transfer from airfoils in conditions of icing has also been conducted by other laboratories. In reference 10, the transfer of heat from surfaces subjected to icing conditions on Mount Washington has been studied. The General Electric Research Laboratory has conducted a number of investigations on this phase of icing. A summary of this work and a list of reports is presented in reference 11. A comprehensive report by the Army Air Forces on the development and application of heated wings is contained in reference 12.

In continuation of the present icing program, the C-46 airplane was equipped with special meteorological and electrically heated test apparatus, and flown in natural-icing conditions during the winters of 1945-46 and 1946-47. Flight tests were conducted mainly along airline routes over most of the United States. The meteorological data recorded during the icing conditions encountered in the two seasons are presented and discussed in references 13 and 14.

This report presents an analysis of the data obtained during the 1945-46 and 1946-47 winter seasons with two electrically heated airfoil sections. The data were analyzed using the heat-transfer equations developed by Hardy. (See references 5 and 6.) A consideration of the area and rate of water impingement on one of the airfoil sections based on an analytical study of water-drop trajectories (reference 15) is also presented. An attempt is made to further the knowledge of the process of airfoil thermal ice-prevention.

The appreciation of the NACA is extended to United Air Lines, Inc., the United States Weather Bureau, and to the Air Materiel Command of the Army Air Forces for aid and cooperation in the research. In particular, the services of Major James L. Murray of the Air Materiel Command, Army Air Forces, and Captain Carl M. Christenson and First Officer Lyle W. Reynolds of United Air Lines, who served as pilots of the research airplane, were a valuable aid to the conduct of the investigation.

SYMBOLS

The following nomenclature is used throughout this report:

a	radius of water drop, feet
c	airfoil chord length, feet
c_p	specific heat of air at constant pressure, Btu per pound, degree Fahrenheit
c_{p_w}	specific heat of water at constant pressure, equal to 1 Btu per pound, degree Fahrenheit
C	concentration factor, defined in equation (6), dimensionless
e	saturation vapor pressure with respect to water, millimeters of mercury
E	water-drop collection efficiency, defined in equation (10)
g	acceleration of gravity, equal to 32.2 feet per second, second
h	convective surface heat-transfer coefficient, Btu per hour, square foot, degree Fahrenheit
H	total surface heat-transfer coefficient, Btu per hour, square foot, degree Fahrenheit
J	mechanical equivalent of heat, equal to 778 foot-pounds per Btu
k	thermal conductivity, Btu per second, square foot, degree Fahrenheit per foot
K	dimensionless drop-inertia quantity, defined in equation (5)
L_s	latent heat of vaporization of water at surface temperature, Btu per pound
m	liquid-water concentration of icing cloud, pounds of water per cubic foot of air
M_a	weight rate of water-drop impingement per unit of surface area, pounds per hour, square foot
M_b	weight rate of water flow aft of area of water-drop impingement per foot of span for one side of airfoil, pounds per hour, foot

M_s	weight rate of water-drop impingement per foot of span for one side of airfoil, pounds per hour, foot
n	concentration of liquid water contained in drops of each size in a drop-size distribution, pounds of water per cubic foot of air
P	barometric pressure, millimeters of mercury
Pr	Prandtl number $(c_p\mu/k)$, dimensionless
q	unit rate of heat flow, Btu per hour, square foot
R_c	Reynolds number for airfoil $(Vc\gamma/\mu)$, dimensionless
R_U	free-stream Reynolds number of water drop relative to speed of airfoil $(2Va\gamma/\mu)$, dimensionless
s	distance measured chordwise along airfoil surface from stagnation point, feet
t	temperature, degrees Fahrenheit
U	local velocity just outside boundary layer, feet per second
V	free-stream velocity, feet per second
W_a	weight rate of evaporation of water per unit of surface area, pounds per hour, square foot
W_s	weight rate of evaporation of water per foot of span for one side of airfoil, pounds per hour, foot
x	distance measured chordwise along airfoil chord line from zero-percent chord point, feet
X	evaporation factor, defined in equation (22), dimensionless
y	airfoil ordinate, feet
y_o	starting distance of water drop above projected chord line of airfoil, feet
Z_p	pressure altitude, feet
α_s/α_d	ratio of saturated to dry adiabatic lapse rates
β	exponent of Prandtl number, 1/2 for laminar flow, 1/3 for turbulent flow

γ specific weight of air, pounds per cubic foot

γ_w specific weight of water, equal to 62.4 pounds per cubic foot

μ viscosity of air, pounds per second, foot

Subscripts

1 refers to conditions at edge of boundary layer

k kinetic

o refers to free-stream conditions

me mean effective

s refers to conditions at airfoil surface

SL sea level

ANALYSIS

During flight in icing conditions a heated wing is cooled by convective heat transfer, by evaporation of the water on the surface, and, in the region of droplet interception, by the water striking the wing.[1] The rate at which heat must be supplied in order to maintain the wing surface at a specified temperature is, therefore, a function of the rates of convection, evaporation, and water impingement. Equations for expressing this heat requirement are presented in references 5 and 6. These equations, with slight modification, are used throughout this report.

Expressed as an equation, the unit heat loss q from a partially or completely wetted surface exposed to icing conditions may be stated:

$$q = q_w + q_c + q_e \tag{1}$$

where

q_w heat loss due to warming the intercepted water

q_c heat loss due to forced convection

q_e heat loss due to evaporation of the impinging water

Each of these individual heat flows will be analyzed.

---

[1]The heat loss due to radiation is small and can be neglected.

Heat Loss Due to Warming the Intercepted Water

In the region where water droplets strike the wing, the heat required per unit area to heat the water to surface temperature is

$$q_w = M_a \left[t_s - \left(t_o + \Delta t_{k_w} \right) \right] \tag{2}$$

The term Δt_{k_w} is the kinetic temperature rise of the water caused by stoppage of the droplets as they strike the wing. The value of Δt_{k_w} is given by

$$\Delta t_{k_w} = \frac{V^2}{2gJc_{p_w}} \tag{3}$$

where V is the free-stream velocity in feet per second. The value of Δt_{k_w} is less than 2° Fahrenheit for airplane speeds up to 200 miles an hour and, for the calculations presented in this report, the term has been neglected. Equation (2) thus becomes:

$$q_w = M_a (t_s - t_o) \tag{4}$$

The weight rate of water impingement on the wing, the area of impingement, and the distribution of the water over that area are important factors in the heat-transfer analysis. In addition to the effect of the amount of water intercepted on the value of q_w in equation (4), the evaluation of M_a provides an indication of the quantity of water which must be maintained in a liquid state until it either evaporates or runs off the trailing edge if the formation of ice aft of the area of impingement, normally termed "runback," is to be avoided. The area of impingement influences the extent of heated region to be provided at the leading edge, while knowledge of the distribution of water impingement is required in the calculation of the heating requirement in areas where water is striking.

Calculations have been made by Glauert (reference 16) for the trajectories of water drops about cylinders and an airfoil. In this work the assumption was made that the drops obeyed Stokes' law of resistance. At the speeds of flight, however, Stokes' law no longer strictly holds, and Langmuir and Blodgett (reference 17) computed a series of drop trajectories about cylinders, spheres, and ribbons, taking into consideration deviations from Stokes' law. These computations were undertaken on the assumption that the trajectories for

cylinders would apply to airfoils if the airfoil were replaced by an "equivalent" cylinder (reference 12).

Preliminary calculations based on references 16 and 17 indicated that, for large values of drop size and airspeed, the assumption of the equivalent cylinder would not hold for airfoils. Therefore, more extensive calculations were undertaken to determine the drop trajectories for one of the test airfoils of this research, an NACA 0012 airfoil at 0° angle of attack. In these calculations, presented in detail in reference 15, a Joukowski airfoil (the contour of which closely approximates that of the NACA 0012) was used to supply the stream lines since the Joukowski stream lines and velocity field can be computed with relative ease. The basic equations presented in reference 16 were used with modifications for deviation from Stokes' law as given in reference 17. The procedure followed was to start a given distance forward of the airfoil and calculate the paths of the drops using a step-by-step integration process. Results of these computations are presented in figure 1. The curves shown establish the distance s, measured from the stagnation point, at which a given drop will strike the airfoil when starting a distance y_o above the projected chord line. Curves are presented for various values of K, where

$$K = \frac{2}{9}\frac{\gamma_w}{\gamma}\left(\frac{a}{c}\right)^2\left(\frac{Vc\gamma}{\mu}\right) \tag{5}$$

It should be noted that the curves of figure 1 apply strictly only for a drop Reynolds number R_U of 95.65, that is, only for particular combinations of drop size, airspeed, altitude, and air temperature. The value of 95.65 was chosen as being the Reynolds number corresponding to average conditions of drop size, airspeed, altitude, and air temperature experienced during the tests of this investigation. However, the curves of figure 1 can be used for a range of Reynolds numbers on either side of 95.65 without serious error. Due to practical considerations, these curves were used in the analysis of the data presented in this report, even though the Reynolds number differed somewhat for every case.

Area of water impingement.- The end points of the curves shown in figure 1 denote the extreme location at which drops of a particular K value will strike the airfoil. Beyond this value of s/c no drops of this K value will hit. Thus, the broken line in figure 1 establishes the area of impingement for all values of K.

Rate of water impingement.- The rate of water impingement at a specified point on an airfoil is a function of the area of impingement, the velocity of flight, the liquid-water concentration of the air

stream, and the distribution of the intercepted water over the surface. This latter factor, called the concentration factor C is represented by the ratio of y_o to s, or:

$$C = \frac{y_o}{s}$$

For point values,

$$C = \frac{\Delta y_o}{\Delta s}$$

or more exactly,

$$C = \frac{dy_o}{ds} \tag{6}$$

The weight rate of water impingement per unit of surface area in pounds per hour, square foot, then, is

$$M_a = 3600\ V\ m\ C \tag{7}$$

It is apparent from equation (6) that C is simply the slope of the curves shown in figure 1. A plot of the measured slopes of these curves as a function of s/c is presented in figure 2. Using values of C obtained from figure 2, the weight rate of water impingement at any point on the surface can be calculated from equation (7).

In the case of a cloud, where the water drops are not of uniform size, but instead follow a pattern of size distribution, the rate of impingement can be computed if the distribution is known or assumed. The rate of water impingement at any point is the sum of all the rates of impingement of the volume of water contained in each drop size. Equation (7) then becomes

$$M_a = 3600\ V \sum nC \tag{8}$$

where n is the concentration of liquid water contained in drops of a particular size and C is the concentration factor for the K value corresponding to that drop size.

In order to establish the possibility of runback forming aft of the heated area of a wing, it is necessary to know the total quantity of water intercepted per unit of wing span. This rate of impingement, denoted as M_s in pounds per hour, foot span, is given by

$$M_s = \int_0^s M_a \, ds \tag{9}$$

A more rapid method for the evaluation of M_s utilizes a curve of collection efficiency E as a function of K (fig. 3). Collection efficiency is defined as

$$E = \frac{y_{o_{limit}}}{y_{max}} \tag{10}$$

where $y_{o_{limit}}$ is the value of y_o for which drops of a particular K value just miss the airfoil, and y_{max} is the maximum ordinate of the airfoil. The equation for computing M_s, then, is

$$M_s = 3600 \, EVm \, y_{max} \tag{11}$$

Using figure 3, the rate of water impingement can be computed for each of the drop sizes in the assumed or measured drop-size distribution. The total rate of impingement is the summation of these individual rates.

Heat Loss Due to Forced Convection

The unit heat flow from the surface of a body in an air stream resulting from convective heat transfer can be expressed:

$$q_c = h \, (t_s - t_{o_k}) \tag{12}$$

where t_s is the surface temperature and t_{o_k} is the kinetic temperature of the free-stream air at the point for which the heat flow is being computed. The factor h is the convective heat-transfer coefficient and may be evaluated by measurements in clear air or by calculation using the methods presented in references 18 and 19. Evaluation of the term t_{o_k} will now be discussed.

The surface of an unheated wing moving through the air will assume a temperature somewhat higher than that of the free air stream because of stoppage of the air particles in the boundary layer next to the surface. This temperature rise is of importance in the calculation of heat requirements for ice prevention in that it establishes

the datum point from which the temperature of the surface must be raised to obtain the desired temperature, t_s. The value of the temperature rise in clear air, from equations derived in reference 5, is, for laminar flow,

$$\Delta t_k = \frac{V^2}{2gJc_p}\left[1 - \frac{U^2}{V^2}\left(1 - Pr^{\frac{1}{2}}\right)\right] \tag{13}$$

and for turbulent flow,

$$\Delta t_k = \frac{V^2}{2gJc_p}\left[1 - \frac{U^2}{V^2}\left(1 - Pr^{\frac{1}{3}}\right)\right] \tag{14}$$

where U is the local velocity just outside the boundary layer at the point along the surface where the value of Δt_k is being calculated.

In clouds, the kinetic temperature rise is reduced, due to evaporation of water from the surface. Assuming the surface is completely wetted with water, the value of the temperature rise for laminar flow becomes

$$\Delta t_k = \frac{V^2}{2gJc_p}\left[1 - \frac{U^2}{V^2}\left(1 - Pr^{\frac{1}{2}}\right)\right] - 0.622\frac{L_s}{c_p}\left(\frac{e_{o_k} - e_1}{P_1}\right) \tag{15}$$

where

$$e_1 = e_o \frac{P_1}{P_o} \tag{16}$$

and e_{o_k} is the vapor pressure at saturation at the wet kinetic temperature, t_{o_k}. The value of t_{o_k} is

$$t_{o_k} = t_o + \Delta t_k$$

or

$$t_{o_k} = t_o + \frac{V^2}{2gJc_p}\left[1 - \frac{U^2}{V^2}\left(1 - Pr^{\frac{1}{2}}\right)\right] - 0.622\frac{L_s}{c_p}\left(\frac{e_{o_k} - e_1}{p_1}\right) \quad (17)$$

Equation (17) is for laminar flow. The equation for turbulent flow is the same, but with the exponent of Pr changed to 1/3. It can be seen that this equation must be solved by trial, since the value of e_{o_k} is dependent upon the temperature t_{o_k}.

Experiments in clouds, in the process of calibrating a free-air thermometer installation (reference 13), showed that by multiplying the clear-air kinetic-temperature rise by the ratio of the saturated to the dry adiabatic lapse rates, good agreement between the values of kinetic temperature rise calculated in this manner and the measured values was obtained. Since use of the ratio of the adiabatic lapse rates was substantiated experimentally, and since equation (17) must be solved by trial, a somewhat laborious procedure, the following equations were used in this report to calculate values of t_{o_k}:

For laminar flow,

$$t_{o_k} = t_o + \frac{V^2}{2gJc_p}\left[1 - \frac{U^2}{V^2}\left(1 - Pr^{\frac{1}{2}}\right)\right]\frac{\alpha_s}{\alpha_d} \quad (18)$$

and for turbulent flow,

$$t_{o_k} = t_o + \frac{V^2}{2gJc_p}\left[1 - \frac{U^2}{V^2}\left(1 - Pr^{\frac{1}{3}}\right)\right]\frac{\alpha_s}{\alpha_d} \quad (19)$$

Values of α_s/α_d, the ratio of the wet- to the dry-adiabatic lapse rates, are obtained from figure 4. The use of the lapse-rate ratio in equations (18) and (19) is semi-empirical. The limitations of this simplification in the calculation of kinetic-temperature rise of airfoil surfaces in clouds are not known. Below speeds of 200 miles per hour, however, these equations can be used with small error, since the kinetic-temperature rise is low.

Heat Loss Due to Evaporation of the Water on the Surface

The amount of heat removed from a wetted surface as a result of the evaporation of water on that surface can be expressed:

$$q_e = L_s W_a \quad (20)$$

From reference 6 the relation between q_e and the convective heat-transfer coefficient h can be expressed for a completely wetted surface as:

$$q_e = h\,(X - 1)\,(t_s - t_{ok}) \tag{21}$$

where

$$X = 1 + \frac{L_s}{c_p}\left(\frac{e_s - e_{ok}}{t_s - t_{ok}}\right)\frac{0.622}{P_1} \tag{22}$$

By substituting average values for L_s and c_p, equation (22) can be rewritten

$$X = 1 + 3.75\left(\frac{e_s - e_{ok}}{t_s - t_{ok}}\right)\frac{P_{SL}}{P_1} \tag{23}$$

The values chosen for L_s and c_p are 1100 Btu per pound and 0.24 Btu per pound, °Fahrenheit, respectively. The factor P_{SL}/P_1 is the ratio of the standard sea-level pressure to the local static pressure.

It should be noted that the evaporation factor X applies only when the surface is completely wetted. If only partial wetness prevails, the value of X must be modified according to the degree of wetness.

Total Heat Loss from a Wetted Surface

Summarizing the heat losses due to water impingement, convection, and evaporation, equation (1) can be written:

$$q = M_a\,(t_s - t_o) + h\,(t_s - t_{ok}) + h\,(X - 1)\,(t_s - t_{ok})$$

which reduces to

$$q = M_a\,(t_s - t_o) + h\,X\,(t_s - t_{ok}) \tag{24}$$

Aft of the region of water impingement, $M_a = 0$ and equation (24) becomes

$$q = h \times (t_s - t_{o_k}) \tag{25}$$

DESCRIPTION OF EQUIPMENT

All tests reported herein were made in the C-46 airplane shown in figure 5. The airplane had been modified to provide thermal ice-prevention equipment for wings, empennage, windshield, and propellers. A description of the thermal system for the wings and empennage is given in reference 20. The windshield system was altered for the flights as described in reference 21. Protection for the propellers was provided by electrically heated blade shoes.

The meteorological equipment used during the tests to measure the free-air temperature, liquid-water concentration, drop size and drop-size distribution is described in references 13 and 14.

Two electrically heated test airfoils were used to obtain fundamental data on the process of wing thermal ice prevention. Each airfoil was mounted vertically on top of the fuselage of the C-46 airplane, as shown in figure 5. The test airfoil installed during the winter of 1945-46 had an NACA 0012 section. For the tests in the winter of 1946-47 the airfoil had an NACA 65,2-016 section in order to provide test data for low-drag sections, as well as conventional sections. Both sections are symmetrical, and the models were installed with the chord line in the plane of symmetry of the airplane; that is, at zero angle of attack for unyawed flight. Ordinates for an NACA 0012 airfoil are given in reference 22, and for an NACA 65,2-016 airfoil, in reference 23. Figure 6(a) shows the NACA 0012 airfoil mounted on the fuselage. the NACA 65,2-016 airfoil was mounted as shown in figure 6(b). A clear plastic blister, shown in figures 6(a) and 6(b), allowed the airfoils to be viewed and photographed in flight.

Both airfoils had an 8-foot chord and a 4.7-foot span, with a faired square tip. A heated test section of 1-foot span was located 2 feet above the top of the fuselage. It had been determined previously, by means of a pressure survey, that the test-section location was well above the edge of the fuselage boundary layer. Electrically heated guard sections were built around the leading-edge region on both sides of the test section for the purpose of preventing any disturbance of the air flowing over the test section which might have been caused by ice accretions in the region of the guard sections.

NACA 65,2-016 Airfoil Model

Construction details of the 65,2-016 airfoil model are shown in figure 7. The metal portion of the structure consisted of aluminum ribs and skin supported from the fuselage by two spars. The test section was made up of a 3/8-inch-thick plastic base and a sheet of plastic-impregnated fabric, 1/64-inch-thick, on top of which 1/2-inch wide, 0.002-inch-thick, electrical resistance heating strips were cemented in a spanwise direction spaced 1/32 inch apart. A covering of the 1/64-inch-thick plastic-impregnated sheet was laid over the resistance strips, and on top of this was cemented a skin of 0.006-inch-thick aluminum. Each 1/2-inch-wide heating strip was connected to individual lugs located along the edges of the test section. This provided means for chordwise adjustment of the power distribution by 1/2-inch increments. The heated area of the test section extended back to 77 percent chord on the left side and to 17 percent chord on the right side.

The guard sections were constructed in the same manner as the test section, with the exception that the aluminum skin was 0.011 inch thick. The heated area of the guard sections extended to 17 percent chord on both sides of the model.

Measurements of the temperature of the aluminum surface of the test section were obtained by means of thermocouples. Fine iron-constantan thermocouple wire was rolled flat to produce a strip approximately 0.002 inch thick and 1/16 inch wide. These strip thermocouples were laid in spanwise grooves about 3 inches long cut in the aluminum skin. The thermocouple junctions were located in the middle of the grooves, and the leads passed through holes at the ends of the grooves into the interior of the model. Aluminum was sprayed into the groove over the strip thermocouple for a distance of about 3/16 inch on either side of the junction. Thus, the thermocouple junction was bonded to the aluminum skin, allowing accurate surface-temperature measurements to be made. The remainder of the groove on either side of the aluminum spray was filled with a nonelectrically conducting material. Thermocouples were located at the center of the test section at 1-inch chordwise intervals in the leading-edge and calculated transition regions, and at 1-1/2-inch chordwise intervals in other regions. Surface temperatures were recorded by means of self-balancing automatic-recording potentiometers.

The flow of heat through the outer surface was calculated from measurements of the power dissipated in the electrical heating strips. This power was determined by measuring the resistance of the strips and the current flowing through them. Thermocouples placed on both surfaces of the plastic base at a number of chordwise stations gave an indication of the heat flow into the model interior.

These thermocouples were connected to the same recording potentiometers used to record surface temperatures.

Pressure taps were installed flush in the test-section surface about 3 inches down from the top edge of the test section at various chordwise points for the purpose of measuring surface pressure distribution. A standard NACA 60-cell pressure recorder was used to record the pressures.

A source of 400-cycle, single-phase, alternating current was supplied to the test and guard sections for heating these surfaces. The heating strips for the test section were grouped into 30 chordwise blocks. Control of the current flowing through each block was provided, so that a large variation in the chordwise distribution of heat flow was possible during flight. Before the icing operations started the heating strips for the guard sections were connected to maintain a constant surface-temperature rise during flight in clear air. Controls were provided so that the total heat input to the guard sections, but not the chordwise distribution, could be varied during flight.

NACA 0012 Airfoil Model

With a few exceptions, the construction of the 0012 airfoil model was substantially the same as that of the 65,2-016 model. These exceptions will be noted.

The top layer of plastic-impregnated fabric covering the electrical resistance strips constituted the outer skin of the test and guard sections. This was painted and sanded, after the test-section thermocouples had been installed. The heated area of the test section extended back to 58 percent chord on the left side and to 11 percent chord on the right side. The heated area of the guard sections extended to 11 percent chord on both sides of the airfoil.

Strip thermocouples of the same type as installed in the 65,2-016 model were used to measure surface temperatures of the test section. Spanwise grooves were cut in the plastic-impregnated fabric sheet at various intervals along the chord. The strip thermocouples were laid in the grooves and cemented in place. The surface was then painted and sanded so that only a thin layer of paint covered the thermocouple junctions. Thermocouples were located at the center of the test section at 1-inch chordwise intervals in the leading-edge and calculated transition regions, and at 2- to 2-1/2-inch chordwise intervals in other regions. Surface temperatures were recorded by means of an automatic-recording potentiometer.

The flow of heat through the surface of the test section was calculated from measurements of the power dissipated in the electrical

heating strips, in a manner similar to that described for the 65,2-016 airfoil.

Installation of surface pressure taps for the measurement of pressure distribution was the same as for the 65,2-016 model. The pressures were recorded by photographing a multiple-tube manometer to which the pressure taps were connected.

A source of 400-cycle, single-phase, alternating current was supplied to the test and guard sections for heating these surfaces. In the test section, provisions were made for obtaining a limited number of chordwise heating distributions as well as for control of the total heat input with each distribution. A small degree of variation of each heat distribution was also provided. During flight it was possible to control only the total heat input, and to vary, to a small extent, each distribution. As with the 65,2-016 airfoil, the heating strips for the guard sections were connected to give an approximately constant surface-temperature rise in clear air. No control of the heat distribution or the total power input to the guard sections was provided.

TEST PROCEDURE

The test airplane was flown into natural-icing conditions over most of the northwestern area of the United States during the winter of 1945-46. During the winter of 1946-47 the area of operations was extended to include a few flights in the central and eastern part of the United States. The usual test procedure, during flight in icing conditions, was to record airfoil data simultaneously with the measurement of the meteorological conditions. The rotating cylinders, described in reference 13, which constituted the means of measuring liquid-water concentration, drop size, and drop-size distribution, were extended as often as was conveniently possible. Records of free-air temperature, airspeed, and altitude were taken several times a minute. The recording potentiometer used to obtain airfoil temperatures was operated continuously. During this time, the values of current flow through the electrical heating strips of the airfoil were recorded. Photographs of the test-section surface and records of pressure distribution were taken at frequent intervals.

RESULTS

A tabulation of the flight and meteorological conditions for which simultaneous airfoil data were obtained is presented in tables I and II. Table I contains the flight and icing conditions for which corresponding heat-transfer measurements were made with the NACA 0012

airfoil. Table II gives similar information for the NACA 65,2-016 airfoil. All measurements were made during flight in natural-icing conditions. During most of the flights, large variations in liquid-water concentration, and occasionally drop size, were experienced. The rotating cylinders, used to measure liquid-water content and drop size, were extended for about 1 to 2 minutes, thus giving average values for 1- to 2-minute intervals. A complete cycle of the recording potentiometers used to record airfoil temperatures required 4 to 6 minutes, during which time the meteorological conditions may have changed considerably. For these reasons, an effort was made to select, for analysis and discussion herein, only the airfoil data recorded during flight in relatively uniform clouds and/or where close correlation existed between the cylinder measurements and the airfoil-temperature records. Of these data, only a part, chosen as being typical, are presented in this report. These are the thermal data for which the flight and icing conditions are given in tables I and II.

NACA 0012 Airfoil Data

Figures 8(a) to 8(g), inclusive, present the measurements of surface temperature, surface heat flow, and resulting heat-transfer coefficients obtained with the 0012 airfoil model during flight in the conditions presented in table I. The heat-flow distribution illustrated in these figures had been found by experiment to give an approximately uniform temperature rise over the test-section surface during flight in clear air. Variations in the intensity of the distribution for the different conditions of table I occurred as a result of the heat supply procedure followed during the tests. In general, during an icing test the total heat input was reduced until the surface temperature was observed to fall close to freezing temperature at some point on the test section. Typical values of surface temperature, heat flow, and convective heat-transfer coefficient obtained during flight in clear air are shown in figure 8(h).

The data presented in all figures except figure 8(g) were taken with the entire test section heated. Figure 8(g) presents data secured with only the leading-edge region heated, from 11 percent chord on the right side to 8 percent chord on the left side. At the time of this test, insufficient heat was supplied to the leading-edge area to evaporate all the water striking the surface, and streamers of ice formed aft of the heated region, similar to those shown in figure 9.

The heat-flow values given in figures 8(a) to 8(h), inclusive, were calculated from measurements of the total power dissipated in the electrical resistance strips and the internal heat loss. The

measurements of surface temperature, which were obtained with the thermocouple installation previously described, were corrected for errors incurred by the presence of a layer of paint covering the junction. Magnitude of these errors was determined from knowledge of the thickness and thermal conductivity of the paint and the amount of heat flowing through it.

The kinetic temperature of the free-stream air t_{o_K} used in computing the heat-transfer coefficients, was calculated for the 0012 airfoil from equations (18) and (19), using experimentally determined values of the expression

$$1 - \frac{U^2}{V^2}(1-Pr^{\beta})$$

where β is 1/2 for laminar flow and 1/3 for turbulent flow. Values of this expression for various points along the airfoil surface, were obtained from figure 10, which presents data obtained during flight in clear air.

A typical record of pressure distribution over the 0012 airfoil model test-section surface is shown in figure 11.

NACA 65,2-016 Airfoil Data

Figures 12(a) to 12(j), inclusive, present the measurements of surface temperature, surface heat flow, and resulting coefficients of heat transfer obtained with the 65,2-016 airfoil model during flight in the conditions presented in table II. The distribution of heat flow shown in these figures had been experimentally established to provide an approximately uniform temperature rise above free-air temperature over the test-section surface during flight in clear air at an altitude of 11,000 feet and a true airspeed of 175 miles per hour. This heat-flow profile was used throughout all the flight tests. Slight variations in heating intensity are due to variations in internal heat flow and chordwise heat conduction in the thin aluminum skin. Typical values of surface temperature, heat flow, and convective heat-transfer coefficient for flight in clear air are given in figure 12(k).

The results shown in all figures (except figs. 12(h) to 12(j), inclusive) were obtained with the test section heated to approximately 55 percent chord. Heating aft of this point was precluded by a malfunctioning of the heating equipment in this area. Figures 12(h) to 12(j), inclusive, present data secured with only the leading-edge region heated, from 17 percent chord on the right side to 17 percent

chord on the left side. During the time when the measurements of figures 12(i) and 12(j) were taken, an insufficient quantity of heat was being supplied to the leading-edge region to evaporate all the water striking the surface, and ice accumulated aft of the heated area. This is shown in figure 13.

The heat-flow values given in figures 12(a) to 12(k), inclusive, were calculated from measurements of the total power dissipated in the electrical resistance strips, in a similar manner to that used for establishing the heat flow for the NACA 0012 airfoil. In addition to the determination of the internal heat loss in computing the surface heat flow for the NACA 65,2-016 airfoil, the flow of heat chordwise in the thin aluminum surface was considered. The chordwise heat conduction is a function of the chordwise variation in surface temperature. It was assumed that the quantity of heat flowing from point to point along the surface, as indicated by the difference in surface temperature between the two points, originated from the heating strip under the higher temperature and flowed away from the surface into the air stream in the area of surface over the heating strip at the lower temperature. This method, although inexact, offered a rapid means of estimating the effect of chordwise conduction. A more exact determination of this effect can be obtained using the "relaxation" method of reference 10. No corrections were applied to the surface-temperature measurements, since it was assumed that the surface thermocouple junctions were at surface temperature.

The kinetic temperature of the free-stream air t_{o_k} was calculated using equations (18) and (19). Values of the expression $1 - (U^2/V^2)(1-Pr^{\beta})$ were calculated and are plotted in figure 14.

A picture of the conditions of wetness which existed on the airfoil during flight in clouds can be seen in figure 15. This figure shows some typical records obtained with strips of blueprint paper which had been fastened to a device that could be extended into the air stream up the leading edge of the airfoil model to a point just below the test section. Since, in effect, these were wrapped around the leading edge of the model, they illustrate the pattern that the water assumes in striking the airfoil and flowing aft. The records were obtained during icing conditions 11, 13, and 14, table II.

A typical measurement of pressure distribution over the 65,2-016 airfoil model test-section surface is shown in figure 16.

DISCUSSION

The ultimate in performance of a wing thermal ice-prevention system is one which will prevent the accretion of ice on any portion of the wing. This ideal operation requires that any water on the wing surface must be maintained in a liquid state until it evaporates, or blows off the wing at the trailing edge. In many wing designs, heating of the entire surface is not practicable because of such features as integral fuel tanks, and in these instances any water flowing aft of the heated region is apt to freeze and form the type of ice accretion normally termed runback. In the following discussion the ice-prevention action of a heated wing will be examined in detail, and the reliability of the equations and assumptions presented in the analysis section for the prediction of surface temperature and rate of water evaporation from the surface will be established. If these equations and analytical methods can be shown to define correctly the process of thermal ice prevention, the fundamental design procedure for a heated wing initially conceived in reference 6 will be more firmly established. The empirical design method of providing a specified temperature rise in clear air can then be replaced by the more fundamental and flexible concept of supplying sufficient heat to maintain the surface temperature above freezing until the water is either evaporated or carried away.

An analysis of the action of a heated wing requires the consideration of three factors: namely (1) the meteorological and flight conditions for which the wing must provide protection; (2) the area of water impingement, and the rate and distribution of impingement over that area; and (3) the rate at which the water is evaporated from the wing surface.

Meteorological and Flight Conditions

The specification of a meteorological condition for the design of thermal ice-prevention equipment depends upon the geographical areas over which the airplane will fly, the seasons of operation, and other factors dictated by the intended service of the aircraft. Obviously, the establishment of design conditions for a specific area requires a knowledge of the conditions prevailing over the area. If, on the other hand, the ice-prevention system is to provide protection for all-weather operation, general specifications of a meteorological condition must be established which will encompass all conditions likely to be encountered.

The most recent and extensive information in regard to the severity of icing conditions likely to be experienced in all-weather operation in the United States is contained in references 13 and 14.

In reference 13, estimates of the maximum continuous icing conditions as well as the maximum probable icing conditions apt to be encountered are presented. Since the duration of the maximum probable icing condition is quite short (1 to 2 minutes), and icing of this severity is entirely associated with cumulus clouds which should be avoided in all operations, the maximum continuous icing condition is believed to be of greater interest for design purposes. Two conditions of maximum continuous icing are presented based on a relationship of drop size and liquid-water content. These conditions are given in the following table:

Liquid-water concentration (gm/m^3)	[2]Mean-effective drop diameter (microns)	Free-air temperature (^oF)
0.8	15	20
0.5	25	20

It is believed that the conditions in the above table form a good basis for the design of thermal ice-prevention equipment for all-weather operation. In addition to these values, however, the proposed wing thermal system should be analyzed for possible undesirable operation in other icing conditions. For example, reference 13 points out that drops of 35 to 50 microns diameter should not be regarded as exceptional. Although the amount of liquid water associated with such large drops is usually low (about 0.1 gram per cubic meter) the fact remains that the area of water impingement would be very large and would probably exceed the limits of the heated region if this region had been based only on a consideration of the data in the maximum continuous table. Finally, the possibility of encountering icing conditions at low temperatures may be a critical condition for heated wings on some airplanes. For instance, the estimated conditions of maximum continuous icing presented in reference 13 and given in the preceding table were extended in reference 14 to air temperatures as low as -20^o F for the case of 15-micron drops. The conditions of maximum continuous icing suggested are 0.5 gram per cubic meter at 0^o F and 0.25 gram per cubic meter at -20^o F, both with

[2]The mean-effective diameter as defined in reference 13 is the size of drop in a cloud sample for which the amount of liquid water existing in water drops larger than that drop is equal to the amount of liquid water existing in drops smaller than the drop.

a mean-effective drop diameter of 15 microns. Either of these conditions may be more deleterious to the functioning of the wing thermal system than those in the table.

From the foregoing discussion, it is evident that the analysis of a heated wing should give consideration to several possibly critical icing conditions in the same manner that several flight conditions are assumed for the wing structural analysis. The data of references 13 and 14, although somewhat limited in scope, are considered to be sufficiently indicative of icing conditions in the United States to form a meteorological basis for heated-wing design.

The problem of selecting a flight condition for the design of ice-prevention equipment is concerned with the airspeed and altitude at which the airplane will fly. The airspeed will depend upon the specific airplane, and, in general, a cruise condition should be selected. Choosing an altitude for design is dependent upon several factors, which will be discussed later.

Area, Rate, and Distribution of Water Impingement

Having defined the icing conditions for which the heated wing is to be designed, the next step is to determine the region of the leading edge in which the water drops will strike the wing, the rate of water impact at any specified point in that region, and the total rate of impingement per foot of wing span. This subject was discussed at some length for the general case in the analysis section. In that discussion, it was shown that the method of reference 15 could be used to prepare (for any wing section for which the stream lines were known or could be determined) curves similar to those presented in figures 1, 2, and 3. The broken line of figure 1 gives an indication of the area of water impingement, while the rate of impingement at a specified point can be obtained from figure 2 and equation (7).

Two methods are available for the determination of the total rate of impingement per foot of wing span. The calculation of this quantity is of primary importance, as it determines the amount of heat required to disperse the water by evaporation. The first method utilizes the concept of collection efficiency E as mentioned in the analysis section. This method is preferable when only the value of the total rate of impingement is desired, since preparation of the curves of figure 2 is not required. For a thorough analysis of the heat transfer from the surface, however, knowledge of the rate of impingement at a point M_a is required. By employing equation (7) and figure 2 a curve of the distribution of water impingement (M_a against s/c) can be plotted. Figure 17 shows such a curve for the NACA 0012 airfoil, using equation (8) and an "E" type drop-size

distribution. (See reference 17.) A curve of this type presents an interesting picture of the distribution of water impingement and, in addition, the area under the curve denotes the total rate of water interception.

Although the method of reference 15 is considered to provide a complete and quite accurate prediction of the distribution of water impingement on the leading edge of an airfoil, it does have the disadvantages of requiring (1) a knowledge of the velocity components along a number of the airfoil stream lines, and (2) considerable computation. The difficulties associated with the computation of the water-drop trajectories for airfoils have encouraged the substitution of a cylinder with radius equal to the airfoil leading-edge radius in the determination of water impingement. (See references 5 and 6.) The curves of reference 17, which have been calculated for a large range of drop sizes, airspeeds, altitudes, and cylinder diameters, are then used directly to evaluate the anticipated water impingement on the airfoil. This substitution procedure is a useful device but should be employed with a full knowledge of its limitations. One of these limitations is the fact that the curves of reference 17 provide the area and total rate of water impingement, but give no direct indication of the distribution of impingement.

A second restriction of the cylinder-substitution method is concerned with the contour and size of the forward portion of the airfoil. To obtain an indication of this effect, the rate and area of water impingement on the 0012 airfoil, at 0° angle of attack, and on the leading-edge cylinder of that airfoil are compared for the same flight conditions and various drop sizes in figure 18. The values for the 0012 section were obtained from figures 1 and 2, and those for the cylinder from reference 17. At drop diameters up to about 25 microns the rates of impingement on the airfoil and on the leading-edge cylinder are approximately the same, although above 25 microns as the drop size increases, the rate of impingement becomes considerably greater on the airfoil than on the cylinder. At drop diameters up to about 18 microns the area of impingement on the cylinder is roughly equal to that on the airfoil. However, at a drop diameter of 25 microns, which is not unusual (reference 13), and was presented previously in this report as a possible *maximum* continuous condition, the area of impingement on the airfoil is nearly 50 percent greater than on the cylinder. It should be noted that the value of 25 microns for the maximum continuous condition is the mean-effective diameter, and that drops of a larger size probably will be present due to the existence of a distribution of sizes. Although these values provide an indication of the scale limitation of the cylinder-substitution method, the fact should be noted that figure 18 applies to only one airfoil section, with an 8-foot chord, and at one flight condition. The leading-edge radius of the NACA 0012 section for an 8-foot chord is small (1.5 in.)

and the leading-edge cylinder does not match the section contour for any great extent above the chord line. This is shown graphically in figure 19 which presents a comparison of the forward portions of three airfoil sections and the leading-edge cylinder of the 0012 section. In the case of airfoil sections with the leading-edge radius a greater percent of the chord than the 0012 section, and also for airfoils of 0012 section, or similar, with chords greater than 8 feet, the cylinder-substitution method will present a better approximation than that indicated by figure 18 for the same speed range.

For airfoil sections with a leading-edge radius which represents a small percentage of the chord, the substitution of an "equivalent" cylinder (reference 12) with a radius larger than the leading-edge radius would probably provide a better indication of the rate and area of water impingement on the airfoil than would be obtained for the leading-edge cylinder. At the present time there is not sufficient information on water-drop trajectories about airfoils to provide a basis for selecting the proper cylinder in each instance; therefore, the designer must utilize the more complicated, but more accurate, method of reference 15 or assume some cylinder diameter based on his experience. The possibility that the rate and area of impingement on an ellipse would more closely approximate the rate and area of impingement on a series of similar airfoils has been suggested and is worthy of future consideration.

The ability to select a proper drop size for the design of wing ice-prevention equipment is a factor of considerable importance to the designer, as can be illustrated by figure 20. In this figure the rate and area of impingement are presented for the 0012 airfoil as a function of drop size. The rate of impingement for each drop size was calculated for a liquid-water content of 1.0 gram per cubic meter. Consider, then, a change in design drop diameter from 10 microns to 20 microns. The resultant increase in rate of water impingement is 1.75 pounds per hour per foot of span or an increase of 175 percent, although the actual amount of water present per unit volume of cloud has not been changed at all. The same increase in drop size will cause an increase in area of impingement from 1.5 to 4 percent s/c.

In contrast, consider the effect on the rate of water impingement produced by an increase in the quantity of liquid water present, assuming the drop size to remain constant. The area of impingement will remain unchanged, while the rate of impingement will increase only in direct proportion to the increase in water concentration. This example clearly illustrates the fact that the amount of free water present in an icing cloud is only one factor influencing the quantity of water which will actually strike the wing in a specified time interval, and that the size of the cloud drops is a factor of at least equal importance.

The problem of distribution of the sizes of drops in an icing cloud also bears careful consideration. For example, if an "E" type drop-size distribution exists with a mean-effective drop diameter of 25 microns, the largest drops will be 68 microns in diameter. Hence, the area of impingement will be considerably greater than if a uniform drop size of 25 microns prevailed. The data of reference 14 indicate that, in general, the distributions of drop size in icing clouds are fairly narrow, and do not usually follow the broad distributions, such as type "E." Nevertheless, the distribution must be considered, since the largest drops in the cloud determine the area of impingement and the minimum extent of heated area required for ice prevention.

Rate of Evaporation of Water

Having discussed the problem of area and rate of water interception, the next step is to establish the rate at which the intercepted water is evaporated from the wing surface and the validity of the equations presented previously for determining the rate of heat dissipation during the process of evaporation. The problem of rate of evaporation is particularly important because all of the water intercepted by a wing heated only in the region of the leading edge must be dispersed by evaporation if the formation of runback is to be avoided.

From a superficial study of the mechanism by which water is deposited on the surface of a wing, it would be expected that in the area of water impingement the surface is completely wetted, and that equation (24) for calculating the heat loss from a heated wing is valid. Aft of the area of impingement, it would be anticipated that the surface may not be fully wetted, since water does not reach this region directly, but instead must flow back from the area of impingement. If the surface aft of the area of impingement is only partially wetted, the expression for X (equation (23)) must be modified for use in equation (25) to calculate heat requirements.

Observations, made during the airfoil tests, of the water pattern on the leading edge of the airfoils revealed that the above suppositions are correct. At a very short distance back of the region of impingement, the film of water was observed to reach a state of instability and break into small rivulets. A picture of the conditions of wetness which actually exist on a wing during flight in clouds can be seen in figure 15. This figure, which shows typical records obtained with the strips of blueprint paper placed around the leading edge of the 65,2-016 airfoil model during flight in icing conditions, illustrates the pattern formed by the water in striking the airfoil leading edge and flowing aft. It is evident

from the patterns that the area of impingement, which is clearly defined, is completely wetted, while back of this area the water collects and forms rivulets, creating a partially wetted surface. A study of the patterns indicated a variation in the fraction of surface area wetted (aft of the impingement area) with rate of impingement of water. Accordingly, the rates of water impingement M_s were calculated using equation (11) for the conditions existing at the time that rivulet patterns were obtained (icing conditions 11 through 15, table II). The curves and values presented previously for the 0012 airfoil were used in the calculations of M_s for the 65,2-016 airfoil. Substitution of the calculations for the 0012 section in computing values for the 65,2-016 section appears to be a good approximation, since the contour of the 65,2-016 section in the leading-edge region is very nearly the same as that of the Joukowski airfoil used in the 0012 trajectory calculations. Figure 19 compares the contours of the three sections.

The values of M_s were plotted against the measured areas of surface wetted, obtained from the strips of blueprint paper. Figure 21 shows the relationship, thus obtained, between the rate of flow of water from the impingement region and the fraction of surface area wetted. For the data shown in figure 21, values of the rate of water flow over the surface aft of impingement M_b were assumed to be equal to the rate of water impingement M_s. The scatter of data points in the figure is believed to be caused by errors in measurement of the liquid-water concentration occurring at the time the rivulet patterns were obtained. Table II shows that the free-air temperature was high during icing conditions 11 through 15, when the blueprint records were taken. The kinetic temperature was close to freezing, and it was observed that the water striking the rotating cylinders, used in the measurement of water concentration, was running back, and possibly off, the cylinders. Thus, the liquid-water concentrations measured may have been lower than the actual concentrations present. The two data points corresponding to a weight rate of water flow of 0.57 pounds per hour per foot of span (fig. 21) represent the rivulet data procured at the lowest free-air temperature of these tests (icing condition 14, table II). These are probably the most reliable data, since the rotating cylinders were subject to smaller losses of water. Therefore, the curve shown in figure 21 was weighted toward these points. The ultimate extent of this curve in the direction of percent of surface wetted is not definitely known. There is evidence, however, indicating that the degree of surface wetness aft of the area of impingement reaches a maximum which is not exceeded, regardless of the rate at which water is intercepted. It was found that a relationship exists between the rate of flow of water in the region aft of impingement and the surface-temperature rise above free-air temperature, and that the temperature rise decreases to a limit as the rate of flow of water

increases. Figure 22 shows the relationship between the rate at which water flows back over the heated surface of the 65,2-016 airfoil test section and the average increase in temperature above free-air temperature of the surface from 10 to 25 percent chord. The values of the rate of water flow were obtained by subtracting from the calculated rates of water impingement for one side of the airfoil the computed rates of evaporation from the region of impingement. Figure 22 illustrates that as the rate of water flowing over the surface increases, the temperature of the surface decreases, but that a limit to the decrease in temperature apparently is reached. This indicates that the rate of evaporation reaches a maximum as the limiting surface temperature is approached, since evaporation is the only variable in the heat-transfer process in the area of surface under consideration. Therefore, if the rate of evaporation attains a maximum, the degree of surface wetness must also approach a limit. It can be demonstrated, using equation (25) and the values presented in figures 21 and 22, that the maximum fraction of surface area wetted is about 50 percent.

Although the data from which the curve of figure 21 was computed were obtained with blueprint paper strips wrapped around the leading edge of the 65,2-016 airfoil, the values given in this figure are believed to be sufficiently indicative of the conditions of wettability existing on all clean wing surfaces not specially treated to be applicable for general airfoil thermal design. For purposes of design, it is suggested that the limit of surface wetness for surfaces not specially treated be taken as 40 percent. It is of importance to note that in using the curve of surface wetness shown in figure 21, for a heated wing, the total rate of evaporation of water W_S in the region of water-drop impingement must be subtracted from the total rate of water impingement M_S in order to obtain the rate of flow of water rearward from the area of impingement. The values given in figure 21 for degree of surface wetness are believed to be accurate only to the nearest 10 percent.

With the information gained so far, it should be possible to analyze the data obtained with the two electrically heated airfoil models and establish the validity of equations (24) and (25) for calculating heat flow. The curves of measured heat-flow distribution shown in figures 8(a) to 8(g) and figures 12(a) to 12(j) were faired to produce a form more suitable for comparison with heat-flow curves calculated using equations (24) and (25). Comparisons of the measured heat flow and the heat flow calculated to produce the measured surface temperatures, assuming the entire surface to be completely wetted, for the two airfoil sections for typical cases are shown in figures 23 and 24. These curves are also compared to the calculated heat loss due to convection only, that is, assuming the surface to be completely dry (equation (12)). In the previously

mentioned calculations, measured values of convective heat-transfer coefficient, obtained during flight in clear air, were used. In order to calculate the amount of heat dissipated in warming the impinging water (equation (4)) for the calculation of heat flow for the completely wetted case, values of M_a were computed from equation (8) using the measured values of liquid-water concentration, drop size, and drop-size distribution (tables I and II). As was done previously in the analysis of the blueprint-paper rivulet patterns, values of M_a were computed for both airfoil sections using the curves presented for the 0012 airfoil.

A study of the measured and calculated heat-flow curves in figures 23 and 24 shows that in the area of water-drop impingement good agreement is obtained between measured values and the values calculated for a completely wetted surface, indicating that in the region where it is reasonable to assume a fully wetted surface the equations for calculating heat flow are valid. Aft of the area of impingement, in the region of low heat flow, where it has been shown that the surface is only partially wetted, the values calculated for a completely wetted surface are lower than the measured values. Since the surface is only partially wetted, it would be expected that the calculated curve, which represents the values of heat flow required to produce the measured surface temperatures if the surface were completely wetted, would be considerably higher than the measured curve. There appear to be only two possible explanations for this discrepancy: (1) equation (25) gives erroneous values and cannot be relied upon for calculation, and (2) the values of convective heat-transfer coefficient used in equation (25) for calculating the heat-flow values are in error. The first explanation does not appear to be likely in view of the fact that the equation was derived on a sound basis. Also, there is no obvious reason why the equation should hold in the leading-edge region and fail to hold in the area aft of the leading edge. The second explanation, that erroneous values of convective heat-transfer coefficient were used in the calculations, seems entirely possible. Since the values of convective heat-transfer coefficient used in equation (25) are those measured during flight in clear air, it seems reasonable to assume that transition from laminar to turbulent flow moved forward during flight in icing conditions from the position maintained in clear air. Movement of transition to a point near the leading edge would cause the convective heat-transfer coefficients in the region under consideration to be increased several times above the values existing in clear air, since the convective coefficients in turbulent flow generally are considerably greater than those in laminar flow. Such an increase in the convective coefficients would raise the curves calculated for a completely wetted surface (figs. 23 and 24) to a position above the measured curves.

It is very likely that disturbance of the boundary layer, caused by water drops striking the airfoil surface and roughening the surface as they coalesce and flow aft, would effect a forward movement of transition. There is further evidence to support the assumption that the water-roughened surface caused movement of transition forward. Observations of the 65,2-016 airfoil during a flight in clear air with the test section heated indicated that transition had shifted forward by a considerable amount. This was noted by a lowering of the surface temperatures in the region aft of the leading edge. The heat distribution had been set previously to produce a constant surface temperature in clear air, and only a change in the boundary-layer characteristics could cause the evident change in heat-transfer coefficient. After the flight, a close examination of the leading-edge region of the airfoil revealed small insects stuck to the surface where they had hit during the flight. The surface was wiped clean and during a subsequent flight in clear air it was noted that transition had moved back again, as evidenced by the restoration of the surface temperatures to normal. Thus, it appears that very small irregularities in the surface, such as are present on the surface of an airfoil in icing conditions, are sufficient to cause transition to occur prematurely. Tests in wind tunnels also have shown that small protuberances in the leading-edge region of an airfoil will cause the movement of transition forward. (See reference 24.)

Most of the curves of heat-transfer coefficient measured during flight in icing conditions, shown in figures 8(a) to 8(f) and 12(a) to 12(g), display a definite increase in the aft region of high heat intensity, suggesting that transition is located at this point. It should be noted that the increase in heat-transfer coefficient indicated by these curves is believed to be only an apparent increase, caused by the rapid change in heating intensity in this region. If the coefficient is relatively constant throughout this area, as it is believed to be, a sudden increase in heating intensity will not be accompanied by an equally rapid change in the thermal boundary layer, and for a short distance aft the indicated values of heat-transfer coefficient will be erroneously high.

The exact values of the convective heat-transfer coefficient in the region aft of the area of impingement in icing conditions are unknown, but it is believed the values fluctuate due to changes in the location of transition during flight. Very probably, the disturbance to the boundary layer caused by water on the airfoil surface is of such a character as to create instability in the boundary layer, and cause the location of transition to fluctuate.

In the aft region of high heat flow (figs. 23 and 24), the values of convective heat-transfer coefficient are known, since turbulent flow existed in this region in clear air, when the values

were measured, as well as in icing conditions. In this region, the measured heat-flow curve and the calculated curve of convective heat transfer come together, indicating that at the point where the curves coincide all the water on the surface has been evaporated.

Since the equations for calculating heat flow have been shown to be valid in the area where the surface is completely wetted, it is reasonable to assume that the equations hold in regions where the surface is only partly wetted, provided the correct modifications are made to the evaporative factor X. Fairly accurate modifications to the factor X are believed to be possible by using the curve of surface wetness shown in figure 21. By the use of this curve it should be possible to calculate the rate of evaporation of water from the surface aft of the region of water impingement. In the region of impingement the calculation of rate of evaporation is straightforward, since full evaporation occurs. If the rates of evaporation from the two test airfoils can be demonstrated to be equal to the rates of water impingement for the test conditions, the method for calculating rate of evaporation will be substantiated.

Accordingly, calculations of the rates of evaporation from the surfaces of the two test airfoils were made for all the conditions of tables I and II for which thermal data were obtained. The rates of evaporation were determined graphically, using the curves of measured heat flow and calculated convective heat loss similar to those shown in figures 23 and 24. Aft of the area of impingement, the position of the convective curve was established by dividing the measured values of heat flow by the modified values of X (equation (25)). Values of the degree of surface wetness used in modifying X were determined from figure 21, using computed rates of water impingement and evaporation from the area of impingement. The position of the re-calculated curves of convective heat loss are shown typically in figures 23 and 24. The total rate of evaporation, then, was determined by measuring the area between the measured and re-calculated convective heat-flow curves. This gave the total amount of heat dissipated by evaporation of the water in Btu per hour per foot of span. Dividing this value by L_s the latent heat of vaporization, the total rate of evaporation W_s in pounds per hour per foot of span was obtained.

The rates of evaporation, obtained in the previously mentioned manner, are compared with the rates of water impingement, calculated by the method previously presented, for the 0012 and 65,2-016 airfoil models, for the left side only, in tables III and IV. An average agreement of 13 percent for all the conditions analyzed where no runback formed was obtained, indicating the degree of reliability of the method for calculating the rate of evaporation of water from a heated wing.

In order to demonstrate further the dependability of the method for calculating rate of evaporation from a heated wing, the photograph of runback on the 65,2-016 airfoil (fig. 13) was analyzed. If it can be shown that the actual rate of formation of runback compares closely to the rate at which runback is calculated to form under the particular icing conditions, the method for calculating rate of evaporation will be further substantiated.

The runback shown in figure 13 had started forming 10 minutes earlier. At the time of the photograph the formation was estimated, by observation during flight, to be approximately 3/16 inch thick. The area of the formation extended about 2-1/2 inches chordwise and 12 inches spanwise, making a weight of ice of 0.2 pound. This constitutes an actual rate of formation of runback of 1.2 pounds per hour per foot span. During this 10-minute period, two sets of rotating-cylinder and airfoil heat-transfer data were taken. These correspond to icing conditions 9 and 10, table II. Results of calculations of the rates of impingement and evaporation based on these data are given in table IV. For icing condition 9 the rate of water impingement was 1.60 pounds per hour per foot span. The rate of evaporation from the heated area was 0.44 pound per hour per foot span, leaving a calculated rate of formation of runback of 1.16 pounds per hour per foot of span. During icing condition 10 the calculated rate of impingement was 1.79 pounds per hour per foot and the rate of evaporation was 0.51 pound per hour per foot, resulting in a rate of formation of runback of 1.28 pounds per hour per foot of span. The calculated rates of formation of runback (1.16 and 1.28 lb per hr, ft) agree remarkably well with the actual rate of formation (1.2 lb per hr, ft), illustrating the reliability of the procedure for calculating rate of evaporation.

A short time prior to this test, the airfoil was subjected to a much less severe icing condition (condition 8, table II), during which all of the water intercepted was calculated to have been evaporated (icing condition 8, table IV). Photographs of the test section verified the fact that no runback had formed.

The foregoing analyses were based on the assumption that removal of the water striking the airfoil surface is effected by evaporation only, and that none of the water is dispersed by mechanical means. This is consistent with the results reported in reference 10 and 25. It is believed that "blow-off" of water, as suggested in references 5 and 6, does not occur. Also, it is believed there was no "bounce-off" of the water drops striking the airfoil surfaces, as proposed in reference 11. At speeds higher than those encompassed by the scope of this investigation, it is conceivable that mechanical removal of the water by bounce-off could occur. However, in view of the lack of information on this phenomenon, and since neglecting the

possibility that water may be removed by mechanical means tends to be more conservative in the thermal design, it is suggested that bounce-off be neglected in the design of wing thermal ice-prevention equipment.

Calculation of Heat Requirements for an NACA 0012 Airfoil

Since it has been demonstrated that the rate of evaporation of water from a heated wing can be calculated with reasonable certainty, the rate of heat flow required to produce a particular rate of evaporation can be determined with equal dependability, provided the coefficients of convective heat transfer are known. Using the equations and method presented for calculating the rate of evaporation of water from a heated airfoil surface, a calculation was made to establish the extent of heated area required for ice prevention in specified conditions of icing for the NACA 0012 airfoil, assuming a particular heat-flow distribution. The conditions of calculation are as follows:

Chord length	8 ft
Pressure altitude	12,000 ft
True airspeed	170 mph
Free-air temperature	20° F
Liquid-water concentration	0.5 gm/m^3
Mean-effective drop diameter	25 microns
Drop-size distribution	E

The procedure employed was to assume a reasonable intensity and distribution of total heat flow and then calculate the extent of heated area required to evaporate all of the intercepted water. The method of solution will be outlined briefly in the following paragraph. A detailed step-by-step consideration of the problem showing all computations is given in the appendix.

First, the area, rate, and distribution of water impingement on the airfoil were calculated for the assumed conditions. Using the assumed distribution of total heat flow, the heat loss due to convection for the particular conditions was then calculated. Since in an icing cloud the presence of water on an airfoil surface causes premature transition, for these calculations, transition was assumed to start at 5 percent s/c, and the estimated form of turbulent heat-transfer coefficient shown in figure 25 was used. Calculations were

made for a number of chordwise stations, and the results are given in figure 26, which shows the assumed heat-flow distribution and the calculated convective heat loss for one side of the airfoil. The rate of evaporation is represented by the area between the curves of convective heat loss and total heat flow, except in the region of water impingement, where the rate of evaporation is denoted by the area between the curve of heat loss due to warming the intercepted water and the curve of heat loss due to convection. These areas actually give the rate of heat loss due to evaporation; however, by dividing the area value by L_s, the latent heat of vaporization, the rate of evaporation is obtained. The procedure, then, was to extend the total and convective curves until the total rate of evaporation equaled the rate of water impingement. Extension of the heated area to 18 percent s/c was found to be adequate to ensure evaporation of all of the water intercepted.

Several other calculations were made for the 0012 airfoil to determine the effects of altitude, air temperature, and location of transition on the requirements of heat flow and extent of heated area necessary to evaporate all the intercepted water. The results of each of these calculations were compared with the results of the calculations for the conditions previously specified. For each of the calculations, the same total heat-flow distribution was assumed and the extent of heated area required to evaporate all the intercepted water was calculated for each condition.

To determine the effect of altitude on the heat requirement, a comparative calculation was made for sea-level conditions with all other flight conditions as previously specified and with the area and rate of water impingement the same as at the 12,000-foot condition. The results of this calculation are shown in figure 27, which compares the relative convective heat losses at sea level and 12,000 feet. For the conditions at 12,000 feet extension of the heated area to 18 percent s/c was shown previously to be adequate to ensure evaporation of all of the water intercepted. At sea level it would be necessary to extend the heated area to 26 percent s/c for evaporation of all the water intercepted. The curves of figure 27 can also be used to determine the amount of increase necessary in the total heat flow if all the water is to be evaporated in an area forward of a specified chord point. For example, assume that the extent of heated region for the curves of figure 27 is limited to 18 percent s/c. At 12,000 feet all of the water would be evaporated, as has been previously mentioned. At sea level, however, some of the water would not have been evaporated. By measurement of the areas of figure 27 it can be shown that the total heat flow required to evaporate all the water within the area from 0 to 18 percent s/c at sea level is approximately 10 percent greater than the amount required at 12,000 feet. The increase in heat requirement

with decrease in altitude is due to the fact that the rate of evaporation of water decreases as altitude is decreased, because of the decrease in the evaporative factor X (equation (23)). Since the convective heat-transfer coefficient increases with decrease in altitude, due to the increase in air density, it might be expected that the rate of evaporation would be increased with decrease in altitude, because the rate of evaporation is directly proportional to the convective coefficient (equation (21)). However, the increase in the rate of evaporation is more than compensated by the increase in convective heat loss, and the rate of evaporation, for a fixed total heat flow, actually becomes less with decrease in altitude. Apparently, then, airfoil thermal ice-prevention equipment in which the heat flow is fixed, such as electrical systems, should be designed for the minimum altitude at which the airplane is expected to encounter icing. However, if the airplane is designed to utilize some form of air-heated system, the performance of which probably will decrease with increase in altitude, the maximum altitude at which icing is expected to be encountered should also be investigated.

To determine the effect of air temperature on the heat requirement, a calculation was made of the convective heat loss at 0° F free-air temperature and is compared in figure 27 with the convective heat loss at 20° F. In the calculation with the free-air temperature at 0° F, it was determined that the surface temperature dropped to freezing at 24 percent s/c before all the water on the surface was evaporated. However, the total heat flow required to evaporate all the water within the area from 0 to 18 percent s/c with the air temperature at 0° F is approximately only 15 percent greater than the amount required at 20° F. Although this is an appreciable increase in the heat requirement, it is considerably less than that necessary for a similar change in conditions for ice-prevention equipment designed on the basis of maintaining the surface temperature just above freezing, such as for the case of windshields. (See reference 21.) It appears, then, that a wing thermal system which has been designed for a relatively high air temperature will be capable of ice prevention at low air temperatures in icing conditions nearly as severe as those upon which the design was based. Of course, the system is more subject to failure through the possibility of the surface temperature falling below freezing in the low air-temperature conditions, but in general, the surface temperatures required for evaporation of all impinging water in the relatively small heated area of the leading edge will be sufficiently high to obviate this possibility.

To establish the effect of the location of transition on the heat requirement, a calculation was made of the convective heat loss, assuming laminar flow exists throughout the heated area. For this

calculation, the measured values of convective heat-transfer coefficient shown in figure 25 were used. The convective heat loss for laminar flow is compared in figure 27 with the convective heat loss, assuming transition started at 5 percent s/c. In the case of complete laminar flow, it would be necessary to heat only to 14 percent s/c to obtain evaporation of all the water. The total heat flow required to evaporate all the water within the area from 0 to 14 percent s/c with transition at 5 percent s/c is approximately 10 percent greater than the amount of heat required if laminar flow prevails. Apparently, the location of transition moves forward in conditions of icing, even in the presence of a favorable pressure gradient, to a point where a strong favorable pressure gradient is encountered (figs. 11 and 16). As was stated previously, the location of transition is believed to fluctuate, probably over a considerable distance. It is suggested that forward movement of transition to a point close to the leading edge of the wing be assumed in the design of thermal ice-prevention equipment, especially in view of the fact that a greater amount of heat is required for the turbulent-flow condition.

From a comprehensive study of the results shown in figure 27, some general conclusions can be reached. It is apparent that aft of the area of droplet impingement, the efficiency of removal of water by evaporation decreases rapidly. The reason for the decrease in efficiency is that only partial wetness prevails aft of the area of impingement, while the area of impingement is entirely wet. This indicates that the larger the portion of the total amount of water intercepted that is evaporated in the area of interception, the greater the efficiency of the thermal system becomes. The rate of evaporation of water is the determining factor in the efficiency of a wing thermal ice-prevention system. Only the heat that is dissipated in evaporation is used to advantage. The heat lost by convection only warms the air. Thus, the conclusion is drawn that the heating should be concentrated as much as possible in the leading edge of a wing, in the area of drop impingement, if an efficient thermal system is to be obtained.

Calculations for the C-46 Wing Thermal System in Maximum Continuous Icing Conditions

An analysis of the C-46 airplane wing thermal ice-prevention system for the upper surface at wing station 157 was made in an effort to determine whether the thermal system could cope with the maximum continuous icing conditions given previously at the beginning of this discussion. The assumed icing and flight conditions for the calculations are as follows:

	Condition A	Condition B
Altitude (ft)	6000	6000
True airspeed (mph)	180	180
Liquid water content (gm/m^3)	0.8	0.5
Mean-effective drop size (microns)	15	25
Free-air temperature (^oF)	20	20

The heat-flow distribution at station 157 was estimated, based on data presented in references 4 and 26, and is shown in figure 28. The rates of water impingement for the two icing conditions assuming a "C" type drop-size distribution were calculated for the leading-edge cylinder of the airfoil section using the data presented in reference 17. Curves of distribution of water impingement, for the upper surface, for the two cases are given in figure 29. These were constructed using the data from reference 17 for each drop size in the distributions. The value of M_s, obtained from equation (9), for Condition A is 0.65 pound per hour per foot span, while the value of M_s for Condition B is 1.39 pounds per hour per foot span. As in the calculations presented previously, the rate of evaporation of water from the surface was determined by calculating the heat loss due to convection for the two conditions. Values of convective heat-transfer coefficient were taken from figure 30, which shows the values measured during flight in clear air using an electrically heated glove and the estimated convective coefficients for icing conditions, when transition moves forward. The estimated values were used in the calculations. The computed curve of convective heat loss for Condition A is shown in figure 28. Results of the calculations of rate of evaporation for the two conditions indicated that sufficient heat was supplied to the upper wing surface to evaporate all of the water intercepted. For Condition A the wing was shown to be capable of evaporating 0.90 pound per hour per foot span, indicating that the liquid-water concentration could attain a value of at least 1.1 grams per cubic meter at a mean-effective drop size of 15 microns before runback would form. The rate of evaporation for Condition B was calculated to be 1.35 pounds per hour per foot span, suggesting that the liquid-water concentration of 0.5 gram per cubic meter is the limiting condition at 25 microns.

A further analysis was made of the upper wing surface at station 157 using the values of Condition A, excepting that a free-air temperature of 0° F was assumed. The curve of convective heat loss for this condition is shown in figure 28. Under this condition calculations revealed the wing would be able to evaporate 0.70 pound per hour per foot span. The rate of impingement, as before, was 0.65 pound per hour per foot span.

These calculations substantiate the general observations of the successful operation of the C-46 wing thermal ice-prevention system. The absence of runback on the wing upper surfaces during a great many of the icing flights indicates the adequacy of the thermal design.

Selection of Conditions for Design

In selecting values of drop size, liquid-water concentration, air temperature, and altitude for the design of thermal ice-prevention equipment, a combination of these variables normally occurring in nature should be chosen such as to require the highest rate of heating. As stated previously, conditions of maximum continuous icing are believed to form a good basis for design. It is of interest to investigate the effect of different possible combinations of the variables of drop size, liquid-water content, air temperature, and altitude on the heat requirement for ice prevention for the maximum continuous conditions given in the table in the first part of this discussion.

The effect of an increase in the size of drops in an icing condition is to increase the collection efficiency of the airfoil, thereby increasing both the rate at which water is intercepted and the area of impingement. An increase in the liquid-water concentration of the air causes a proportional increase in the amount of water intercepted, for a given drop size. Since all of the water striking the wing must be evaporated to avoid the formation of ice, an increase in the rate of water interception will cause an increase in the heat requirement. Fortunately, a relation between water concentration and drop size appears to exist in icing clouds, and the existence of very large drops generally is accompanied by a small concentration of liquid water (reference 13). The selection of a combination of drop size and water concentration should be such as to produce the highest rate of impingement. It was shown previously that an increase in the drop size produces a greater increase in the rate of water interception than a proportional increase in the water concentration. For this reason, the maximum continuous icing condition of 25 microns, mean-effective drop size, and 0.5 gram per cubic meter, liquid-water concentration, generally will result in a more rapid rate of water impingement than the condition of 15 microns and 0.8 gram per cubic meter.

A decrease in free-air temperature, while increasing the heat requirement for thermal ice prevention, is accompanied by a decrease in the liquid-water concentration (reference 14), which causes a proportional decrease in the rate of water impingement, for the same drop size. The sizes of drops existing at low air temperatures (0° F) in icing conditions tend to be only slightly smaller than those at higher air temperatures (reference 13); therefore, a selection of air temperature for design will be determined by the combination of air temperature and water concentration (and corresponding drop size) to produce the highest heat requirement. It will be found, generally, that the rate of heating required to evaporate the larger quantities of water at the higher air temperatures is greater than the heat needed for ice prevention at the lower temperatures. However, low air-temperature conditions should be investigated to ascertain that the temperature of the heated surface will not fall below freezing.

There appears to be no relation between altitude and the drop size or liquid-water concentration of icing conditions. (See reference 13.) Therefore, the altitude at which the heat requirement is greatest should be chosen. The minimum altitude of operation was shown previously to produce the highest heat requirement for wing thermal ice prevention. However, as was formerly suggested, if the airplane is designed to utilize some form of air-heated system, the maximum altitude at which icing is expected to be encountered should also be investigated.

CONCLUSIONS

From the foregoing discussion, it is concluded that the extent of knowledge on the meteorology of icing, the impingement of water drops on airfoil surfaces, and the processes of heat transfer and evaporation from a wetted airfoil surface has been increased to a point where the design of heated wings on a fundamental, wet-air basis now can be undertaken with reasonable certainty. In addition to this general conclusion, the following conclusions are drawn, based on test data and analytical studies of the processes of heat transfer and evaporation from a heated wing:

1. The heat should be concentrated as much as possible in the leading-edge region of the wing in the area of water-drop impingement, if an efficient thermal system is to be obtained.

2. An increase in altitude, for the same rate and area of water impingement on a wing and for the same conditions of true airspeed and free-air temperature, decreases the heat requirement for thermal ice prevention.

3. A wing thermal ice-prevention system which has been designed to evaporate all impinging water in the leading-edge region for a relatively high free-air temperature (20° F) will be capable of ice prevention at low air temperatures (0° F) in icing conditions nearly as severe as those upon which the design was based.

Ames Aeronautical Laboratory,
National Advisory Committee for Aeronautics,
Moffett Field, Calif.

APPENDIX

Calculation of Extent of Heated Area Required for NACA 0012 Airfoil

The detailed, step-by-step calculations for establishing the extent of heated area required for ice prevention on an NACA 0012 airfoil in specified conditions of icing are presented in this appendix. It is believed that the general procedure outlined herein will be applicable for the design of most wing thermal ice-prevention equipment.

The calculations were made for one side only of the airfoil. The assumed flight and meteorological conditions used in the calculations are as follows:

Pressure altitude	12,000 ft
True airspeed	170 mph
Free-air temperature	20° F
Liquid-water concentration	0.5 gm/m^3
Mean-effective drop diameter	25 microns
Drop-size distribution	E

The chord length of the airfoil was taken as 8 feet.

Step 1.- Calculate area, rate, and distribution of water interception. The area of interception is determined by the largest droplets present in the cloud. For the case of an "E" type drop-size distribution (reference 17), the largest drops will be 2.71 times larger than the mean-effective size, or

Maximum drop diameter = 2.71 × 25 = 68 microns

The K–value corresponding to a drop diameter of 68 microns for the assumed flight conditions was calculated using equation (5). Thus,

$$K = \frac{2}{9}\left(\frac{62.4}{0.053}\right)\left(\frac{34\times3.28\times10^{-6}}{8}\right)^{2}\left(\frac{250\times8\times0.053}{1.16\times10^{-5}}\right) = 0.465$$

From figure 3, the efficiency of impingement E for this K–value is 54 percent. Using equation (10), the starting ordinate of the 68–micron–diameter drop which just hits the surface is

$$y_{o_{limit}} = E\, y_{max}$$

or

$$\frac{y_{o_{limit}}}{c} = E\,\frac{y_{max}}{c}$$

Since the airfoil is 12 percent thick,

$$\frac{y_{max}}{c} = 0.06$$

and

$$\frac{y_{o_{limit}}}{c} = 0.54 \times 0.06 = 0.032$$

Using the broken curve in figure 1, the area of impingement was found to be 10.8 percent s/c.

The distribution of water–impingement rate over the airfoil surface was calculated using equation (8). The individual rates of impingement for each of the drop sizes in the assumed distribution were calculated for various points along the surface. This was accomplished by computing the value of K for each of the drop sizes

in the distribution using equation (5), determining the values of C, for the corresponding K-value, at various points along the surface, then evaluating the expression VnC. By adding these individual impingement rates for each point on the surface, the resulting distribution of water-impingement rate over the surface was obtained. The above calculations were made using a tabular form of computation, as illustrated in table V. Figure 17 shows the resulting distribution of impingement. The total rate of water impingement M_S was calculated, using equation (9), by measuring the area under the curve shown in figure 17. The value of M_S was calculated to be 2.1 pounds per hour per foot span.

Step 2.- Establish the distribution of heat flow from the surface. The distribution of heat flow will depend on the type of ice-prevention system to be used. If an electrical system is planned, the distribution and intensity, once set, will remain unchanged regardless of variations in flight and meteorological conditions. On the other hand, if the system is to be designed to utilize heated air or some other fluid, the distribution of heat flow from the surface will depend upon the characteristics of the internal flow of the fluid as well as the conditions affecting the external heat transfer. If such a system is to be used, calculation of the heat-flow distribution will be rather complex, and it is believed that assuming a distribution will provide a good basis for starting the calculations for design.

The heat-flow distribution and intensity used in these calculations was estimated, based on data presented in references 4 and 26, to be the heat-flow distribution and intensity of the thermal ice-prevention system for the wing of the C-46 airplane (reference 20) at the 8-foot chord station. This distribution, which is believed to be representative of a probable thermal system, is shown in figure 26.

Step 3.- Determine the values of convective heat-transfer coefficient. The values of measured convective heat-transfer coefficient with the estimated form of the turbulent coefficients shown in figure 25 were used.

Step 4.- Calculate values of surface temperature in the area of water impingement, using equation (24), such that the values of q at any point are equal to the assumed heat flow. (See fig. 26.)

Step 5.- From the values of surface temperature calculated in step 4, compute the convective heat loss using equation (12). The curve of convective heat loss is plotted in figure 26.

Step 6.- Calculate the rate of flow of water aft of the region of water interception. This was done by measuring the area in the region of water impingement between the convective heat-flow curve and the curve denoting heat flow to impinging water (fig. 26) to obtain the rate of heat dissipation due to evaporation. The rate of evaporation was computed from equation (20), and was subtracted from the rate of impingement to give the rate of water flow aft of the region of water interception. The rate of evaporation was calculated to be 1.6 pounds per hour per foot span. Subtracting this value from the rate of water striking the surface, 2.1 pounds per hour, foot, the rate of flow of water aft, then, is 0.5 pound per hour per foot span.

Step 7.- Determine the wetness fraction and make the proper modification to the evaporative factor. Using the curve shown in figure 21, the wetness fraction for a water flow rate of 0.5 pound per hour, foot is 30 percent. It is suggested that the values of degree of wetness given in figure 21 be used only to the nearest 10 percent, since more precise usage is considered to be unwarranted.

The evaporative factor X was then modified by the 30-percent wetness fraction, so that equation (23) becomes

$$X = 1 + 1.12 \left(\frac{e_s - e_{o_k}}{t_s - t_{o_k}} \right) \frac{P_{SL}}{P_1}$$

For these calculations, the value of P_1 was taken as the free-stream static pressure, so that

$$X = 1 + 1.77 \left(\frac{e_s - e_{o_k}}{t_s - t_{o_k}} \right)$$

Step 8.- Calculate values of surface temperature aft of the area of water impingement using equation (25) and the revised value of X such that the values of q at any point are equal to the assumed heat flow. (See fig. 26.)

Step 9.- From the values of surface temperature calculated in step 8, compute the convective heat loss, using equation (12). The curve of convective heat loss is shown in figure 26.

Step 10.- Extend the calculation of convective heat loss until the total rate of evaporation, denoted by the area between the curves

of convection and total heat flow (except in the region of impingement), equals the total rate of water impingement. The rate of evaporation was computed from the area between the two curves using equation (20). For the case of the 0012 airfoil, the extent of heated region required for evaporation of 2.1 pounds per hour, foot span was calculated to be to 18 percent s/c, which is equivalent to 16.5 percent chord.

It should be noted that the extent of the heated region can be decreased by increasing the intensity of the total heat-flow distribution and re-calculating the required extent of heated area.

REFERENCES

1. Rodert, Lewis A., Clousing, Lawrence A., and McAvoy, William H.: Recent Flight Research on Ice Prevention. NACA ARR, Jan. 1942.

2. Neel, Carr B. and Jones, Alun R.: Flight Tests of Thermal Ice-Prevention Equipment in the XB-24F Airplane. NACA RMR, Oct. 1943.

3. Look, Bonne C.: Flight Tests of the Thermal Ice-Prevention Equipment on the B-17F Airplane. NACA ARR No. 4B02, 1944.

4. Selna, James, Neel, Carr B., Jr., and Zeiller, E. Lewis: An Investigation of a Thermal Ice-Prevention System for a C-46 Cargo Airplane. IV - Results of Flight Tests in Dry-Air and Natural-Icing Conditions. NACA ARR No. 5A03c, 1945.

5. Hardy, J. K.: Protection of Aircraft Against Ice. Rep. No. S.M.E. 3380, British R.A.E., July 1946.

6. Hardy, J. K.: An Analysis of the Dissipation of Heat in Conditions of Icing From a Section of the Wing of the C-46 Airplane. NACA ARR No. 4Ilia, 1944.

7. Hardy, J. K.: Measurement of Free Water in Cloud Under Conditions of Icing. NACA ARR No. 4Ill, 1944.

8. Lewis, William: Icing Properties of Noncyclonic Winter Stratus Clouds. NACA TN No. 1391, 1947.

9. Lewis, William: Icing Zones in a Warm-Front System With General Precipitation. NACA TN No. 1392, 1947.

10. Bowers, R. D.: Icing Report by the University of California, Fiscal Year 1946. AAF Tech. Rep. 5529, Sections III and VII, Nov. 1946.

11. Bowers, R. D.: Basic Icing Research by General Electric Company, Fiscal Year 1946. AAF Tech. Rep. 5539, Jan. 1947.

12. Tribus, Myron and Tessman, J. R.: Report on the Development and Application of Heated Wings, AAF TR 4972, Add. I. Jan. 1946. (Available from Office of Technical Services, U. S. Department of Commerce as PB No. 18122.)

13. Lewis, William: A Flight Investigation of the Meteorological Conditions Conducive to the Formation of Ice on Airplanes. NACA TN No. 1393, 1947.

14. Lewis, William, Kline, Dwight B., and Steinmetz, Charles P.: A Further Flight Investigation of the Meteorological Conditions Conducive to Aircraft Icing. NACA TN No. 1424, 1947.

15. Bergrun, Norman R.: A Method for Numerically Calculating the Area and Distribution of Water Impingement on the Leading Edge of an Airfoil in a Cloud. NACA TN No. 1397, 1947.

16. Glauert, Muriel: A Method of Constructing the Paths of Raindrops of Different Diameters Moving in the Neighbourhood of (1) a Circular Cylinder, (2) an Aerofoil, Placed in a Uniform Stream of Air; and a Determination of the Rate of Deposit of the Drops on the Surface and the Percentage of Drops Caught. R. & M. No. 2025, British A.R.C., 1940.

17. Langmuir, Irving, and Blodgett, Katherine B.: A Mathematical Investigation of Water Droplet Trajectories. General Electric Rep., 1945. (Available from Office of Technical Services, U. S. Dept. of Commerce as PB No. 27565.)

18. Frick, Charles W., Jr. and McCullough, George B.: A Method for Determining the Rate of Heat Transfer from a Wing or Streamline Body. NACA ACR, Dec. 1942.

19. Boelter, L. M. K., Grossman, L. M., Martinelli, R. C., and Morrin, E. H.: An Investigation of Aircraft Heaters. Part XXIX – Comparison of Several Methods of Calculating Heat Losses from Airfoils. University of California. NACA TN No. 1453, 1947.

20. Jones, Alun R., and Spies, Ray J., Jr.: An Investigation of a Thermal Ice-Prevention System for a C-46 Cargo Airplane. III – Description of Thermal Ice-Prevention Equipment for Wings, Empennage, and Windshield. NACA ARR No. 5A03b, 1945.

21. Jones, Alun R., Holdaway, George H., and Steinmetz, Charles P.: A Method for Calculating the Heat Required for Windshield Thermal Ice Prevention Based on Extensive Flight Tests in Natural-Icing Conditions. NACA TN No. 1434, 1947.

22. Jacobs, Eastman N., Ward, Kenneth E., and Pinkerton, Robert M.: The Characteristics of 78 Related Airfoil Sections from Tests in the Variable-Density Wind Tunnel. NACA Rep. No. 460, 1933.

23. Frick, Charles W., Jr., and McCullough, George B.: Tests of a Heated Low-Drag Airfoil. NACA ACR, Dec. 1942.

24. Abbot, Ira H., von Doenhoff, Albert E., and Stivers, Louis S., Jr.: Summary of Airfoil Data. NACA ACR, Mar. 1945.

25. Gardner, Tracy B.: Investigation of Runback. Air Materiel Command Ice Research Base Rep. No. IRB 46-36-1F, July 1946.

26. Neel, Carr B., Jr.: An Investigation of a Thermal Ice-Prevention System for a C-46 Cargo Airplane. I - Analysis of the Thermal Design for Wings, Empennage, and Windshield. NACA ARR No. 5A03, 1945.

TABLE I.- METEOROLOGICAL AND FLIGHT CONDITIONS FOR WHICH CORRESPONDING DATA WERE OBTAINED FOR THE NACA 0012 ELECTRICALLY HEATED AIRFOIL MODEL DURING FLIGHT IN NATURAL-ICING CONDITIONS

Icing condition	Flight number	Pacific Standard time	Liquid-water content (gm/m^3)	Mean-effective drop diameter (microns)	Drop-size distribution*	Free-air temperature (^oF)	Pressure altitude (ft)	True airspeed (mph)	Cloud type
1	39	2:03 to 2:05	0.38	10	C	24	9100	167	Stratus
2	39	2:13 to 2:16	.41	10	C	24	8980	162	Stratus
3	39	2:19 to 2:22	.38	9	C	23	9020	160	Stratus
4	39	2:23 to 2:26	.07	5	C	24	8950	160	Stratus
5	39	2:28 to 2:31	.32	9	C	24	9010	157	Stratus
6	43	12:27 to 12:29	.58	11	C	25	10650	169	Stratus
7	49	1:25 to 1:26	1.00	16	D	11	8500	148	Cumulus

* Drop-size distributions defined in reference 17.

TABLE II.- METEOROLOGICAL AND FLIGHT CONDITIONS FOR WHICH CORRESPONDING DATA WERE OBTAINED FOR THE NACA 65,2-016 ELECTRICALLY HEATED AIRFOIL MODEL DURING FLIGHT IN NATURAL-ICING CONDITIONS

Icing condition	Flight number	Pacific Standard time	Liquid-water content (gm/m^3)	Mean-effective drop diameter (microns)	Drop-size distribution*	Free-air temperature (^oF)	Pressure altitude (ft)	True airspeed (mph)	Cloud type
1	100	3:15 to 3:19	0.26	13	D	19	10750	167	Stratocumulus
2	102	1:30 to 1:35	.34	18	E	26	11300	168	Altostratus
3	105	11:01 to 11:06	.44	13	B	19	5100	157	Stratocumulus
4	105	11:41 to 11:45	.60	13	A	19	5060	140	Stratocumulus
5	105	2:32 to 2:36	.42	19	D	21	5000	158	Stratocumulus
6	105	3:07 to 3:12	.34	22	C	20	5100	160	Stratocumulus
7	105	3:18 to 3:23	.15	13	E	20	5300	162	Stratocumulus
8	111	12:32 to 12:36	.09	16	A	16	12450	178	Stratocumulus
9	111	1:08 to 1:12	.28	29	A	13	9900	195	Stratocumulus
10	111	1:15 to 1:19	.41	30	A	14	8900	160	Stratocumulus
11	116	11:39 to 11:40	.12	17	B	25	11460	185	Altocumulus
12	116	11:45 to 11:46	.12	16	B	26	11100	184	Altocumulus
13	116	11:58 to 11:59	.11	15	B	26	11100	165	Altocumulus
14	117	12:31 to 12:32	.35	13	B	24	11100	180	Altostratus
15	117	1:13 to 1:14	.17	12	B	26	10540	165	Altostratus

*Drop-size distributions defined in reference 17.

TABLE III.- COMPARISON OF CALCULATED RATES OF WATER IMPINGEMENT AND EVAPORATION OVER THE LEADING EDGE OF THE NACA 0012 ELECTRICALLY HEATED AIRFOIL MODEL FOR ICING CONDITIONS OF TABLE I

Icing condition	Flight number	Pacific Standard time	Calculated rate of water impingement, M_s [lb/(hr)(ft.span)]	Calculated rate of water evaporation, W_s [lb/(hr)(ft.span)]
1	39	2:03 to 2:05	0.30	0.17
2	39	2:13 to 2:16	.35	.41
3	39	2:19 to 2:22	.27	.36
4	39	2:23 to 2:26	.03	.04
5	39	2:28 to 2:31	.19	.19
6	43	12:27 to 12:29	.61	.62
7	49	1:25 to 1:26	1.41	.24*

*Only leading-edge region heated. Runback formed.

TABLE IV.- COMPARISON OF CALCULATED RATES OF WATER IMPINGEMENT AND EVAPORATION OVER THE LEADING EDGE OF THE NACA 65,2-016 ELECTRICALLY HEATED AIRFOIL MODEL FOR ICING CONDITIONS OF TABLE II

Icing condition	Flight number	Pacific Standard time	Calculated rate of water-drop impingement, M_s [lb/(hr)(ft.span)]	Calculated rate of water evaporation, W_s [lb/(hr)(ft.span)]
1	100	3:15 to 3:19	0.47	0.46
2	102	1:30 to 1:35	.94	.96
3	105	11:01 to 11:06	.52	.55
4	105	11:41 to 11:45	.56	.54
5	105	2:32 to 2:36	.97	1.05
6	105	3:07 to 3:12	1.01	1.06
7	105	3:18 to 3:23	.33	.38
8	111	12:32 to 12:36	.18	.20
9	111	1:08 to 1:12	1.60	.44*
10	111	1:15 to 1:19	1.79	.51*

*Only leading-edge region heated. Runback formed.

TABLE V.– CALCULATIONS FOR DETERMINING DISTRIBUTION OF WATER-IMPINGEMENT RATE OVER THE SURFACE OF AN NACA 0012 AIRFOIL

n/m (percent)	5		10		20		30		20		10		5		- - -
a/a_{me}	0.23		0.44		0.65		1.00		1.45		2.00		2.71		- - -
a (microns)	2.9		5.5		8.1		12.5		18.1		25.0		34.0		- - -
K	0.003		0.012		0.027		0.063		0.133		0.253		0.465		- - -
s/c (percent)	C	VnC*	C	VnC	C	VnC	C	VnC	C	VnC	C	VnC	C	VnC	ΣVnC
0	0.25	0.35	0.35	0.98	0.38	2.13	0.48	4.03	0.63	3.53	0.73	2.04	0.81	1.13	14.19
.1	.15	.21	.34	.97	.37	2.11	.48	4.03	.63	3.53	.73	2.04	.80	1.12	14.01
.2	0	0	.31	.87	.37	2.07	.47	4.00	.63	3.50	.72	2.03	.79	1.11	13.58
.5	- -	- -	.15	.42	.32	1.79	.45	3.78	.60	3.38	.71	1.99	.77	1.08	13.44
.7	- -	- -	0	0	.28	1.54	.42	3.57	.58	3.26	.69	1.93	.75	1.05	11.35
1.0	- -	- -	- -	- -	.15	.84	.38	3.19	.54	3.02	.65	1.82	.71	.99	9.86
1.4	- -	- -	- -	- -	0	0	.30	2.52	.47	2.65	.59	1.65	.67	.93	7.75
2.0	- -	- -	- -	- -	- -	- -	1.14	1.18	.35	1.96	1.49	1.37	.57	.80	5.31
2.4	- -	- -	- -	- -	- -	- -	0	0	.27	1.51	.42	1.18	.51	.71	3.40
3.0	- -	- -	- -	- -	- -	- -	- -	- -	.15	.84	.33	.92	.43	.60	2.36
4.0	- -	- -	- -	- -	- -	- -	- -	- -	0	0	.20	.56	.32	.45	1.01
6.5	- -	- -	- -	- -	- -	- -	- -	- -	- -	- -	0	0	.14	.20	.20
10.8	- -	- -	- -	- -	- -	- -	- -	- -	- -	- -	- -	- -	0	0	0

*Values of V in feet per hour.

NATIONAL ADVISORY COMMITTEE FOR AERONAUTICS

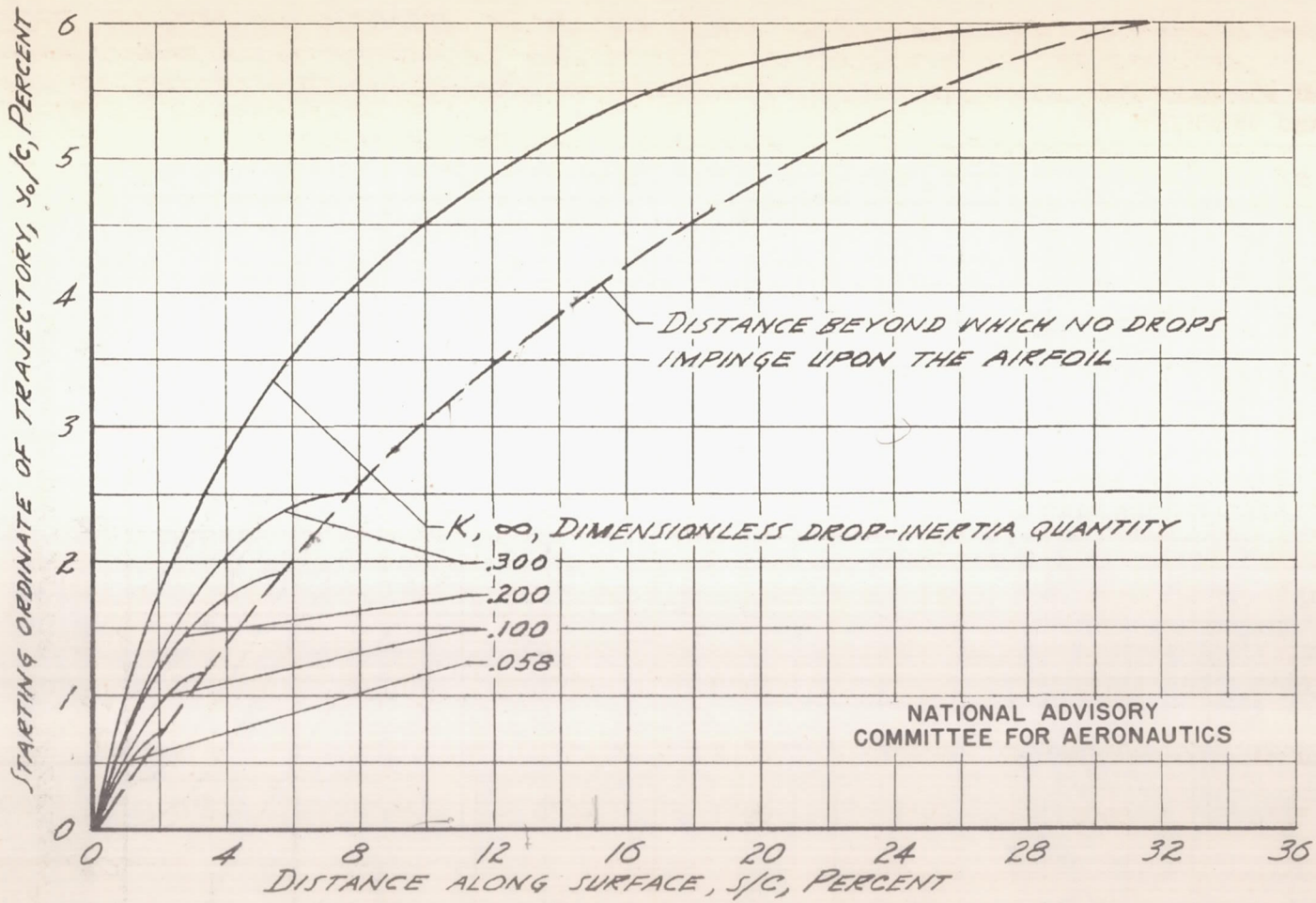

FIGURE 1.- CALCULATED AREA OF WATER-DROP IMPINGEMENT AS A FUNCTION OF DROP INERTIA FOR A 12 PERCENT-THICK SYMMETRICAL JOUKOWSKI AIRFOIL USED TO APPROXIMATE THE CONTOUR OF AN NACA 0012 SECTION AT 0° ANGLE OF ATTACK. FREE-STREAM REYNOLDS NUMBER OF DROP, R_U, 95.65.

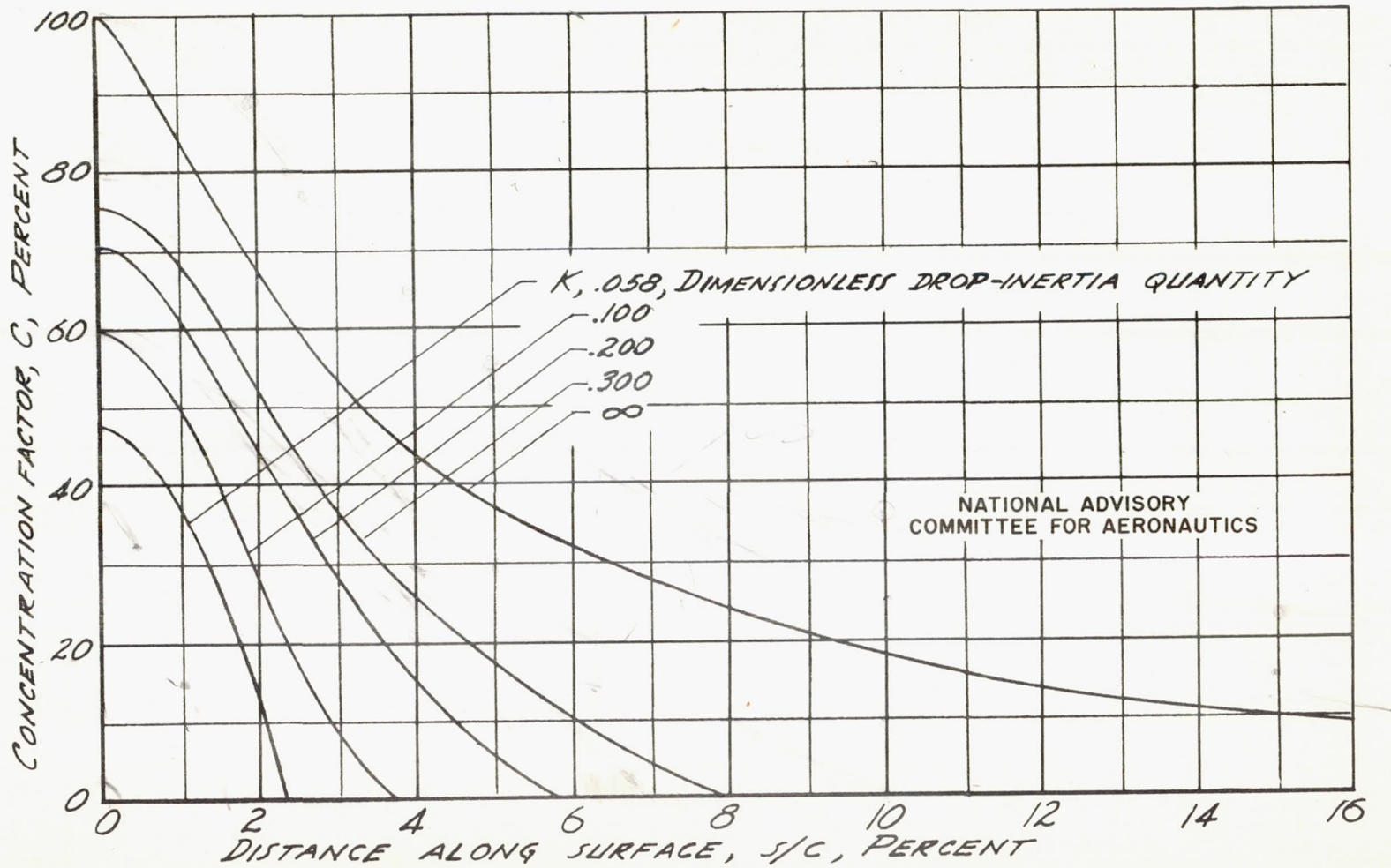

FIGURE 2.- CALCULATED WATER-DROP IMPINGEMENT DISTRIBUTION OVER THE SURFACE OF A 12 PERCENT-THICK SYMMETRICAL JOUKOWSKI AIRFOIL USED TO APPROXIMATE THE CONTOUR OF AN NACA 0012 SECTION AT 0° ANGLE OF ATTACK. FREE-STREAM REYNOLDS NUMBER OF DROP, R_d, 95.65

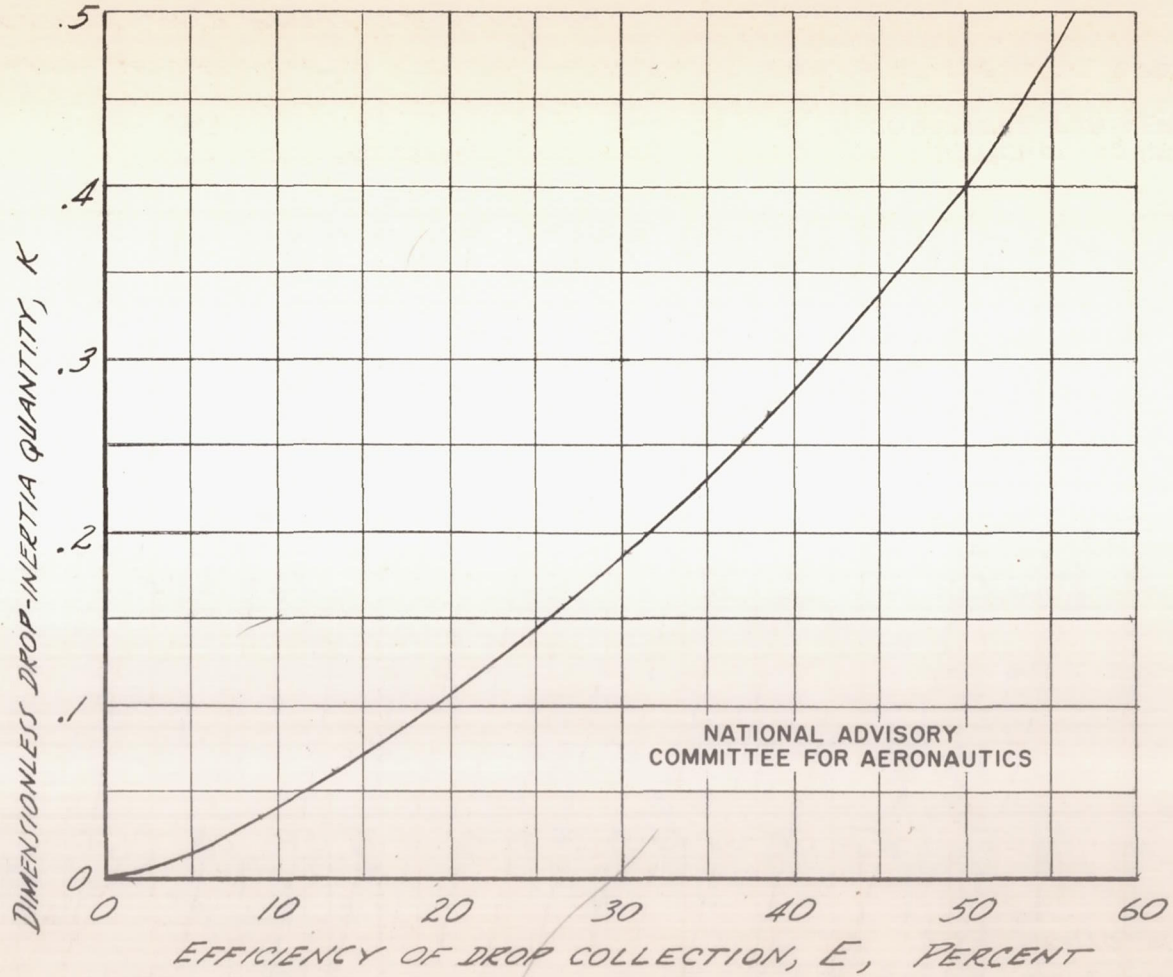

FIGURE 3.- CALCULATED WATER-DROP COLLECTION EFFICIENCY FOR A 12 PERCENT-THICK SYMMETRICAL JOUKOWSKI AIRFOIL USED TO APPROXIMATE THE CONTOUR OF AN NACA 0012 SECTION AT 0° ANGLE OF ATTACK. FREE-STREAM REYNOLDS NUMBER OF DROP, R_d, 95.65.

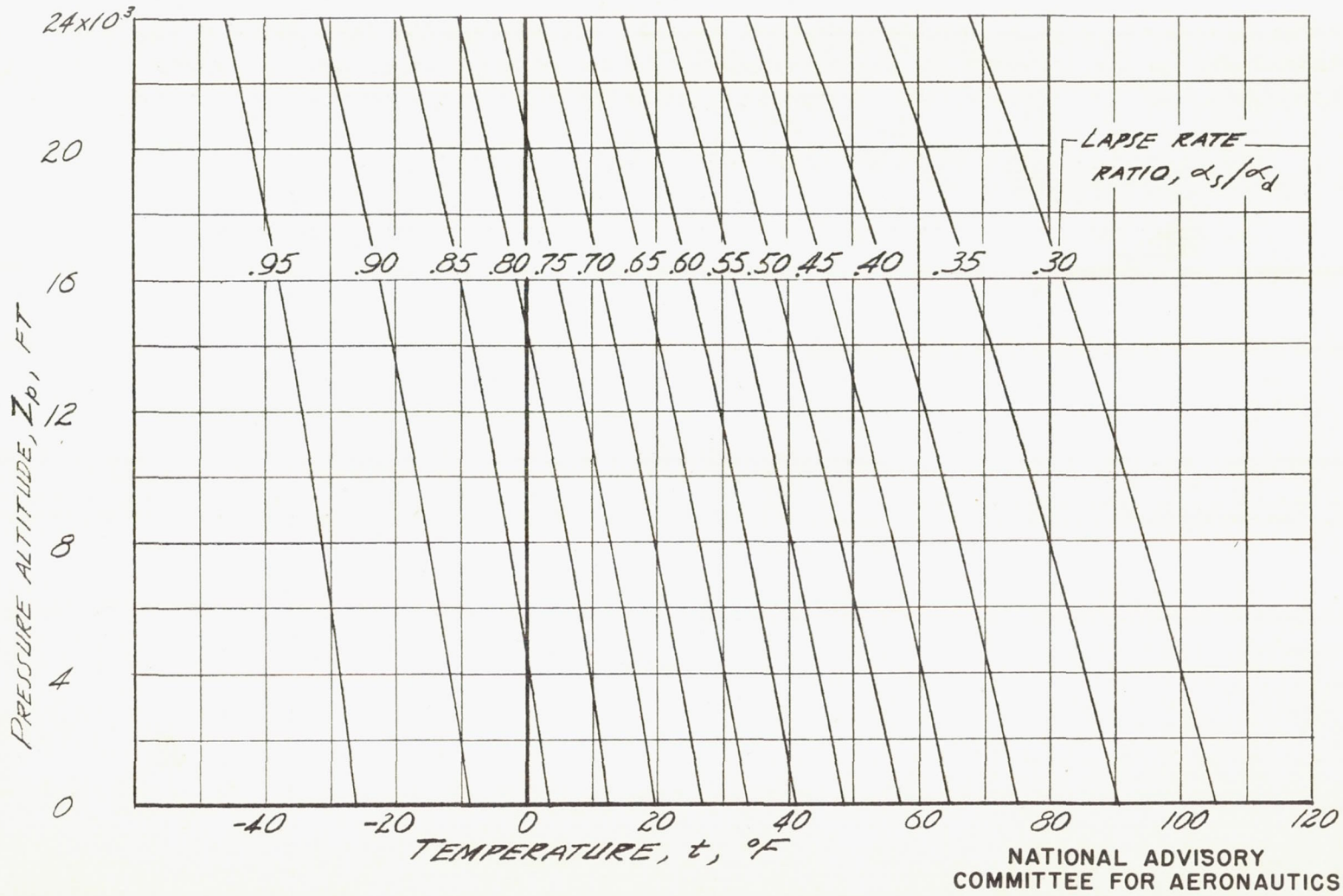

FIGURE 4.- RATIO OF SATURATED- TO DRY-ADIABATIC LAPSE RATES AS A FUNCTION OF TEMPERATURE AND PRESSURE ALTITUDE.

Figure 5.- C-46 test airplane as flown during the winter of 1946-47 showing the position of the airfoil models mounted on the fuselage.

(a) NACA 0012 section mounted on C-46 fuselage for the 1945-46 flight tests.

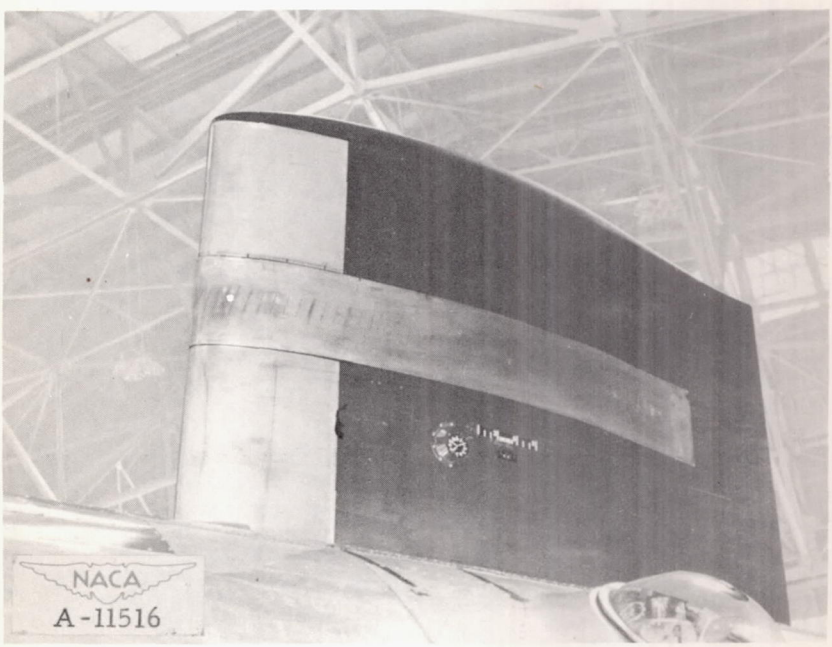

(b) NACA 65,2-016 section mounted on C-46 fuselage for 1946-47 flight tests.

Figure 6.- Electrically heated airfoil models used to obtain data in natural-icing conditions.

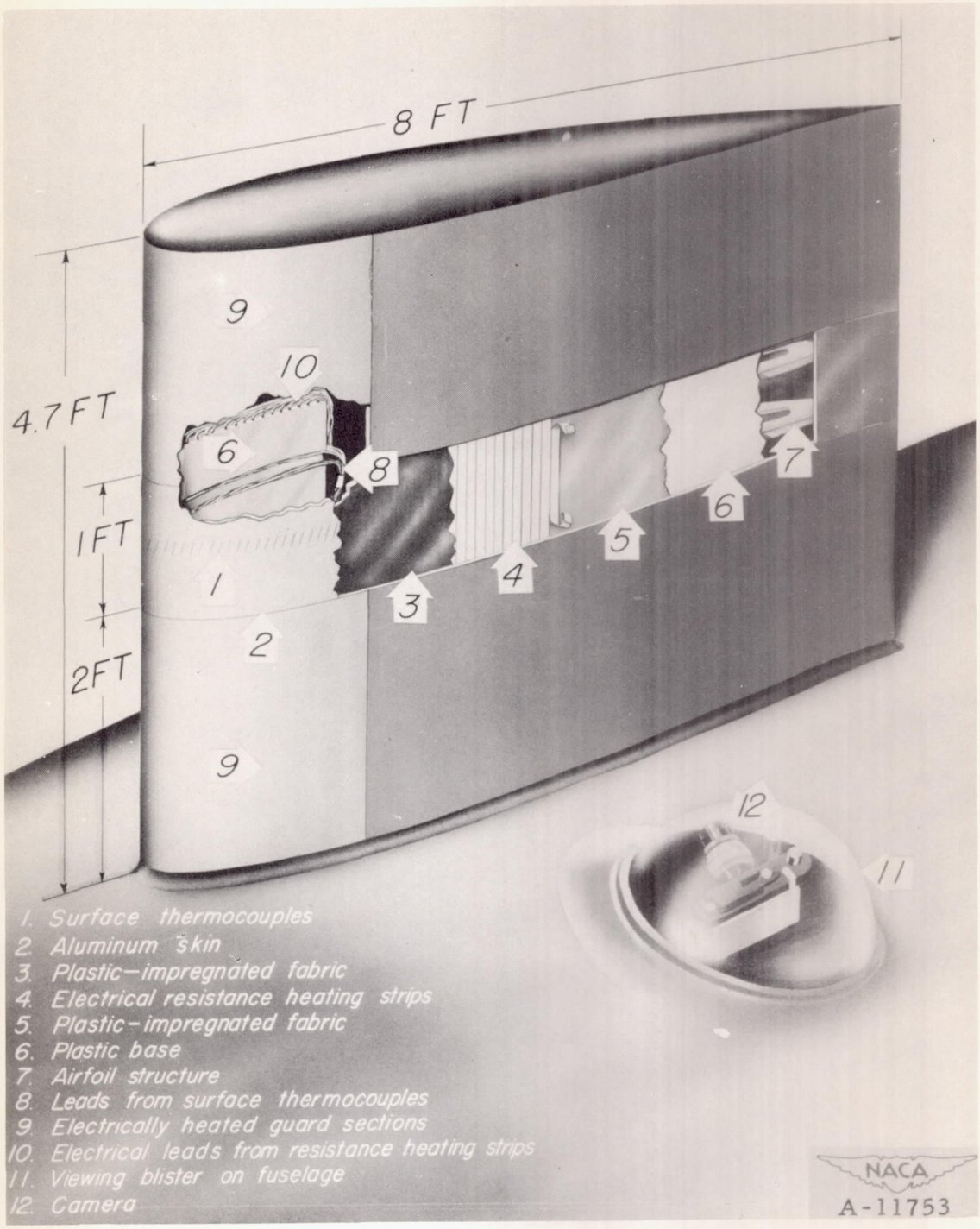

Figure 7.- Cut-away view of the NACA 65,2-016 electrically heated airfoil model showing construction details.

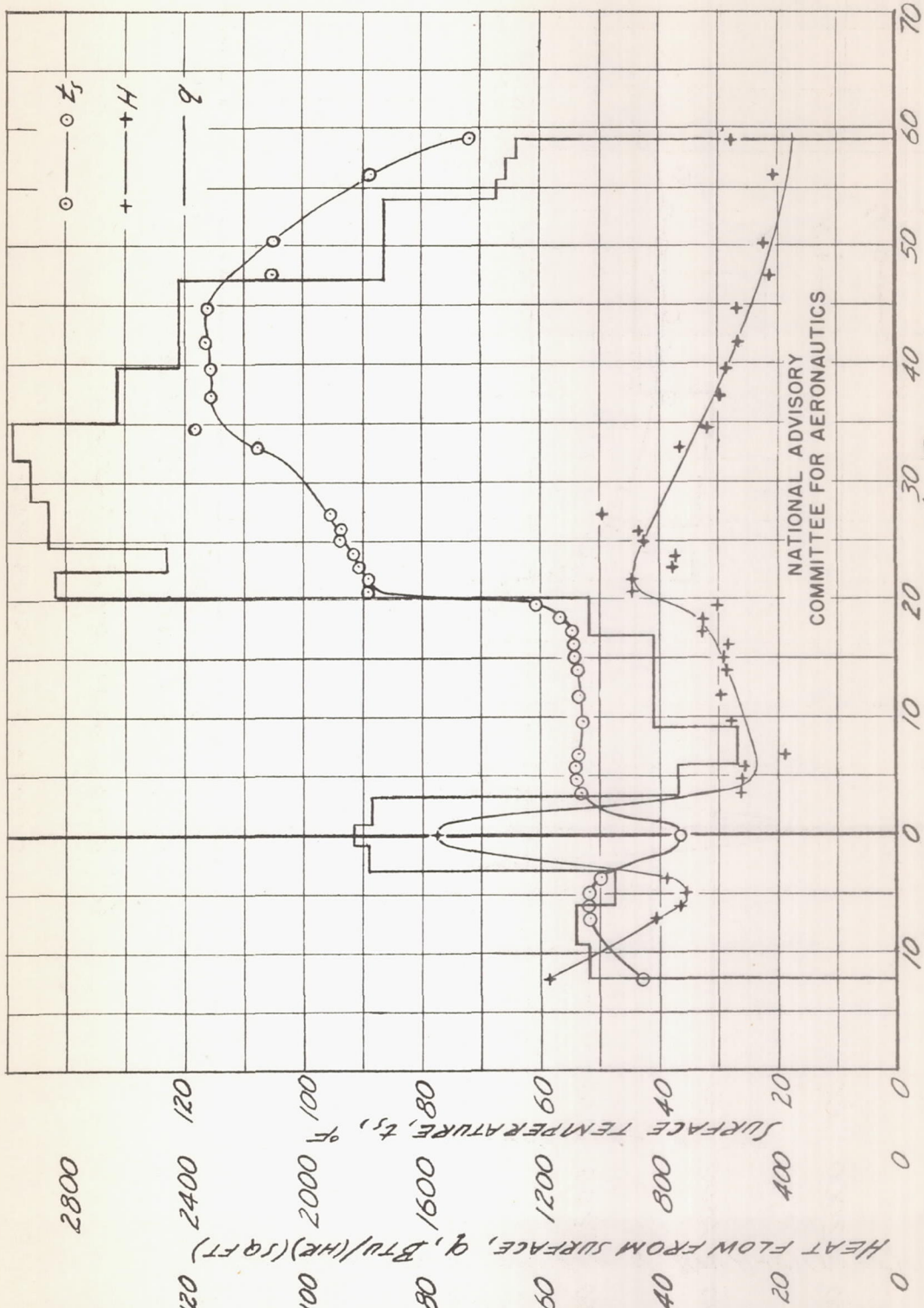

FIGURE 8.- THERMAL DATA OBTAINED WITH THE NACA 0012 ELECTRICALLY HEATED AIRFOIL MODEL.
(a) ICING CONDITION I. TABLE I.

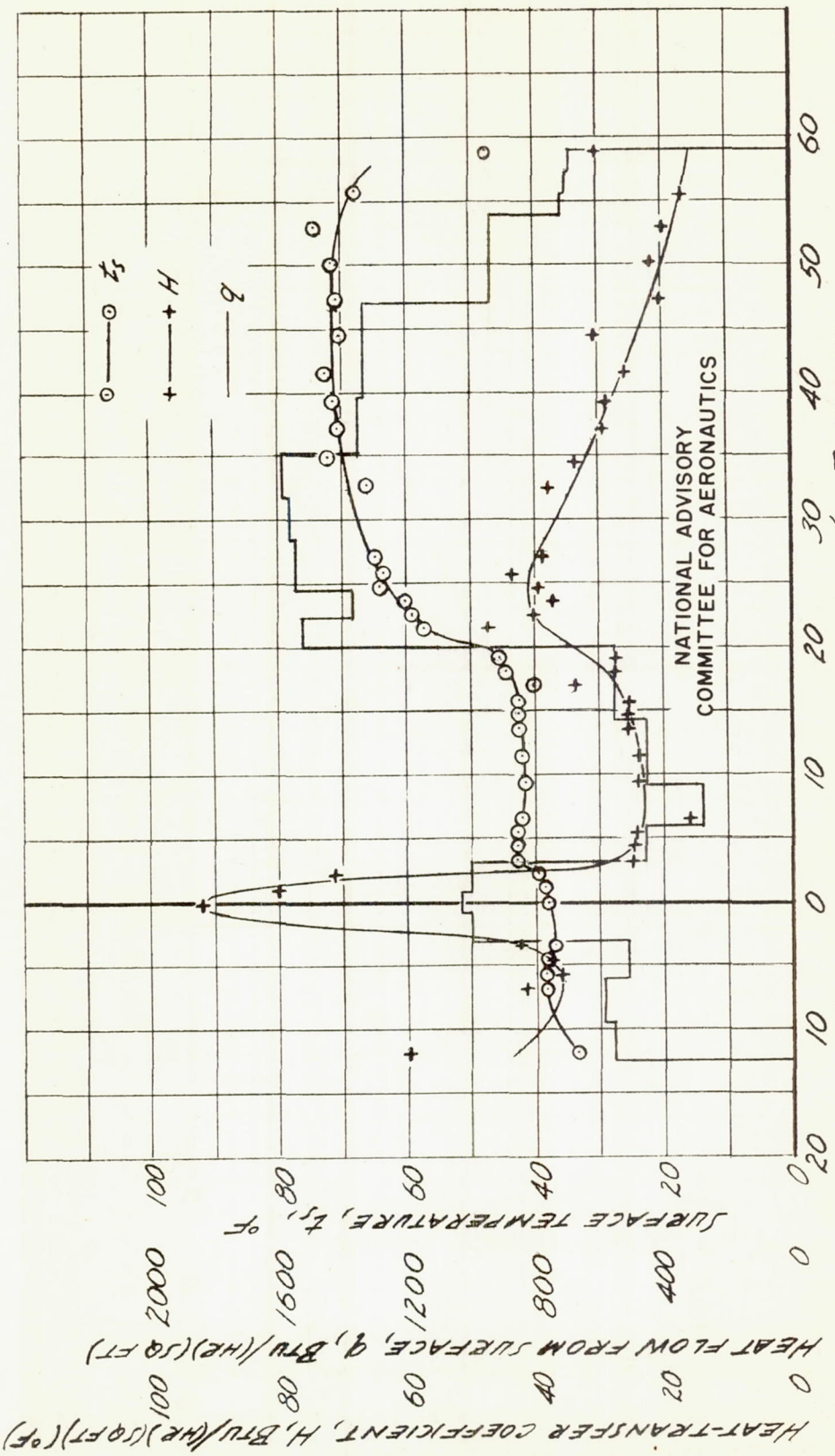

FIGURE 8.- CONTINUED.

(6) ICING CONDITION 2. TABLE I.

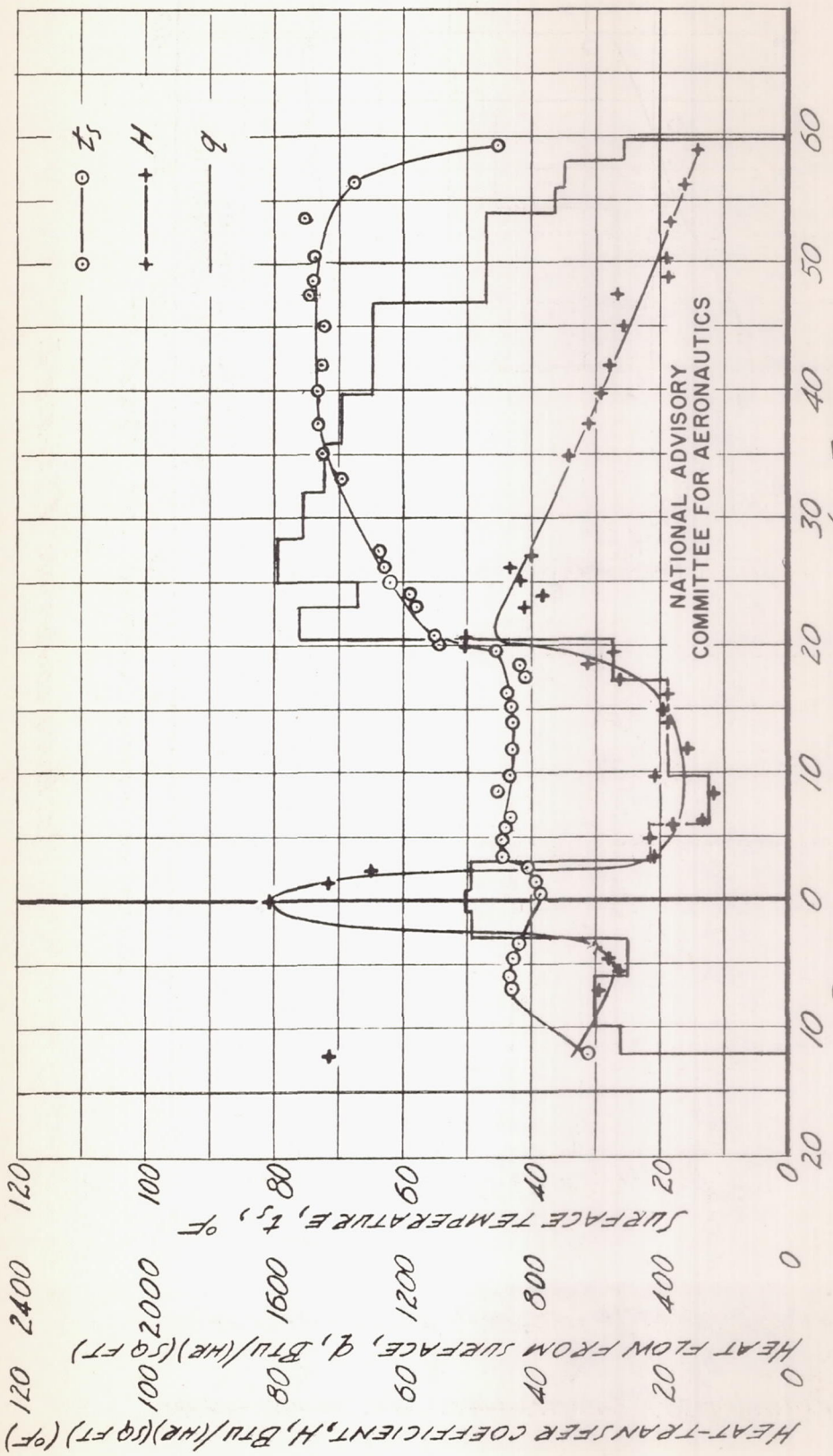

(c) Icing condition 3. Table I.

Figure 8.- Continued.

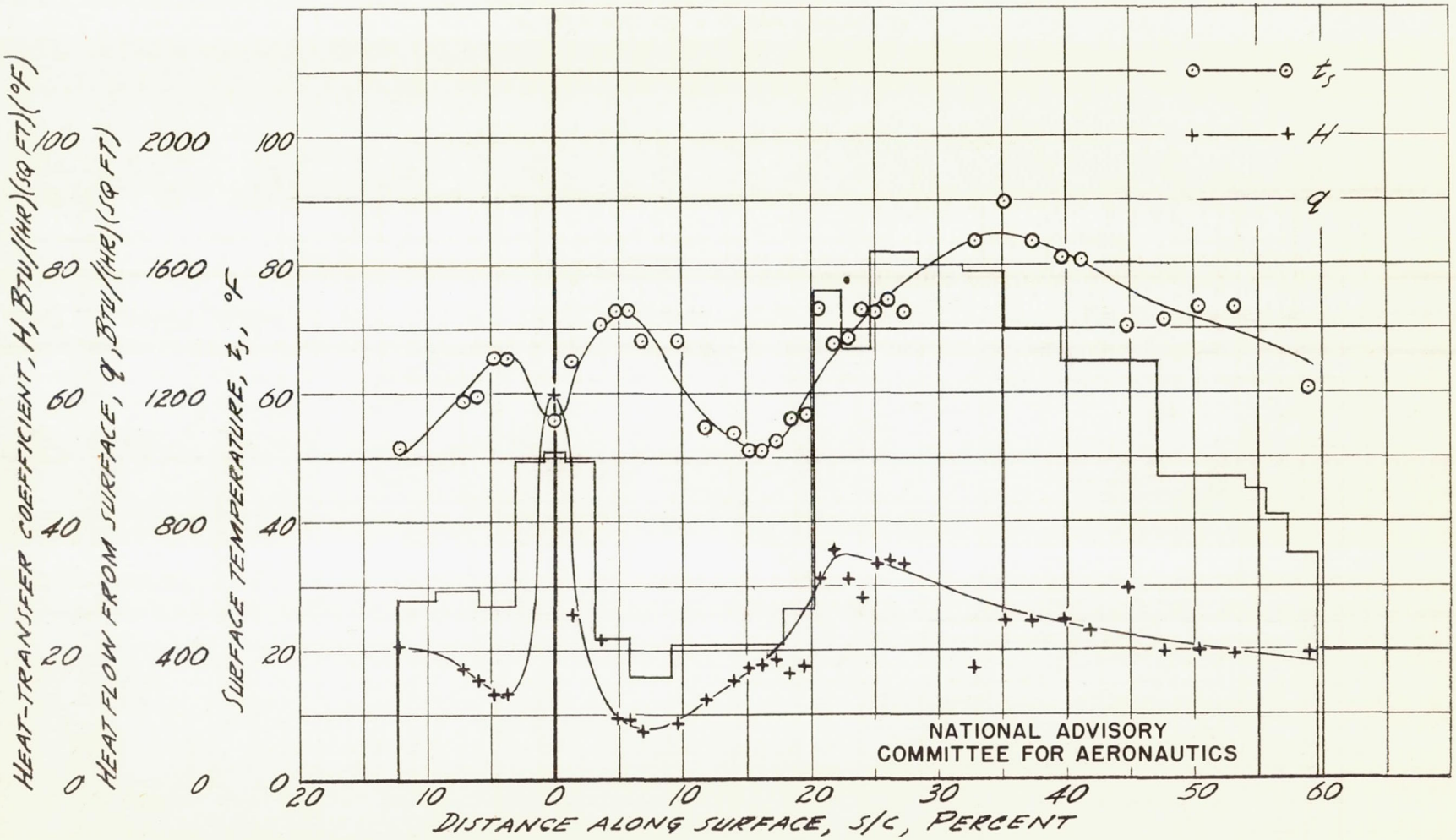

(d) Icing condition 4. Table I.

FIGURE 8. - CONTINUED.

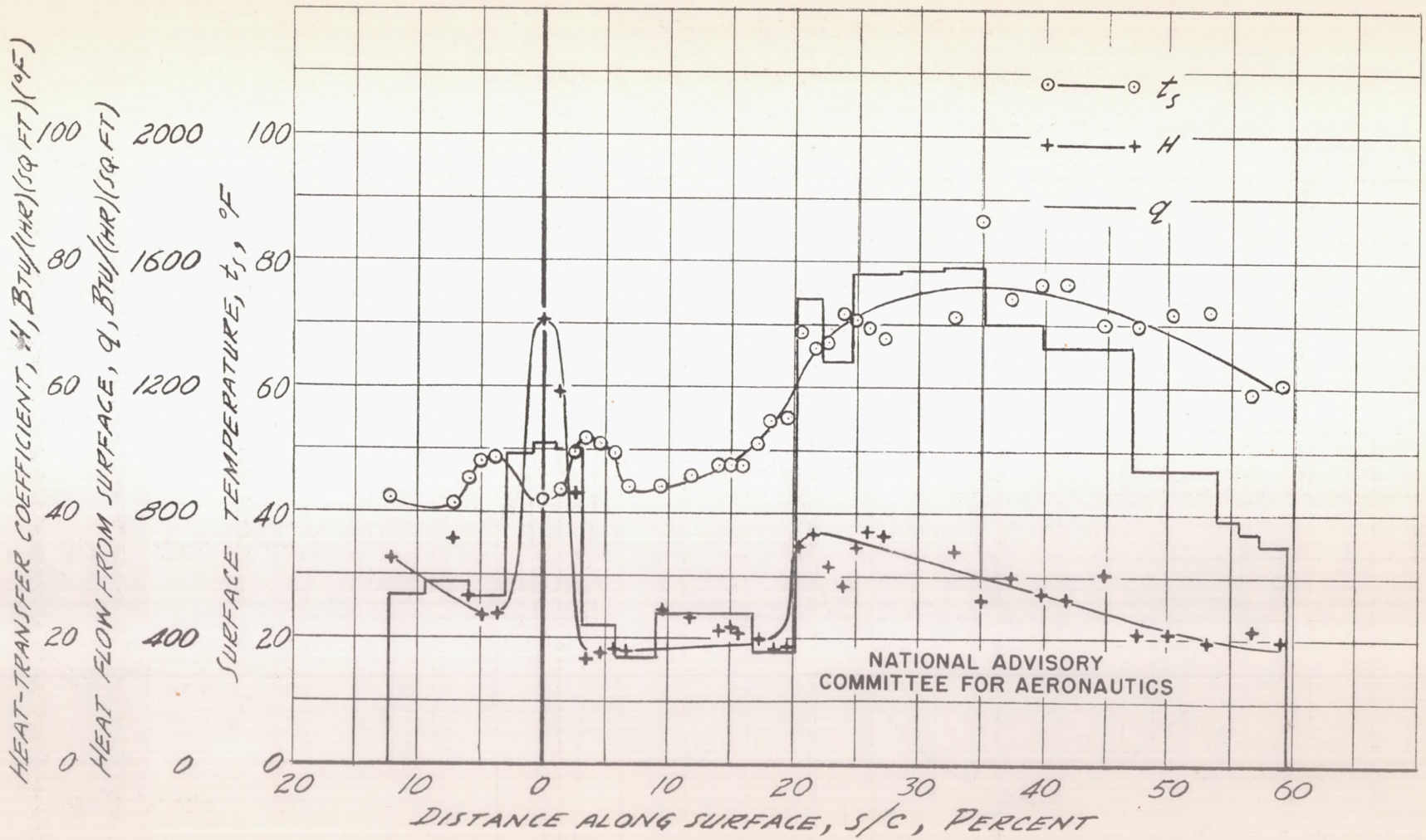

(c) Icing condition 5. Table I

Figure 8.- Continued.

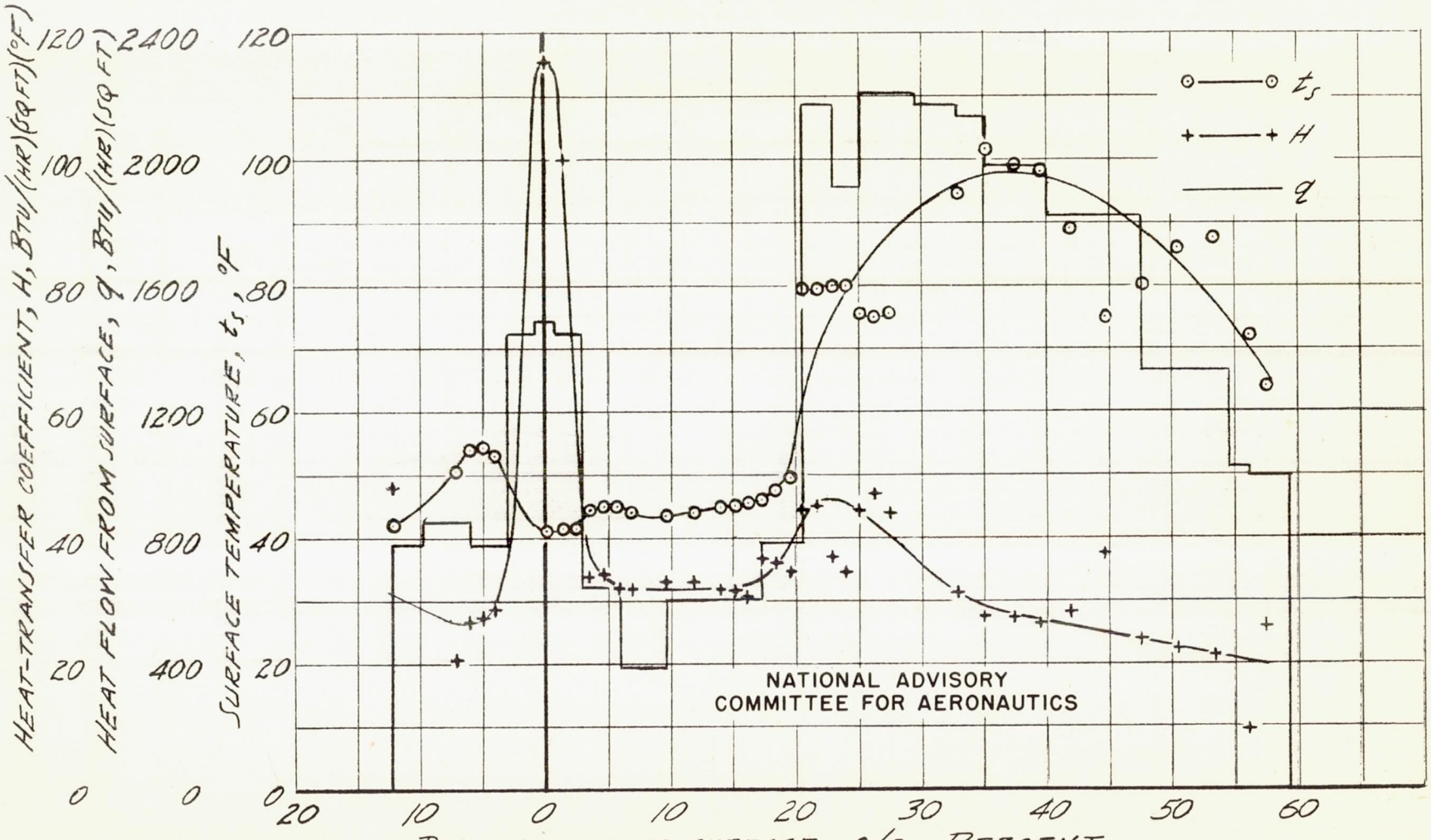

(f) Icing condition 6. Table I.

FIGURE 8.- CONTINUED.

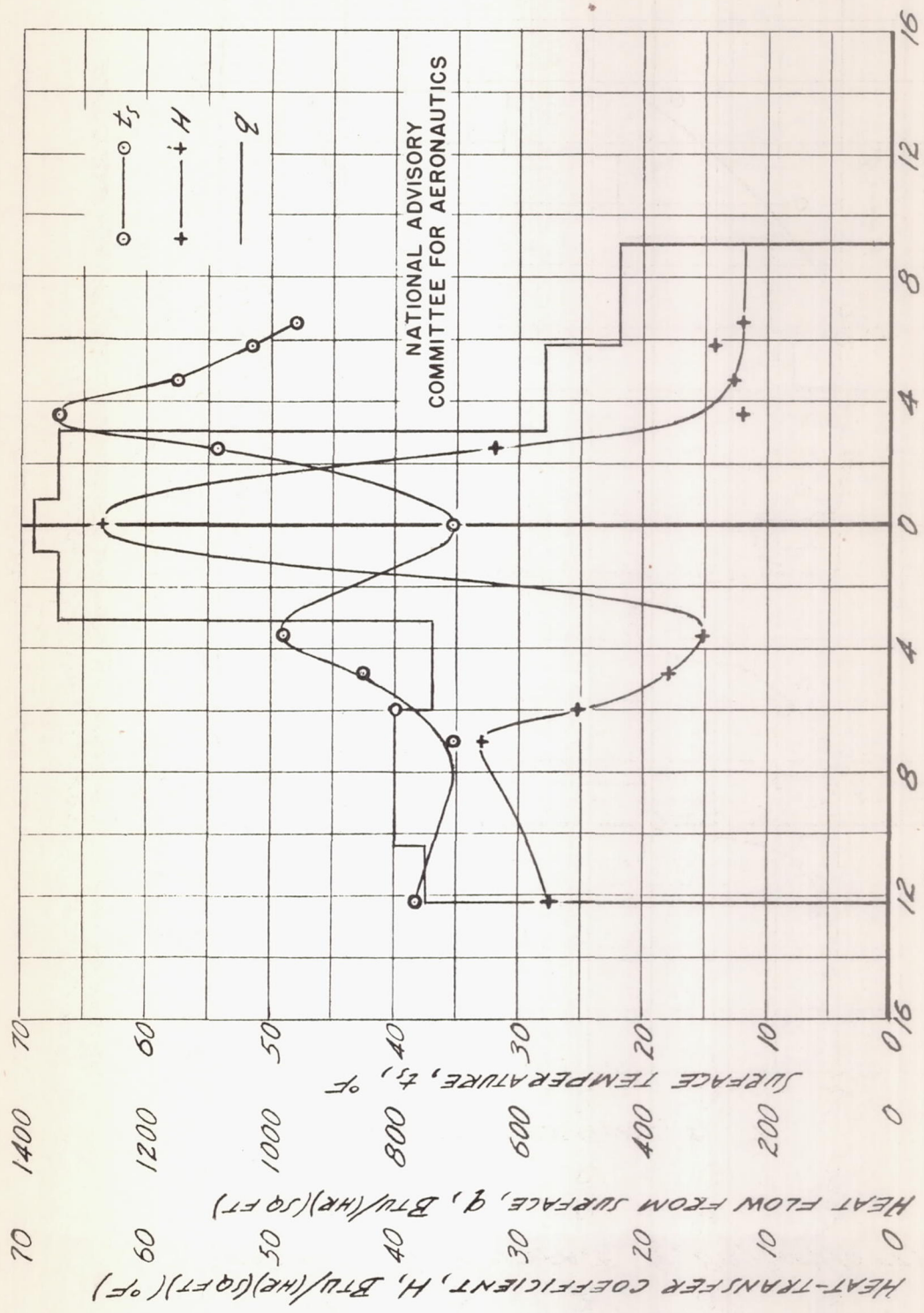

(g) Icing condition 7. Table I.

Figure 8. - Continued.

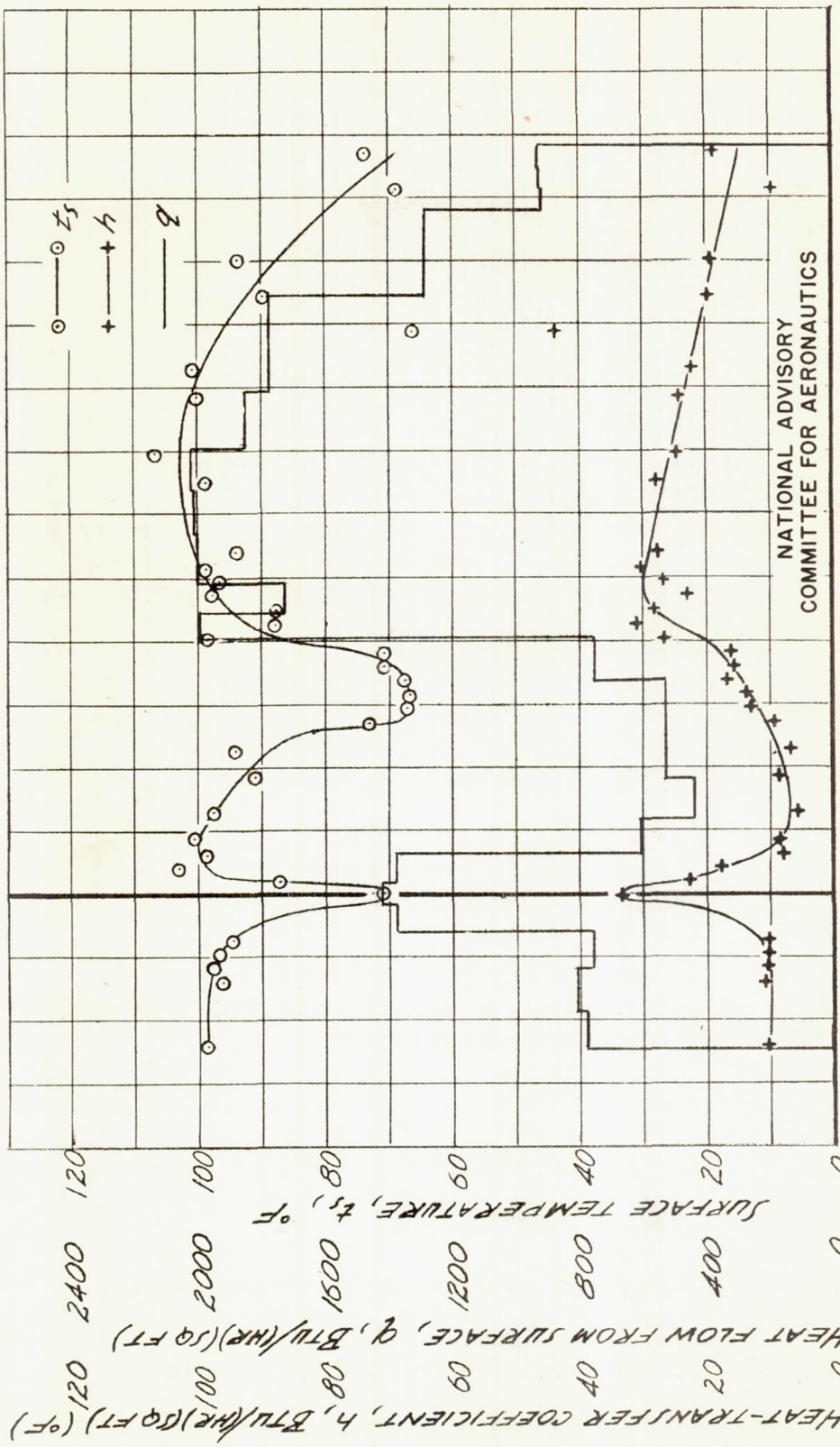

(h) CLEAR-AIR CONDITION. FREE-AIR TEMPERATURE, 23°F; PRESSURE ALTITUDE, 12,300 FT.; TRUE AIRSPEED, 125 MPH.

FIGURE 8.- CONCLUDED.

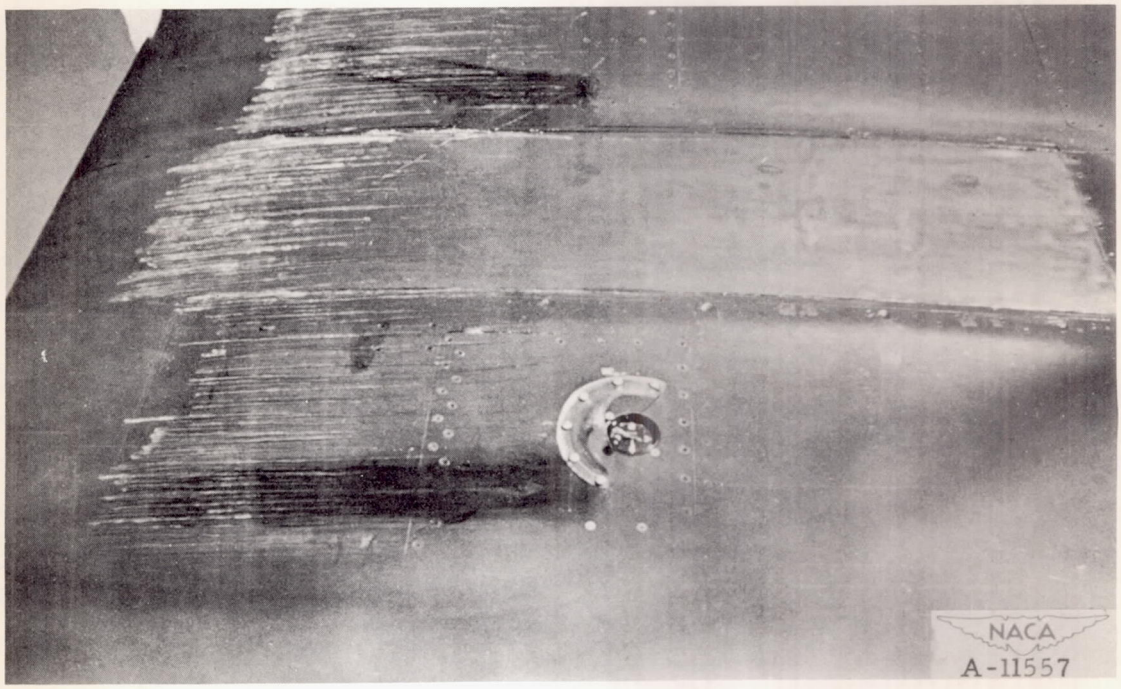

Figure 9.- Typical runback formation obtained on the NACA 0012 airfoil model with only leading-edge region heated.

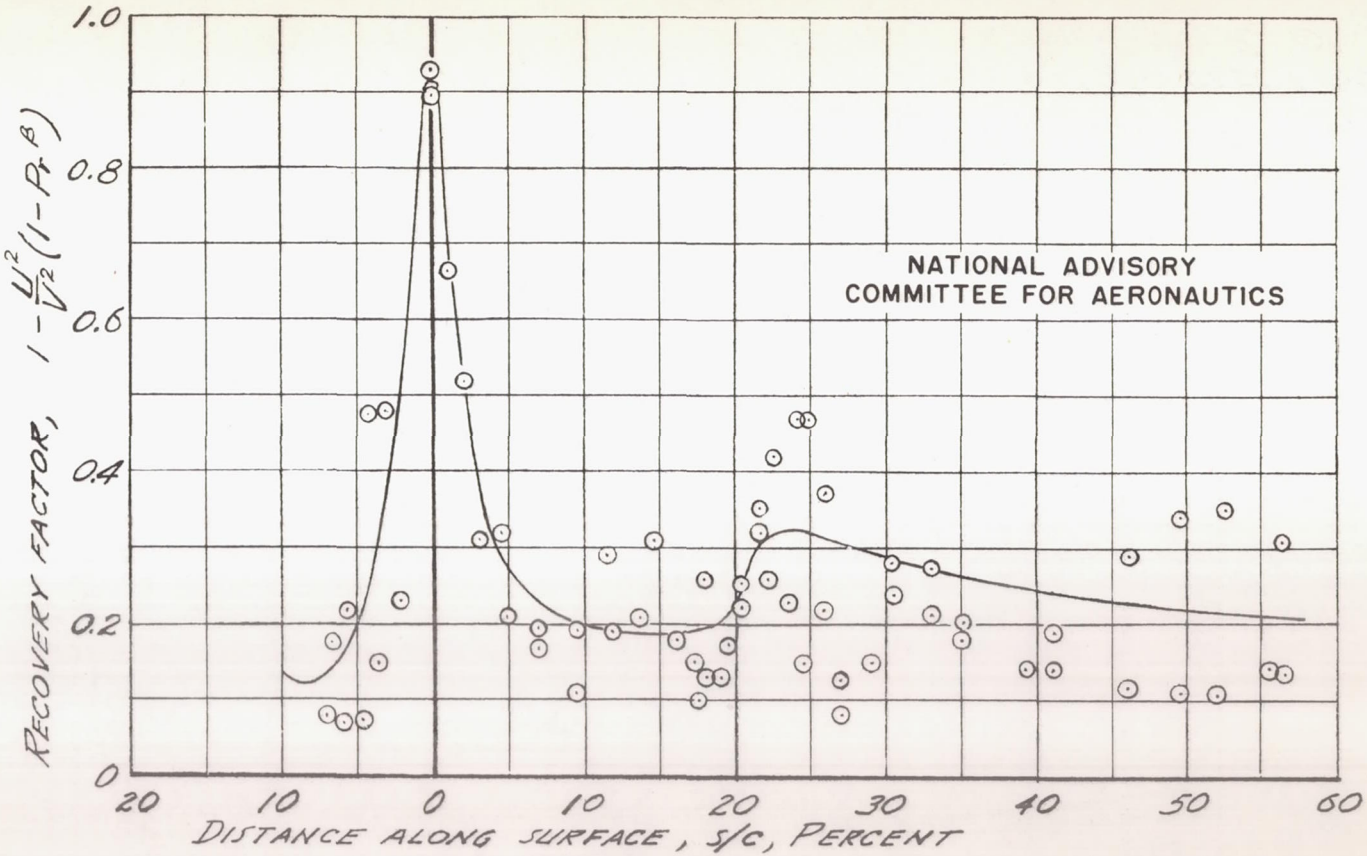

FIGURE 10.- MEASURED CLEAR-AIR RECOVERY FACTOR OVER THE NACA 0012 AIRFOIL SECTION

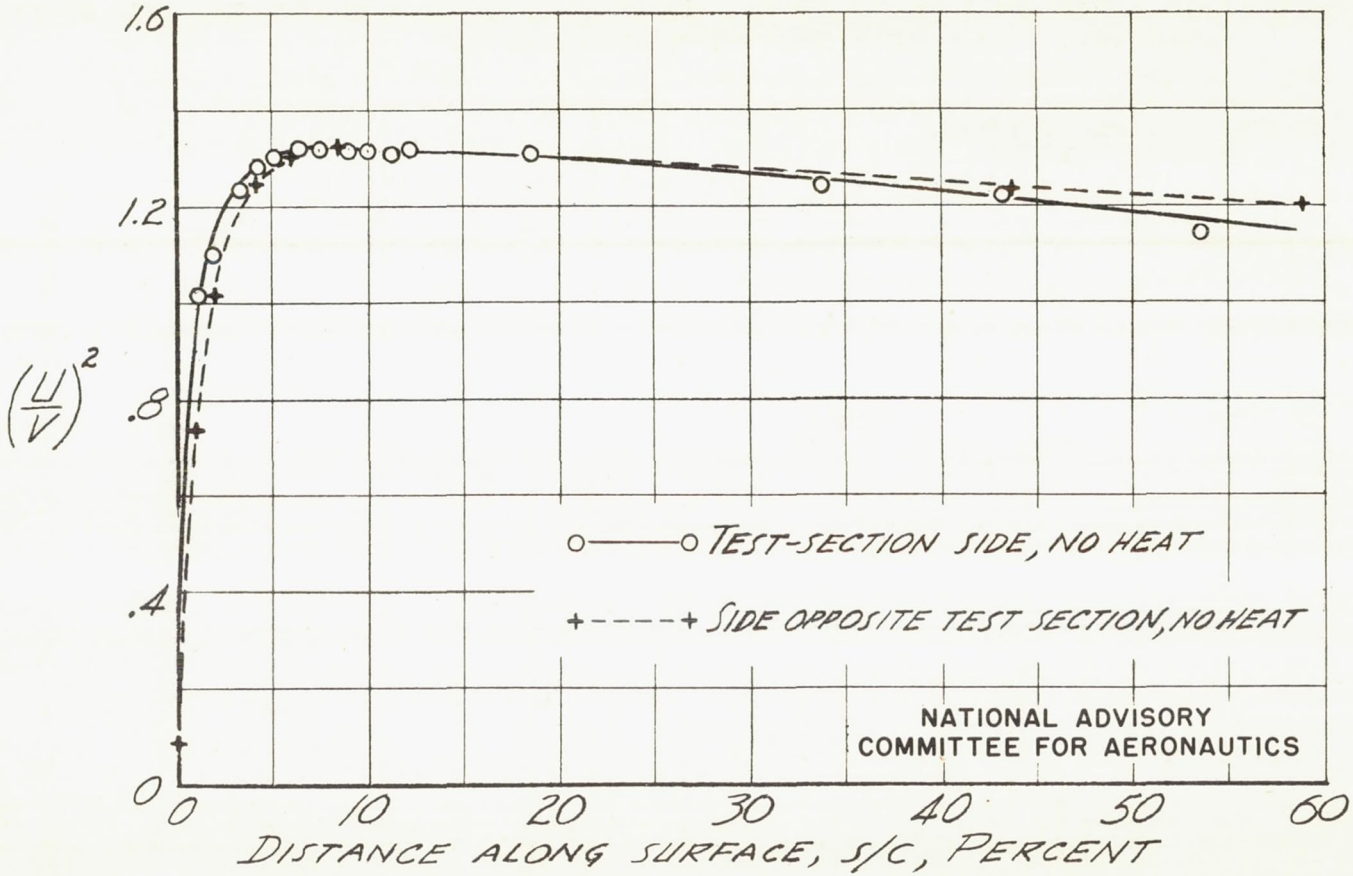

Figure 11.- Pressure distribution over the NACA 0012 electrically heated airfoil section in clear air. Angle of attack, 0°; R_c, 10^7.

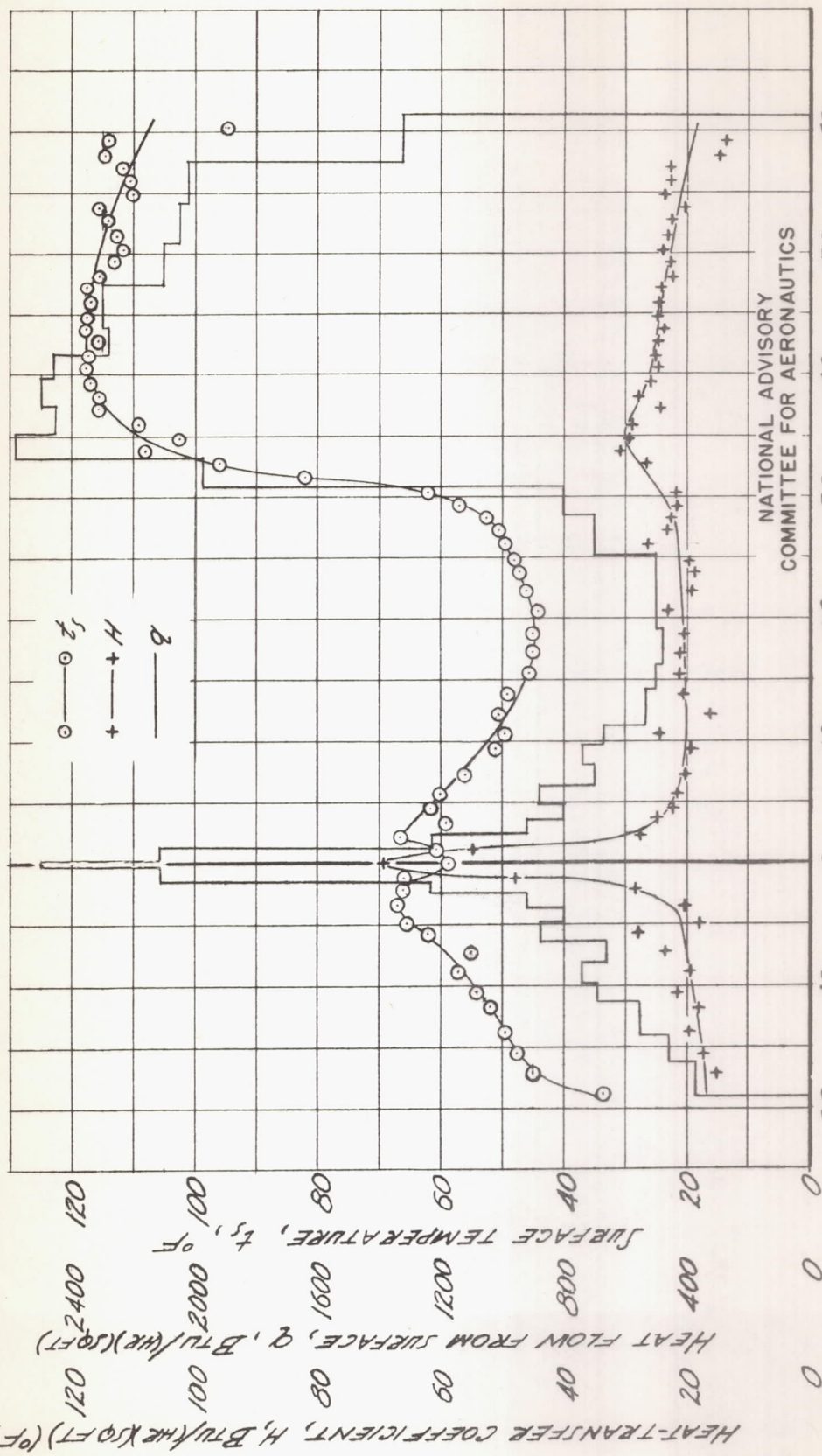

FIGURE 12.- THERMAL DATA OBTAINED WITH THE NACA 65,2-015 ELECTRICALLY HEATED AIRFOIL MODEL.

(a) ICING CONDITION 1. TABLE II.

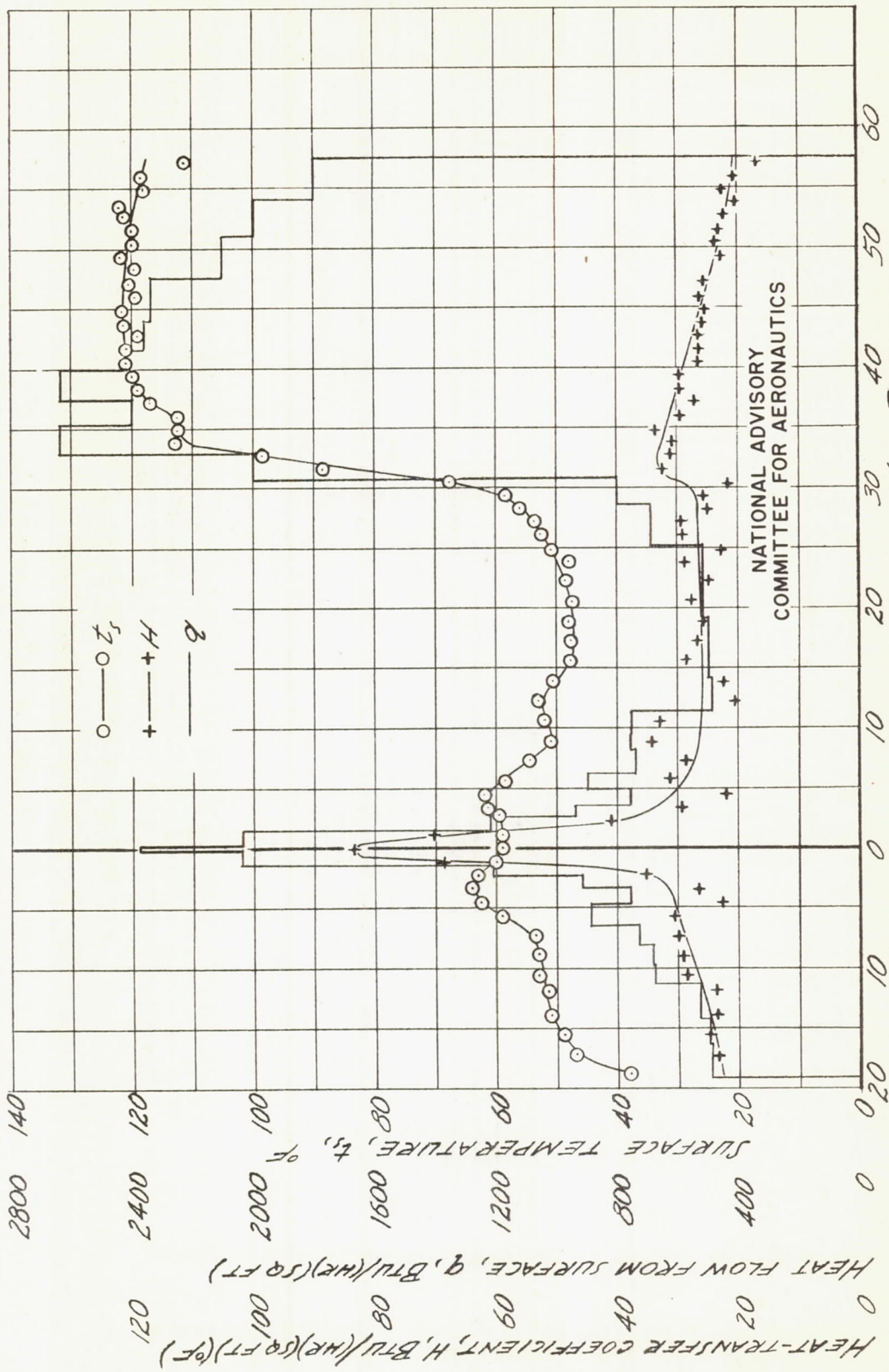

(b) Icing condition 2. Table II

FIGURE 12. - CONTINUED.

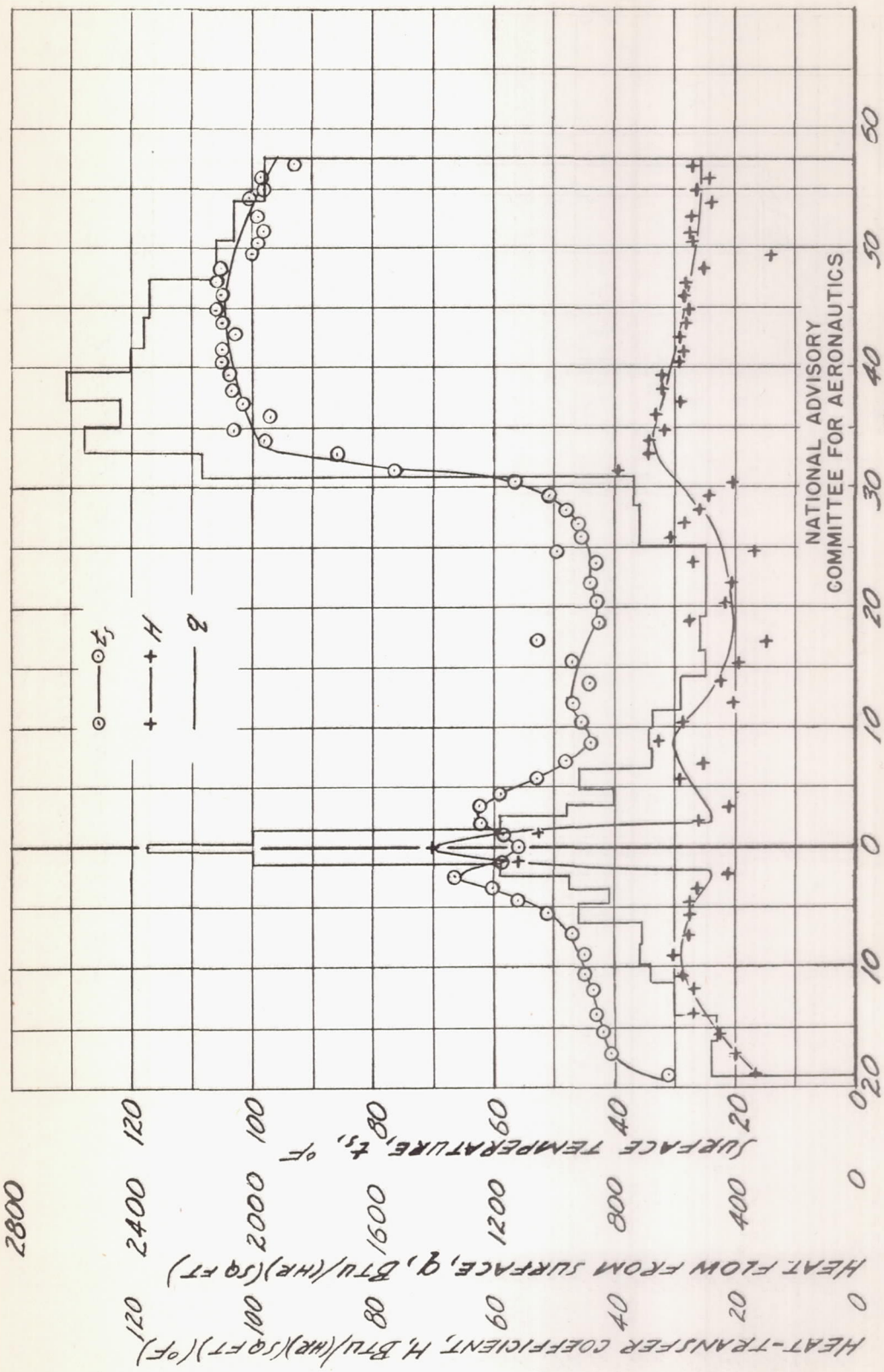

FIGURE 12.- CONTINUED.

(c) ICING CONDITION 3. TABLE II.

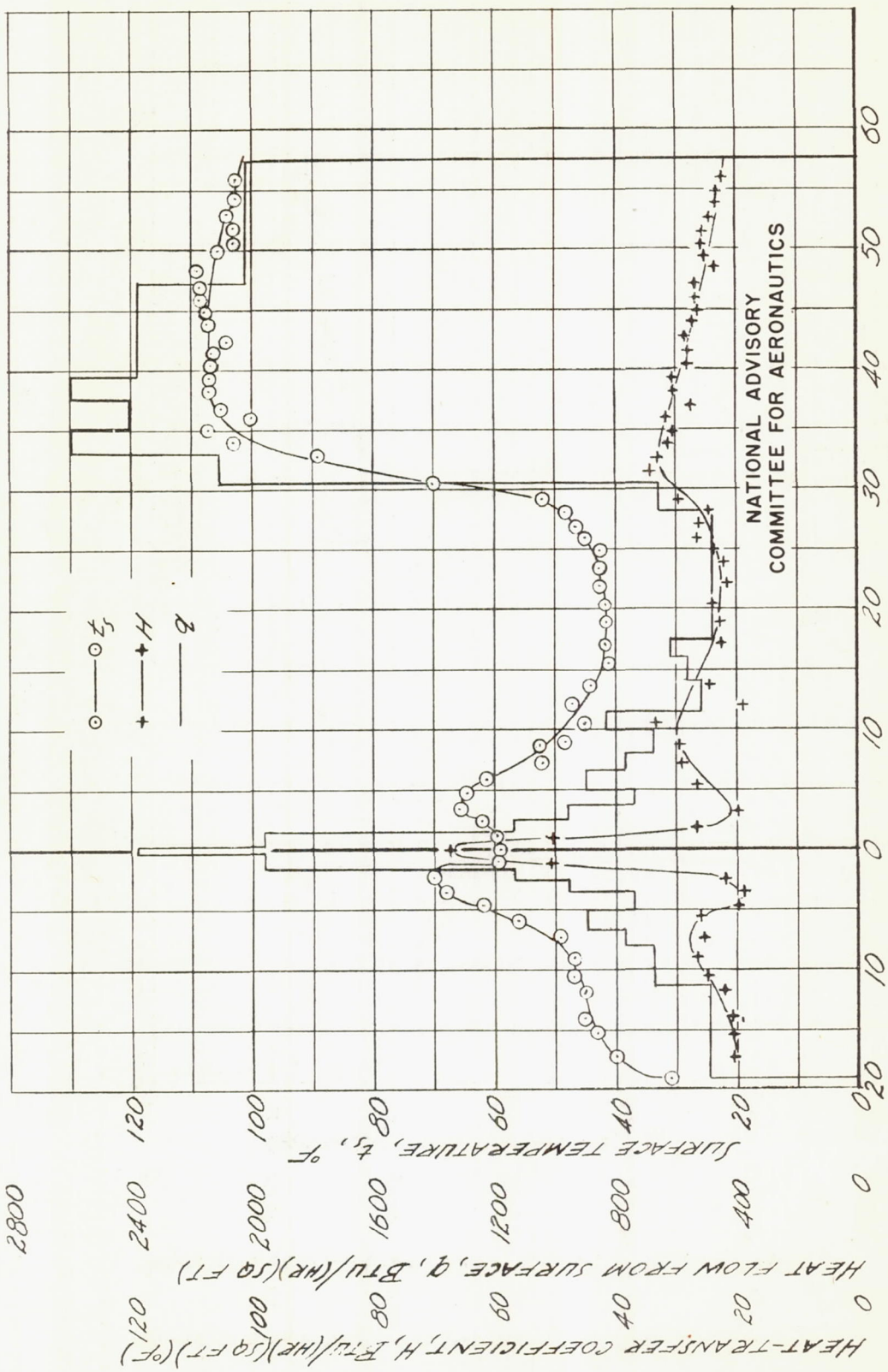

FIGURE 12.- CONTINUED
(d) ICING CONDITION 4, TABLE II.

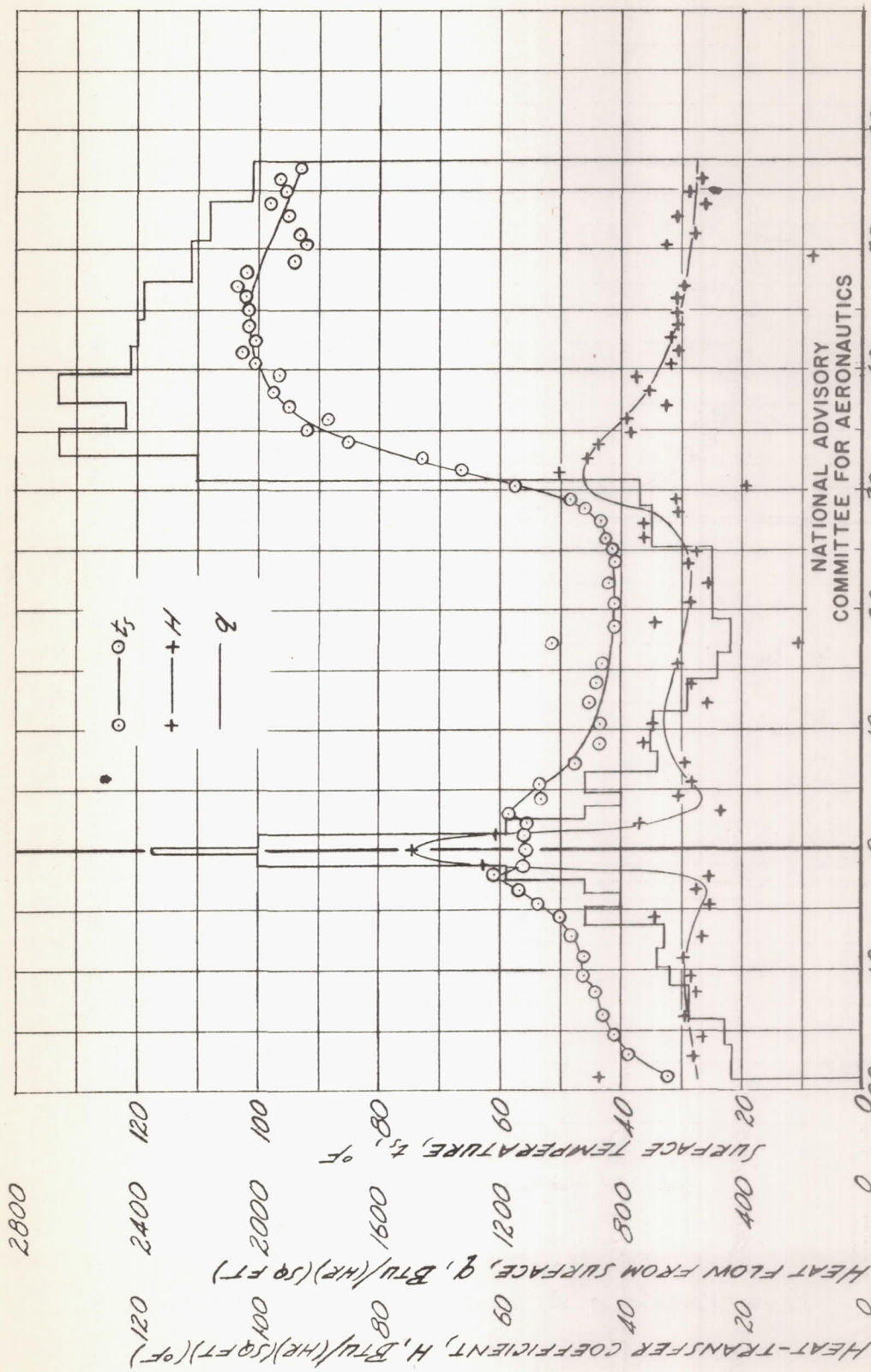

(e) Icing condition 5. Table II.

Figure 12. - Continued.

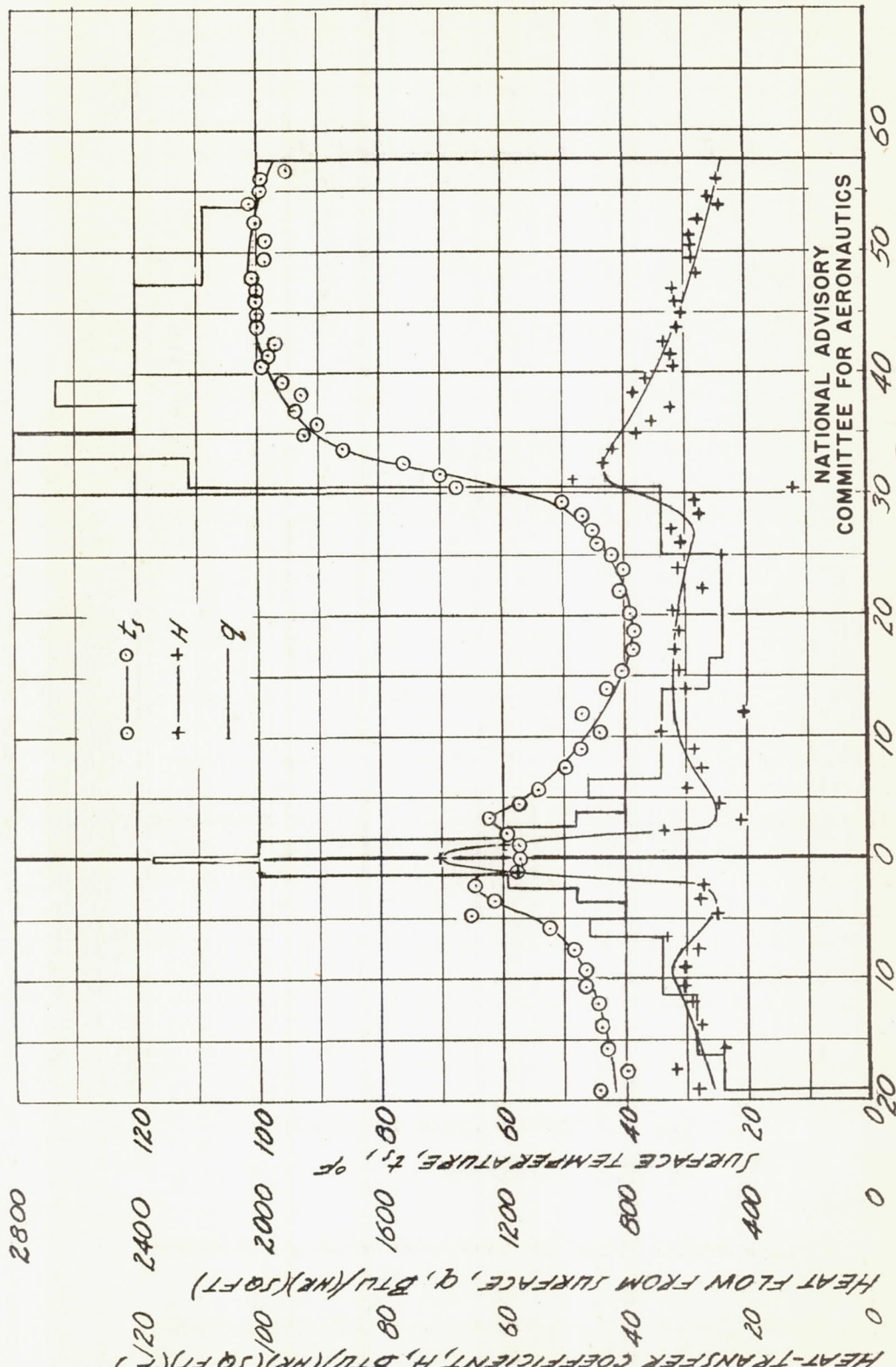

FIGURE 12.- CONTINUED.

(f) ICING CONDITION 6. TABLE II.

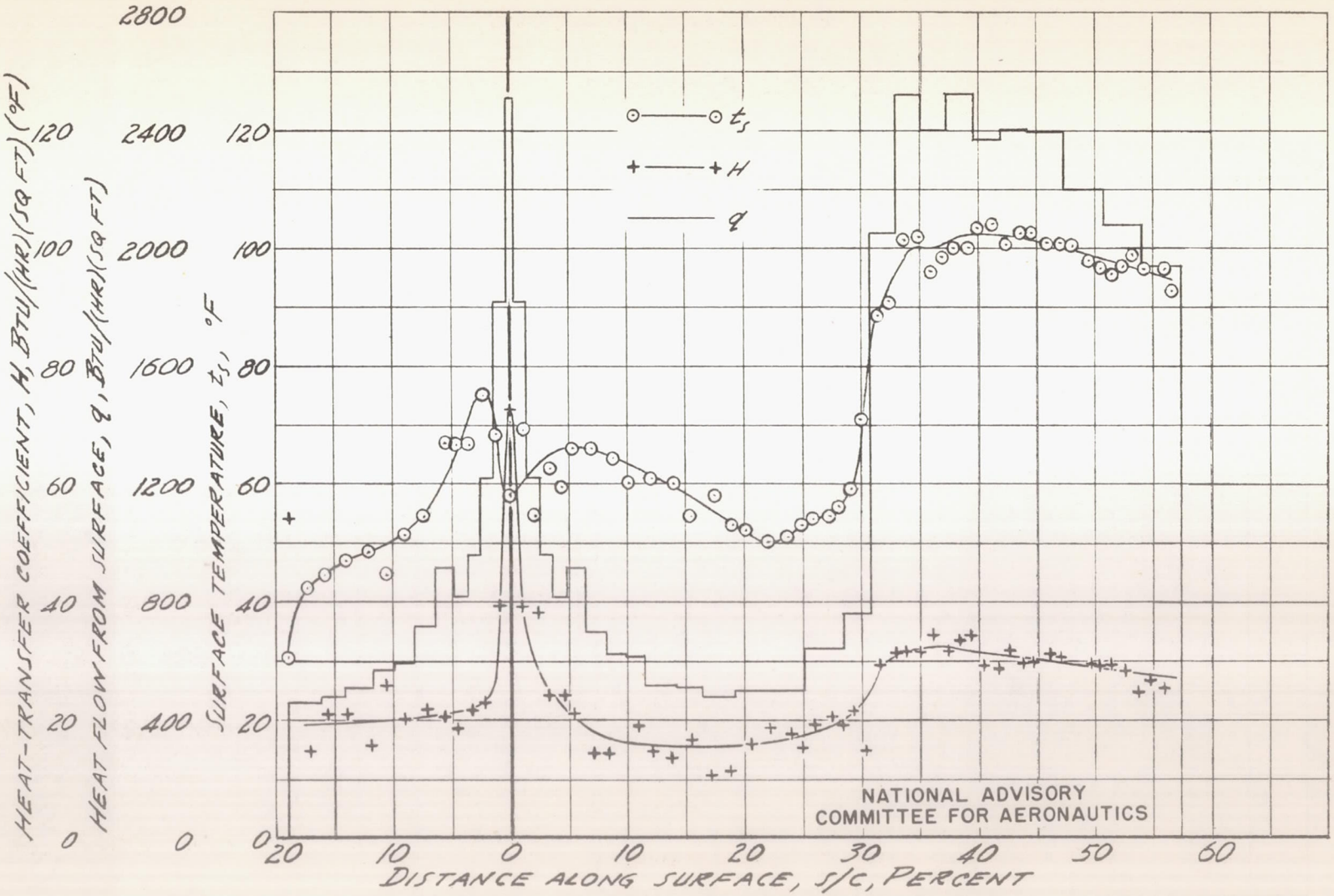

(g) Icing condition 7. Table II.

FIGURE 12. - CONTINUED.

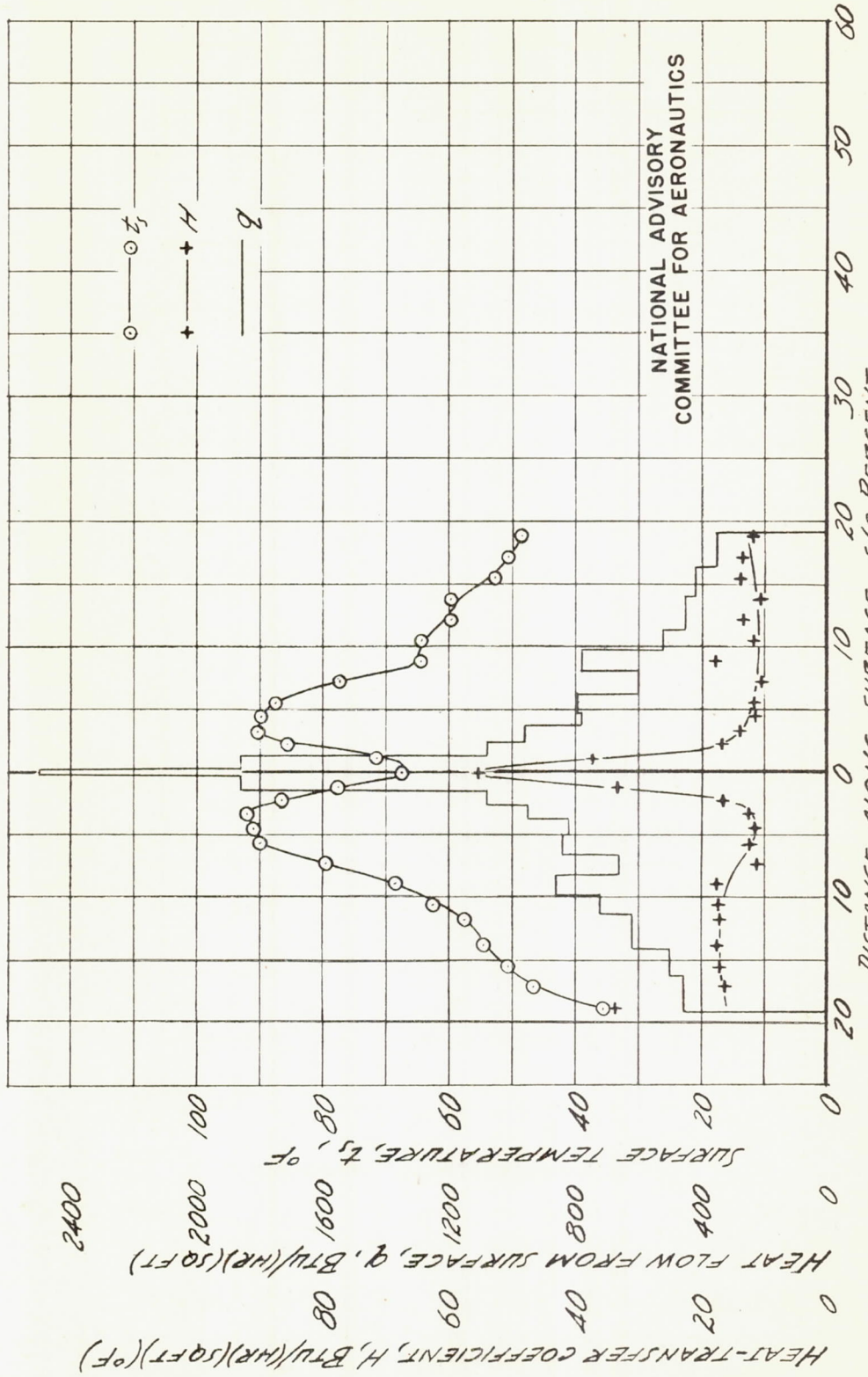

(h) Icing condition 8. Table II.

FIGURE 12.-CONTINUED.

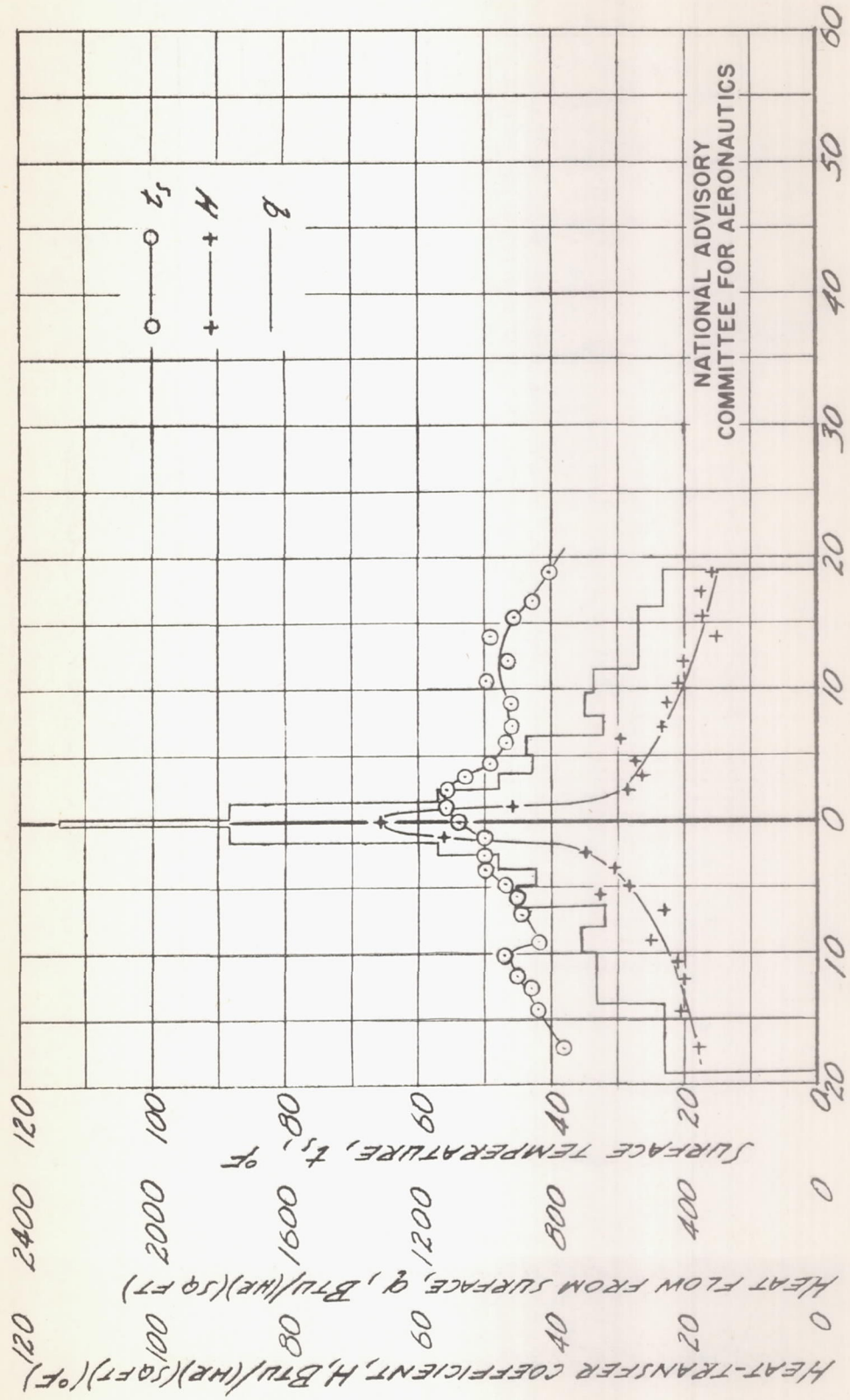

(i) Icing condition 9. Table II.

Figure 12.- Continued.

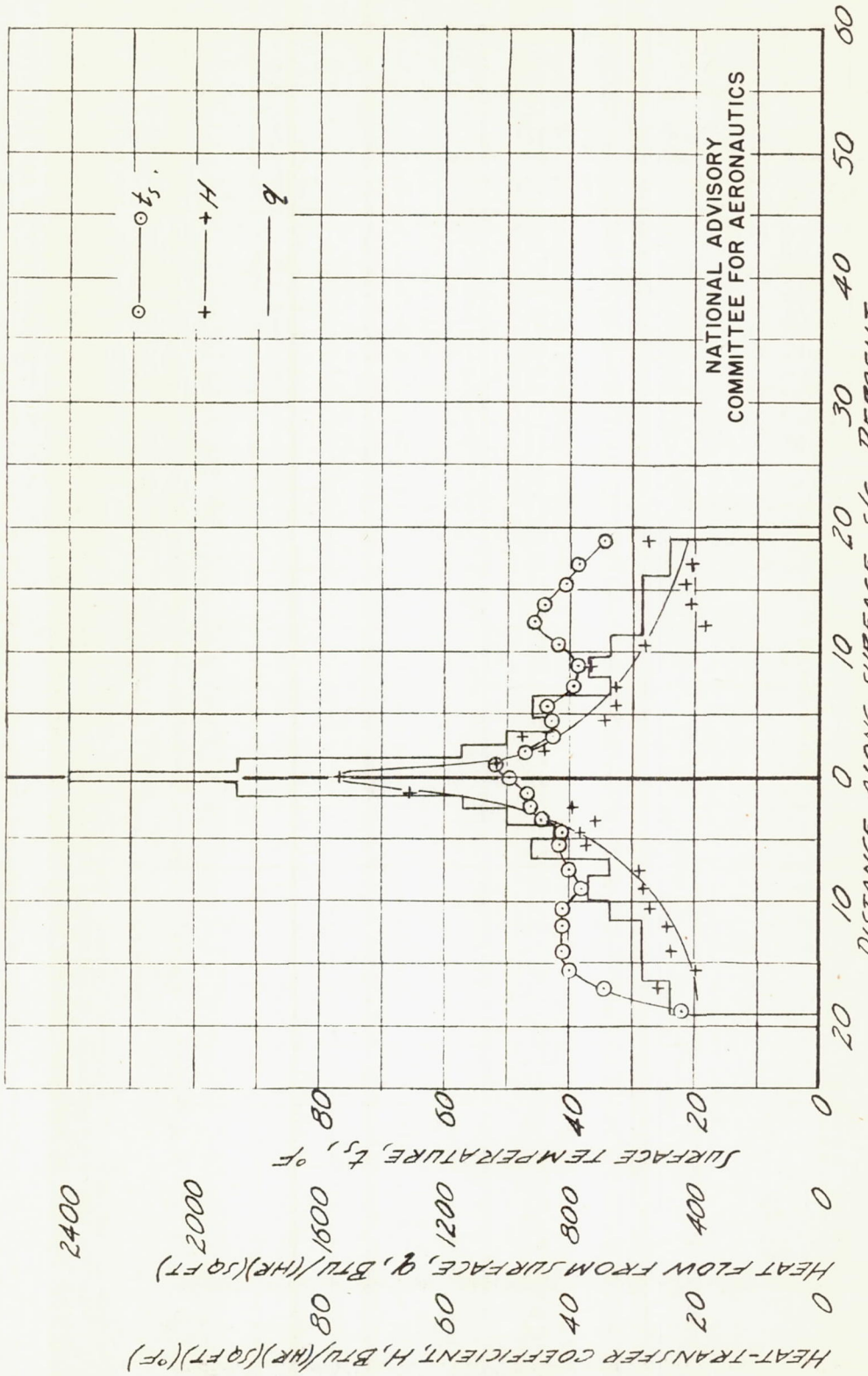

(j) Icing condition 10. Table II.

Figure 12.- Continued.

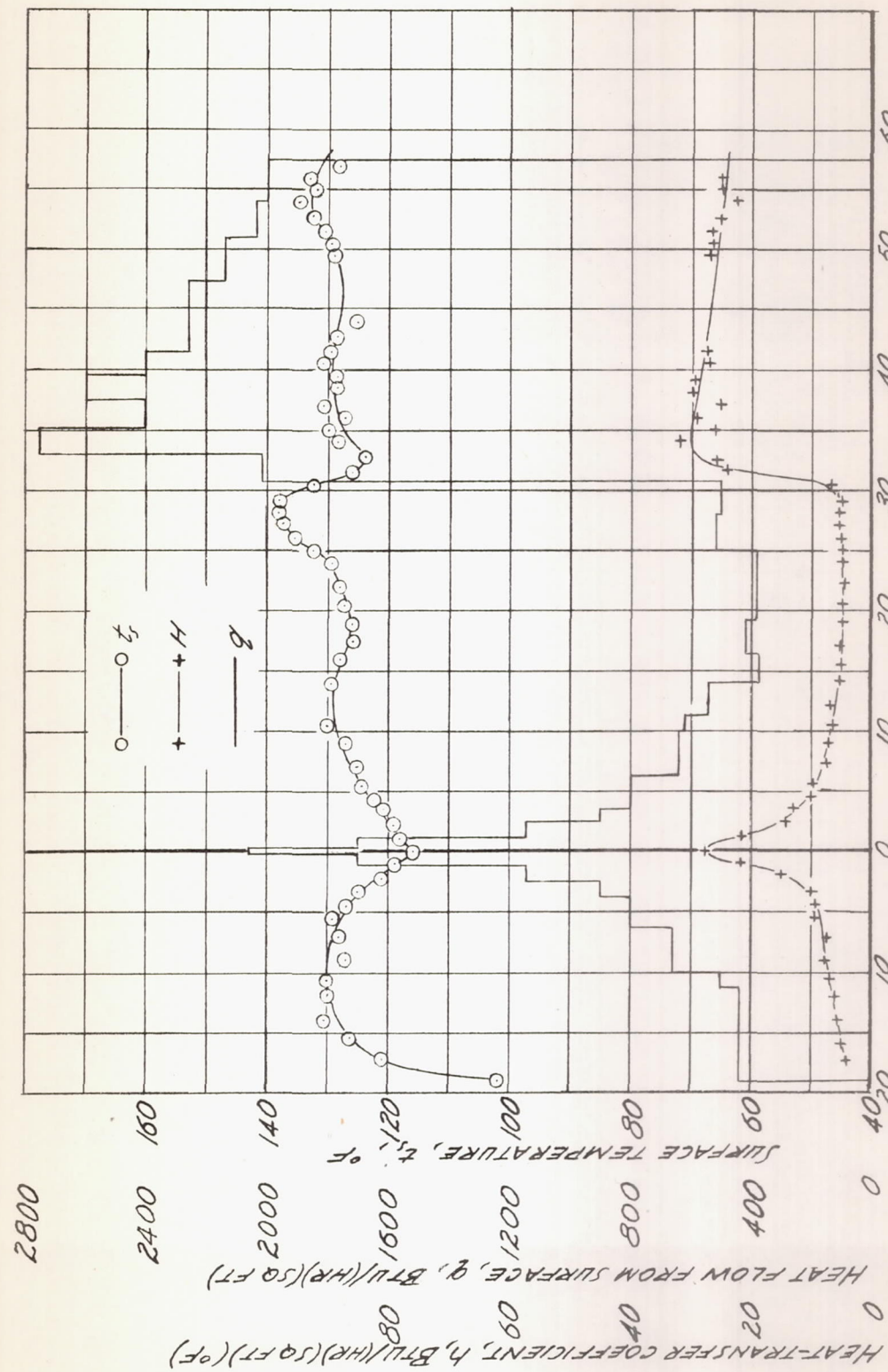

(k) CLEAR-AIR CONDITION. FREE-AIR TEMPERATURE, 38 °F; PRESSURE ALTITUDE, 5200 FT.; TRUE AIRSPEED, 145 MPH.

NATIONAL ADVISORY COMMITTEE FOR AERONAUTICS

FIGURE 12. - CONCLUDED.

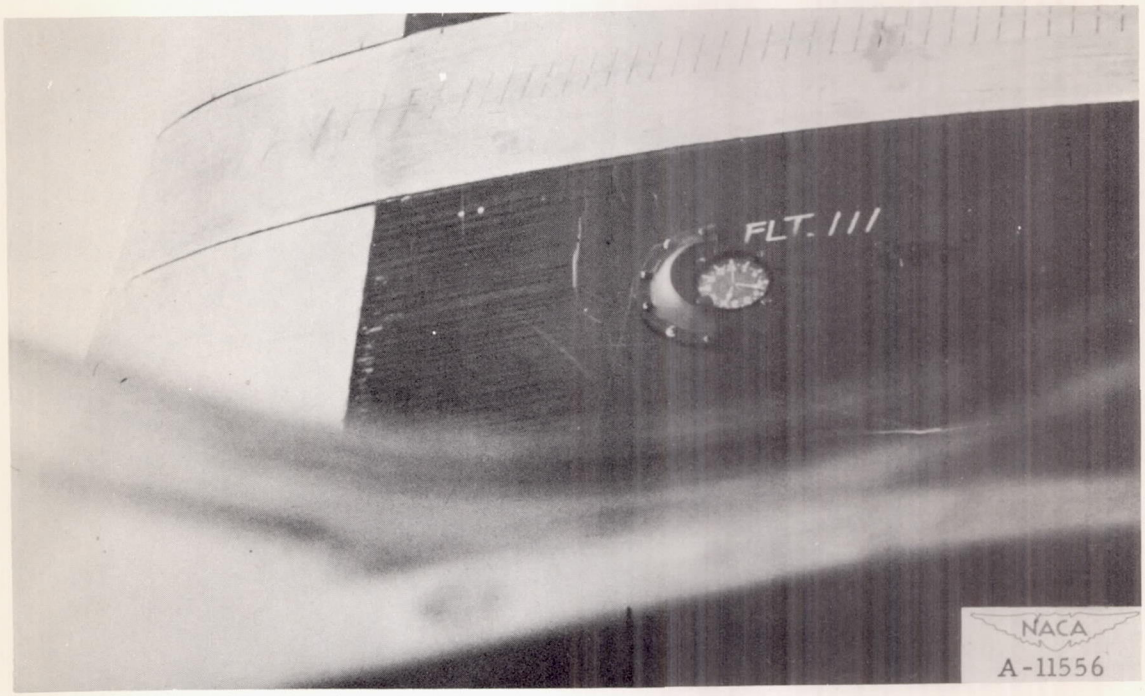

Figure 13.- Runback formation obtained on the electrically heated NACA 65,2-016 airfoil model during icing conditions 9 and 10, table II.

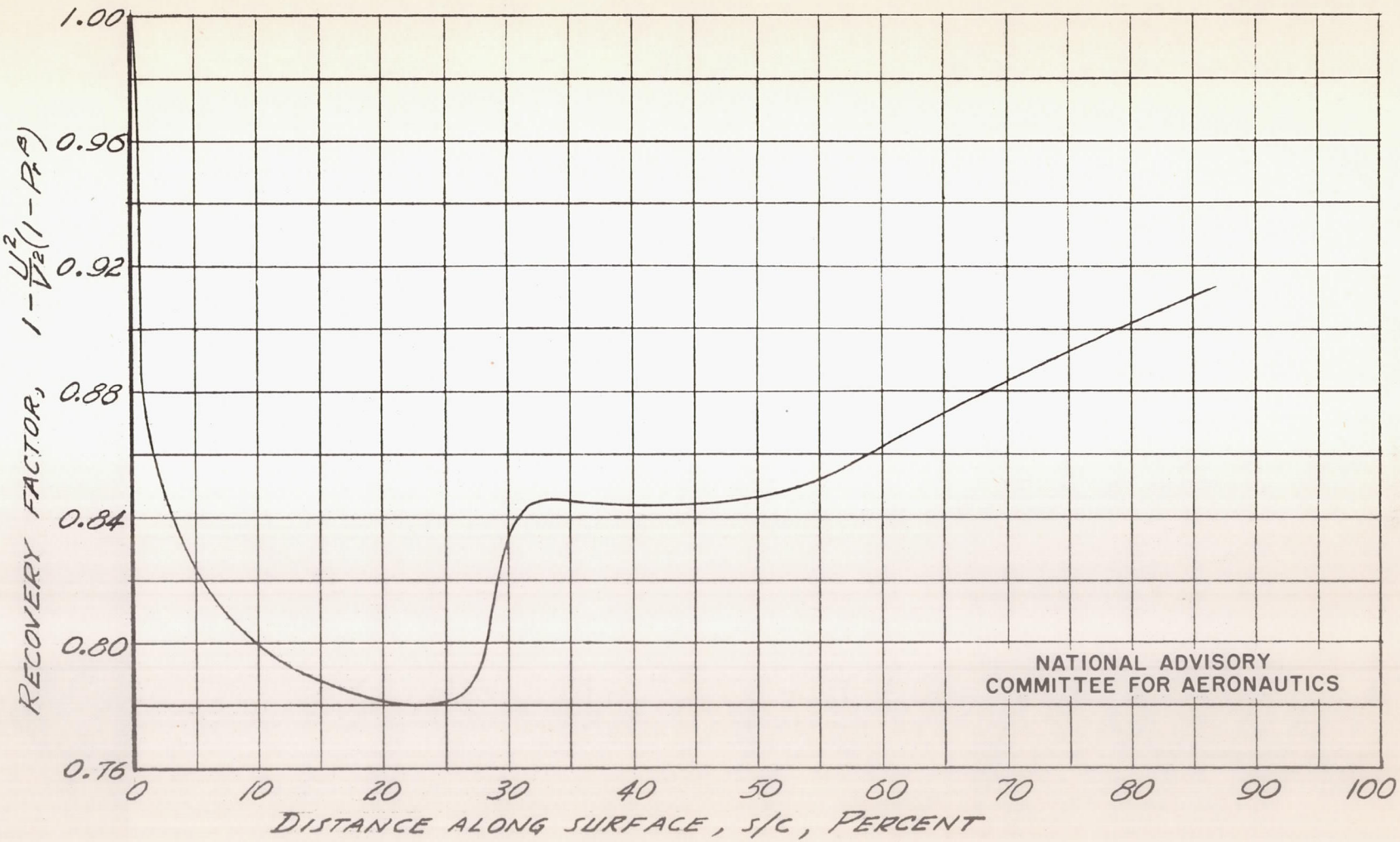

FIGURE 14.- CALCULATED CLEAR-AIR RECOVERY FACTOR OVER THE NACA 65,2-016 AIRFOIL SECTION.

(a) Icing condition 11, table II.

(b) Icing condition 13, table II.

(c) Icing condition 14, table II.

NACA
A-11533

Figure 15.- Typical data records showing area of drop impingement on the NACA 65,2-016 airfoil model, and traces of water flow aft of the region of impingement.

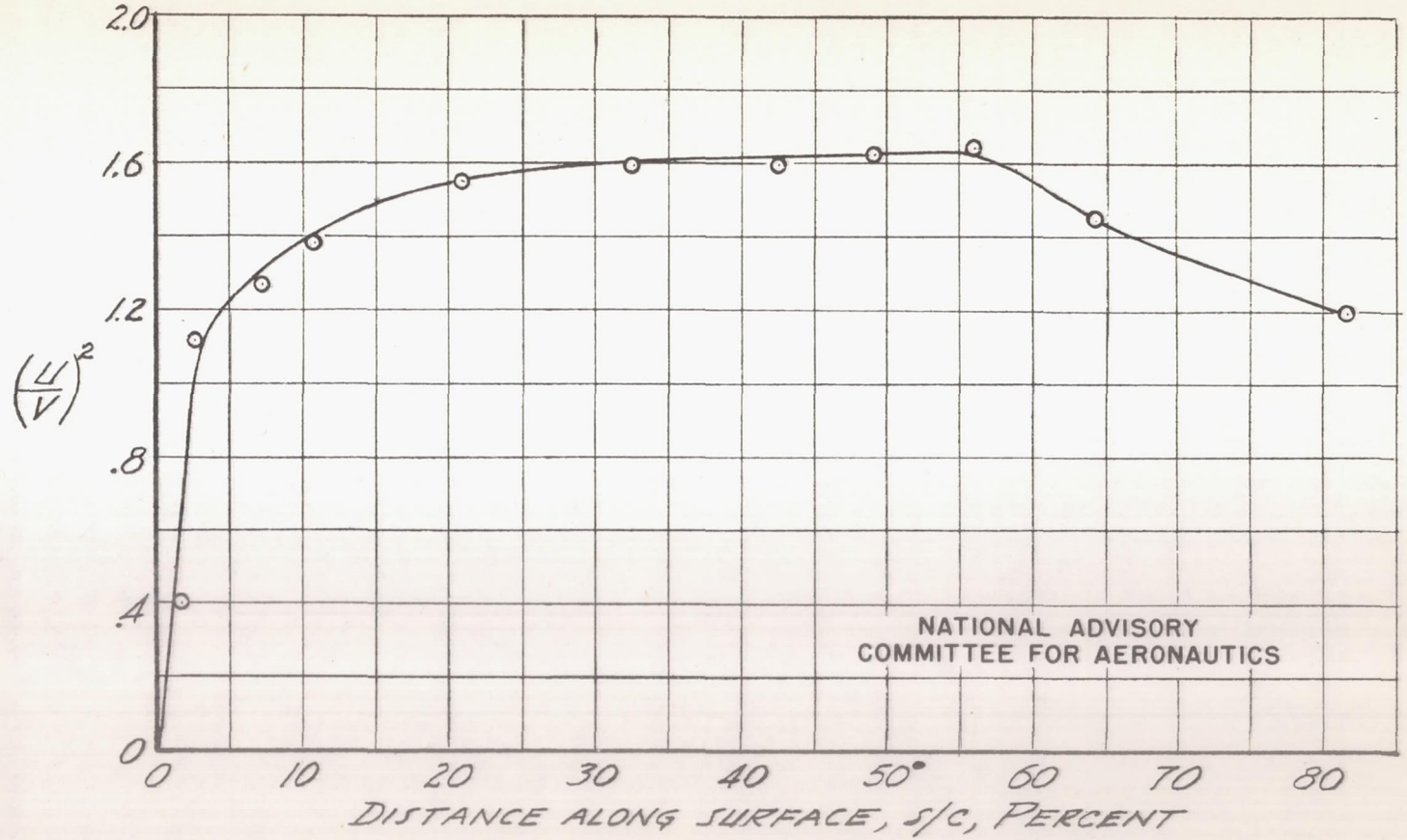

FIGURE 16.- PRESSURE DISTRIBUTION OVER THE NACA 65,2-016 ELECTRICALLY HEATED AIRFOIL SECTION IN CLEAR AIR. ANGLE OF ATTACK, 0°; R_c, 11×10^6.

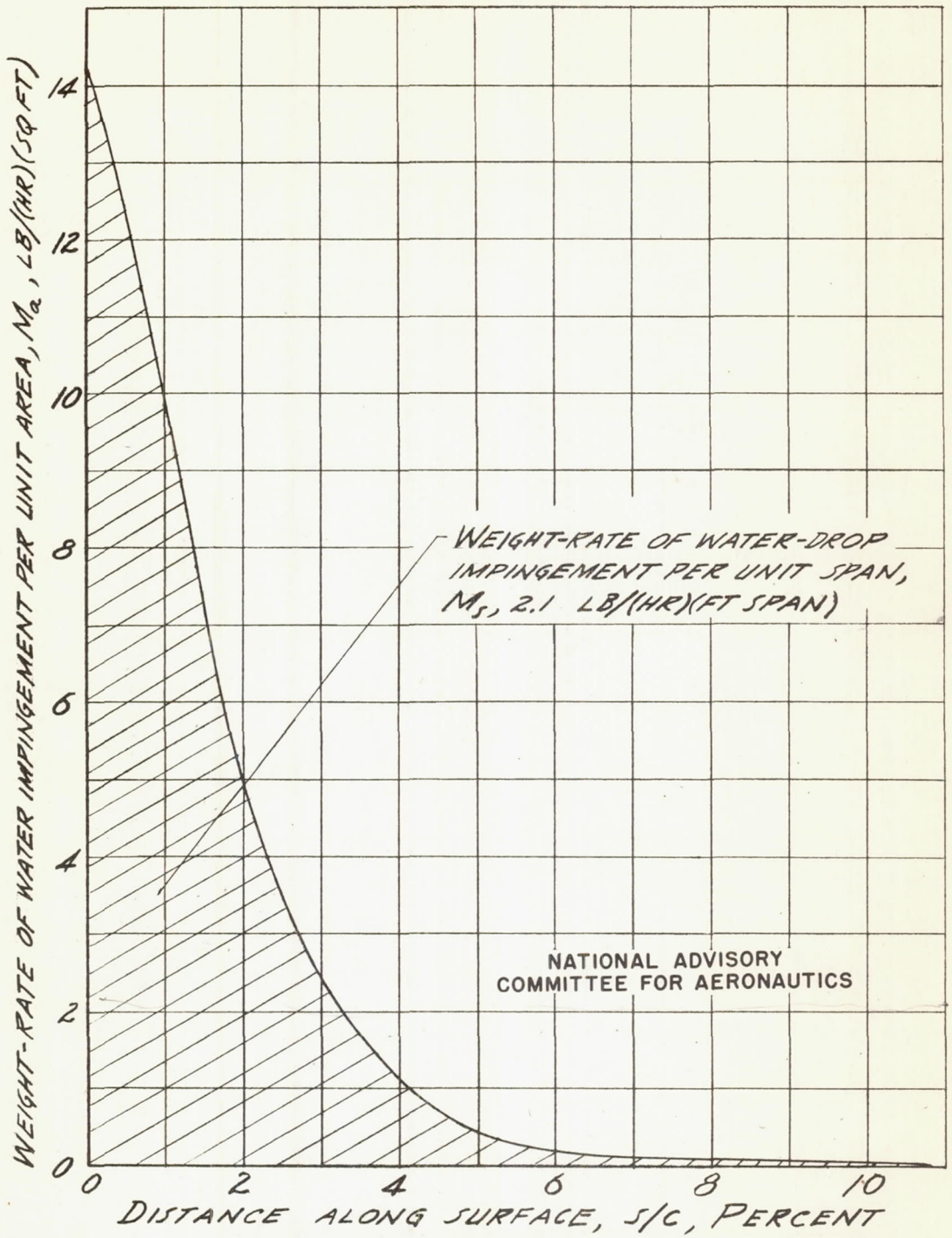

FIGURE 17.-DISTRIBUTION OF WATER-DROP IMPINGEMENT OVER THE SURFACE OF A 12 PERCENT-THICK SYMMETRICAL JOUKOWSKI AIRFOIL USED TO APPROXIMATE THE CONTOUR OF AN NACA 0012 SECTION AT 0° ANGLE OF ATTACK. PRESSURE ALTITUDE, 12,000 FT.; TRUE AIRSPEED, 170 MPH.; LIQUID-WATER CONTENT, 0.5 GRAM/CUBIC METER; MEAN-EFFECTIVE DROP SIZE, 25 MICRONS; DROP-SIZE DISTRIBUTION, E; AIRFOIL CHORD LENGTH, 8 FT.

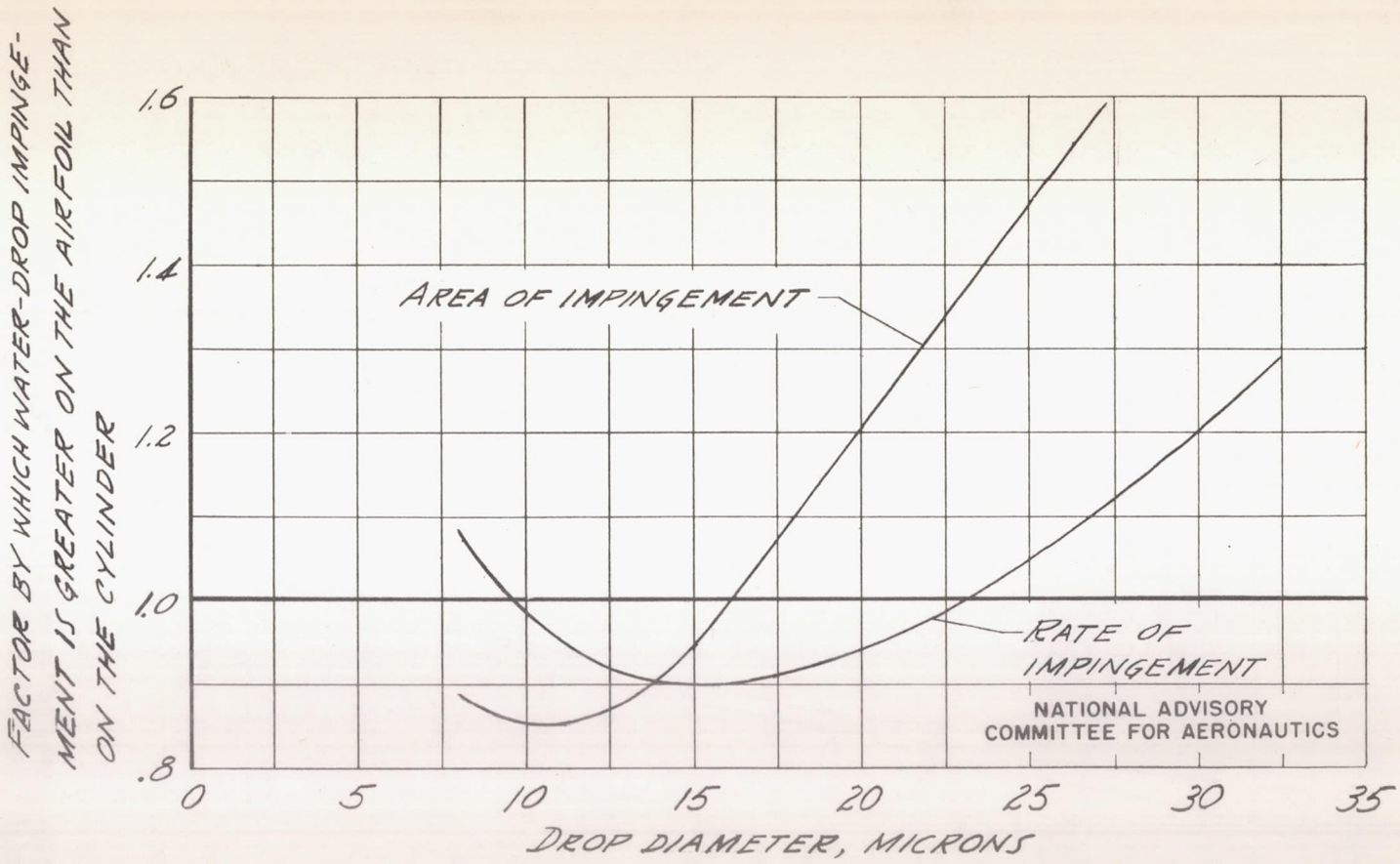

FIGURE 18.- COMPARISON OF RATE AND AREA OF WATER-DROP IMPINGEMENT ON A SYMMETRICAL JOUKOWSKI AIRFOIL 12 PERCENT THICK, 0° ANGLE OF ATTACK, AND A CYLINDER WITH RADIUS EQUAL TO THE AIRFOIL LEADING-EDGE RADIUS. AIRFOIL CHORD LENGTH, 8 FEET; PRESSURE ALTITUDE, 7000 FEET; TRUE AIRSPEED 170 MPH.

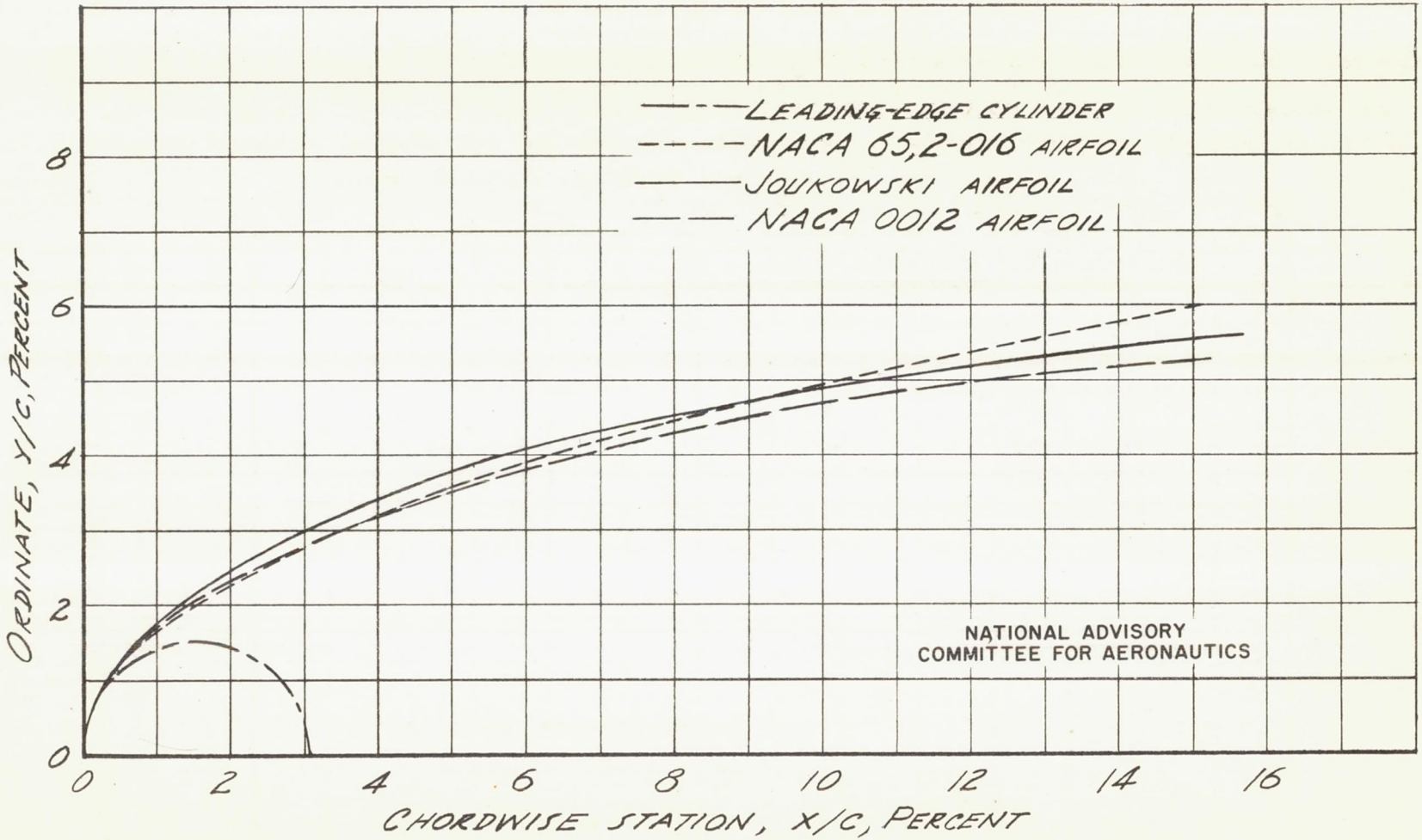

FIGURE 19.- COMPARISON OF CONTOURS OF THREE AIRFOIL SECTIONS AND A CYLINDER OF RADIUS EQUAL TO THE LEADING-EDGE RADIUS FOR ESTIMATING THE SIMILARITY OF WATER-DROP DEPOSITION ON EACH.

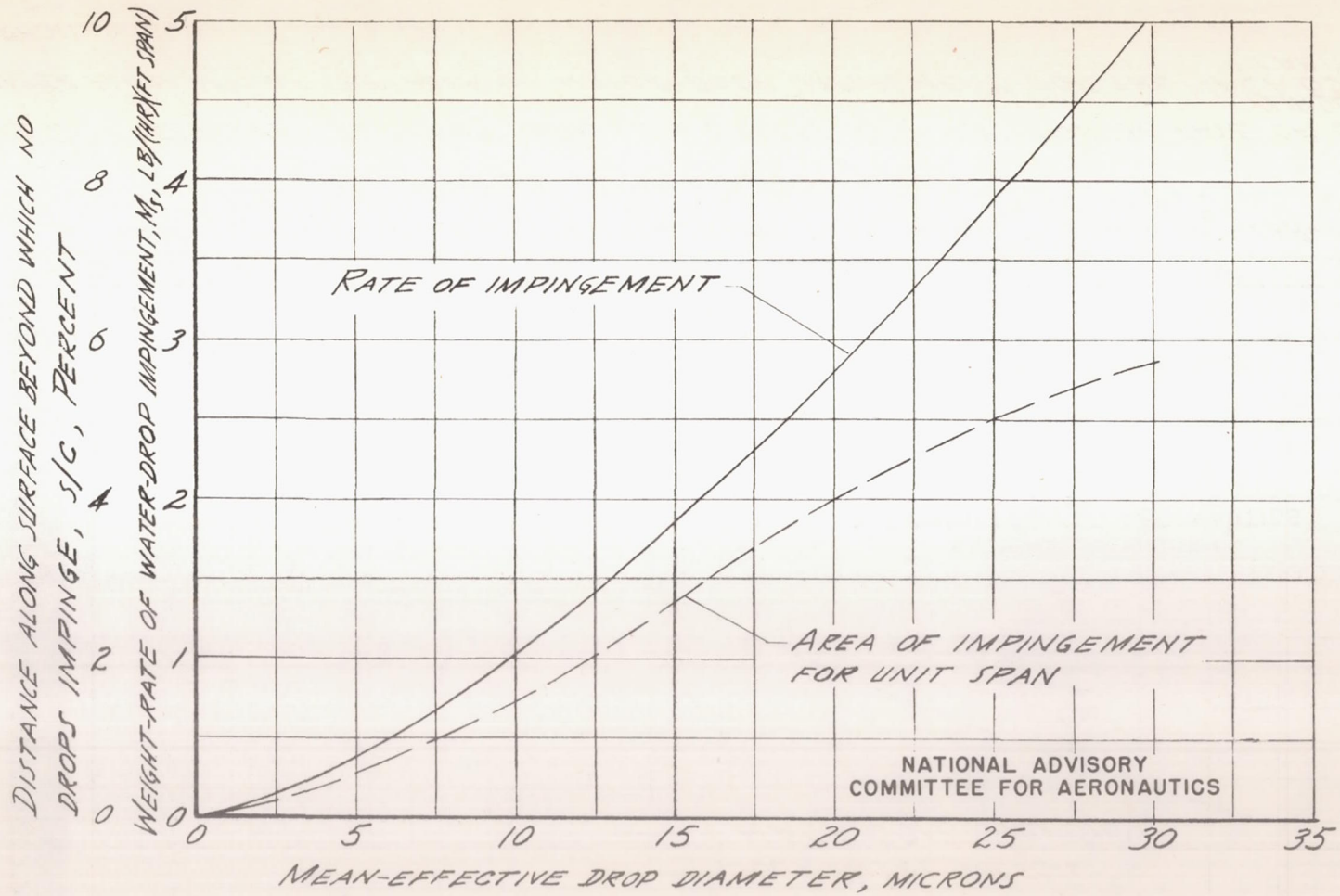

FIGURE 20.- EFFECT OF DROP SIZE ON AREA AND RATE OF WATER-DROP IMPINGEMENT ON THE LEADING EDGE OF A 12 PERCENT-THICK SYMMETRICAL JOUKOWSKI AIRFOIL USED TO APPROXIMATE THE CONTOUR OF AN NACA 0012 SECTION AT 0° ANGLE OF ATTACK. PRESSURE ALTITUDE, 7,000 FT.; TRUE AIRSPEED, 170 MPH.; LIQUID-WATER CONTENT, 1.0 GRAM PER CUBIC METER; DROP-SIZE DISTRIBUTION, C; AIRFOIL CHORD LENGTH, 8 FEET.

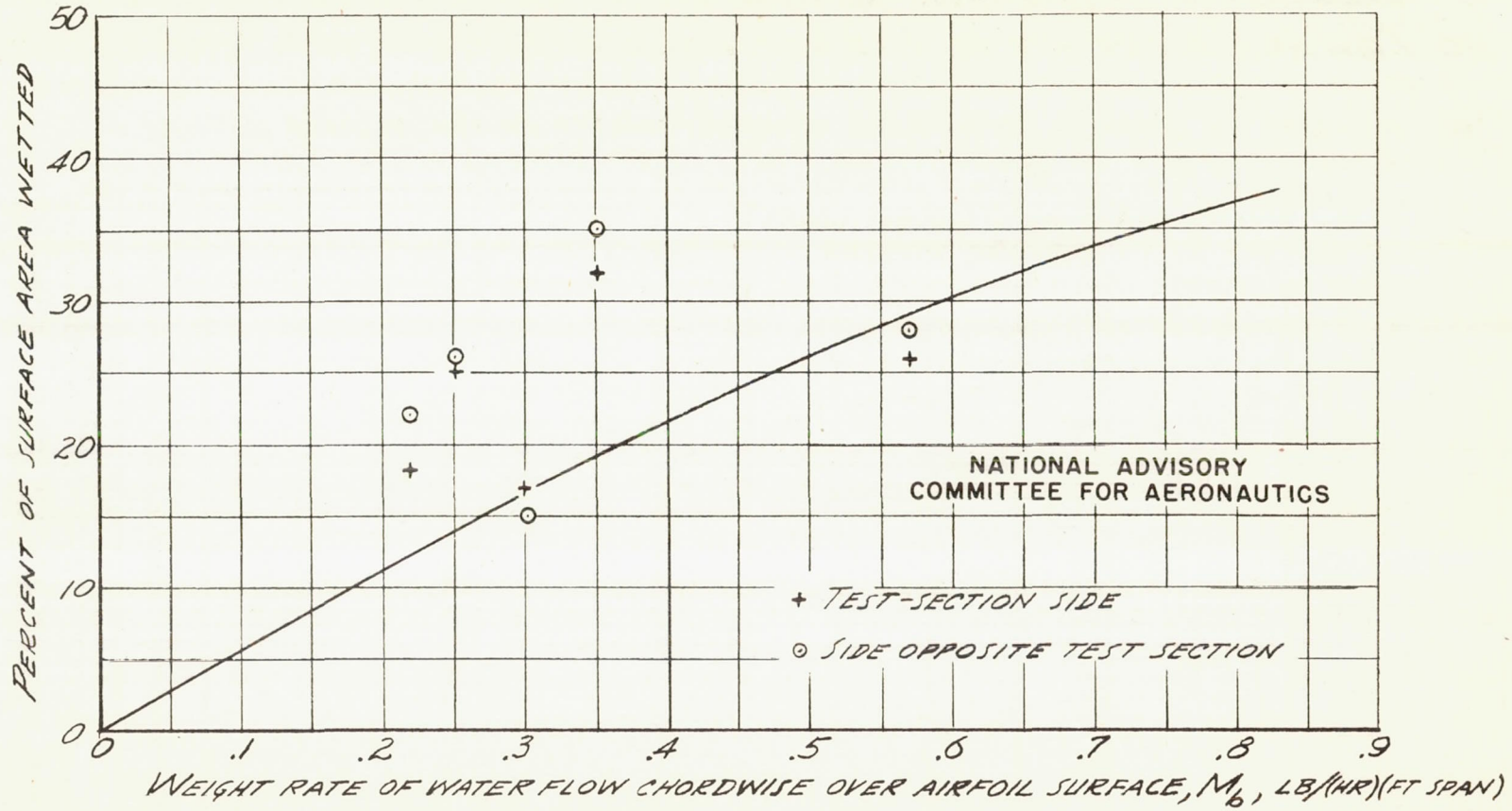

FIGURE 21.- MEASURED PERCENT SURFACE WETNESS AS A FUNCTION OF RATE OF CHORDWISE WATER FLOW AFT OF THE AREA OF WATER-DROP IMPINGMENT FOR THE NACA 65,2-016 AIRFOIL.

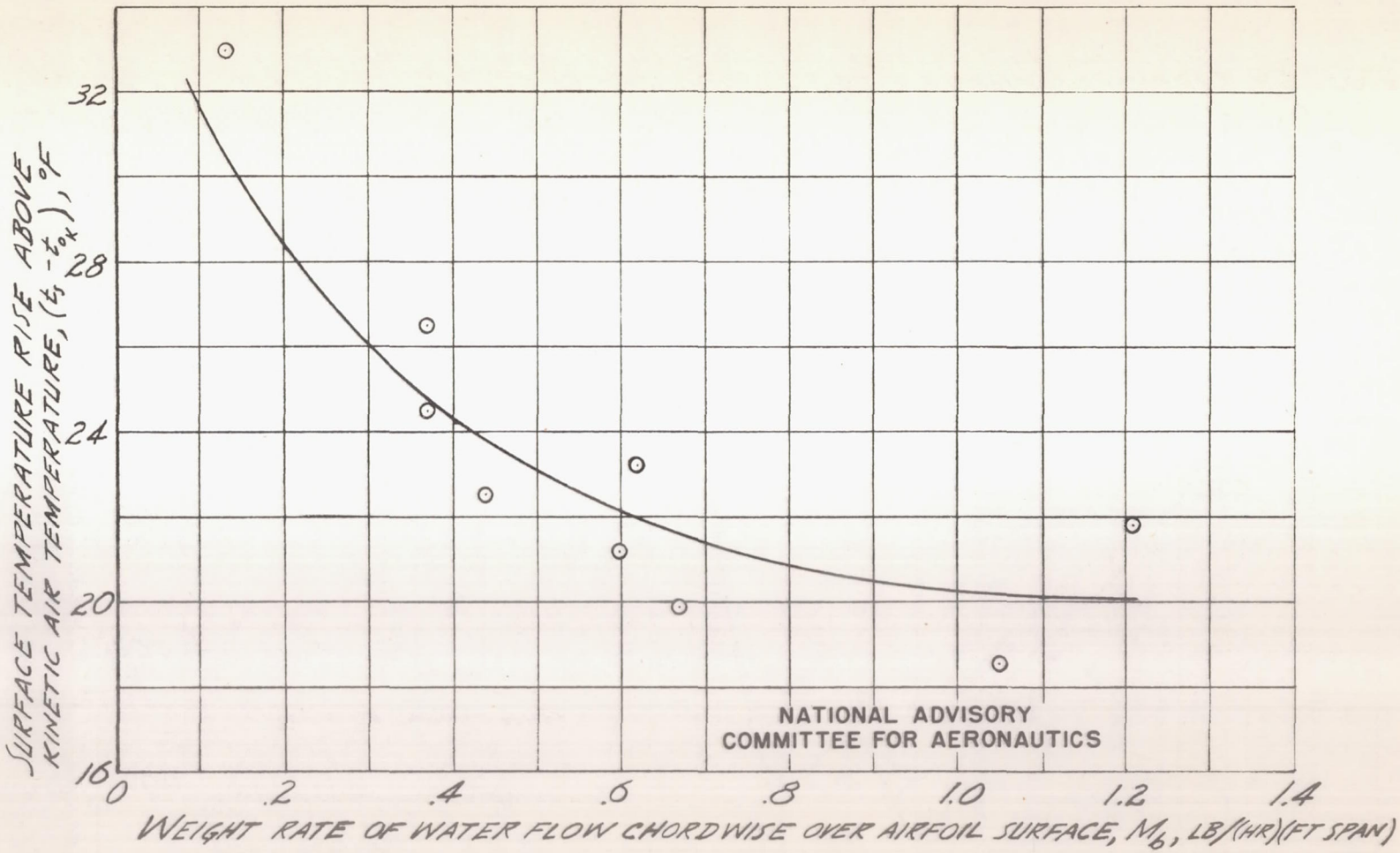

FIGURE 22.- MEASURED SURFACE TEMPERATURE RISE AS A FUNCTION OF RATE OF CHORDWISE WATER FLOW AFT OF THE AREA OF WATER-DROP IMPINGEMENT FOR THE NACA 65,2-016 AIRFOIL.

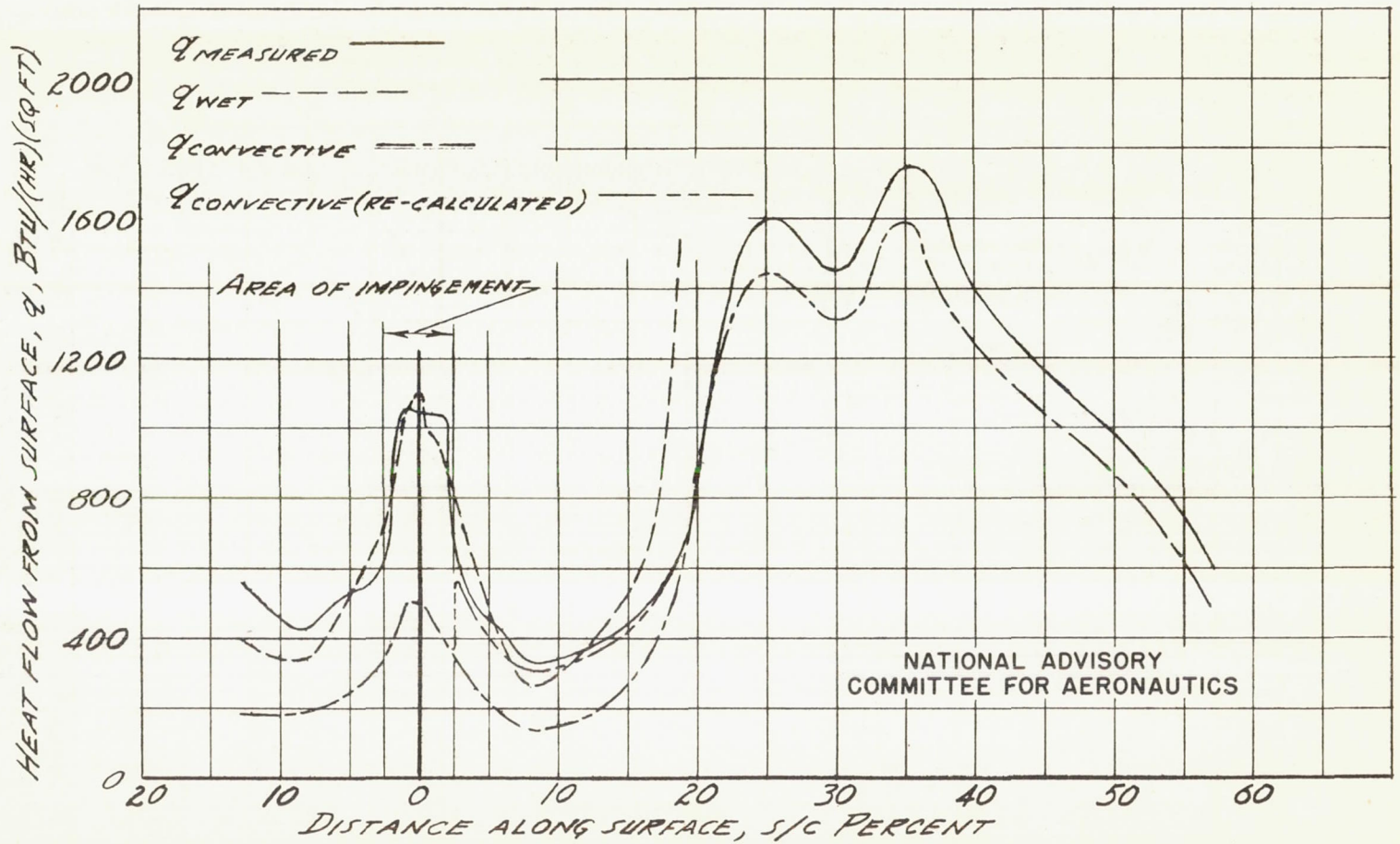

FIGURE 23.- COMPARISON OF MEASURED HEAT FLOW WITH HEAT FLOWS CALCULATED TO PRODUCE THE MEASURED SURFACE TEMPERATURES FOR A COMPLETELY WET AND COMPLETELY DRY SURFACE, FOR THE NACA 0012 AIRFOIL MODEL. ICING CONDITION 5, TABLE I.

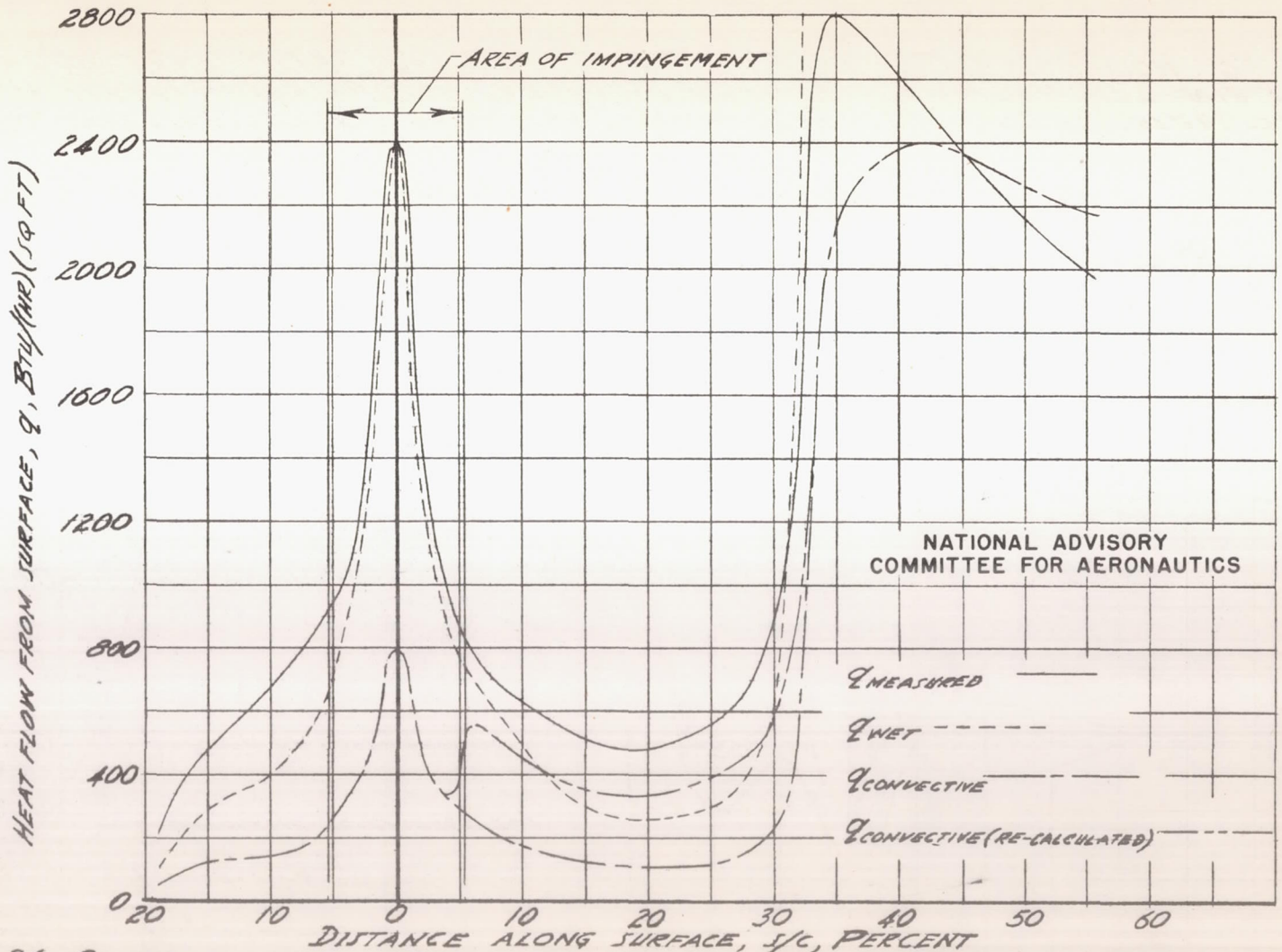

FIGURE 24.-COMPARISON OF MEASURED HEAT FLOW WITH HEAT FLOWS CALCULATED TO PRODUCE THE MEASURED SURFACE TEMPERATURE FOR A COMPLETELY WET AND COMPLETELY DRY SURFACE, FOR THE NACA 65,2-016 AIRFOIL MODEL. ICING CONDITION 2. TABLE II.

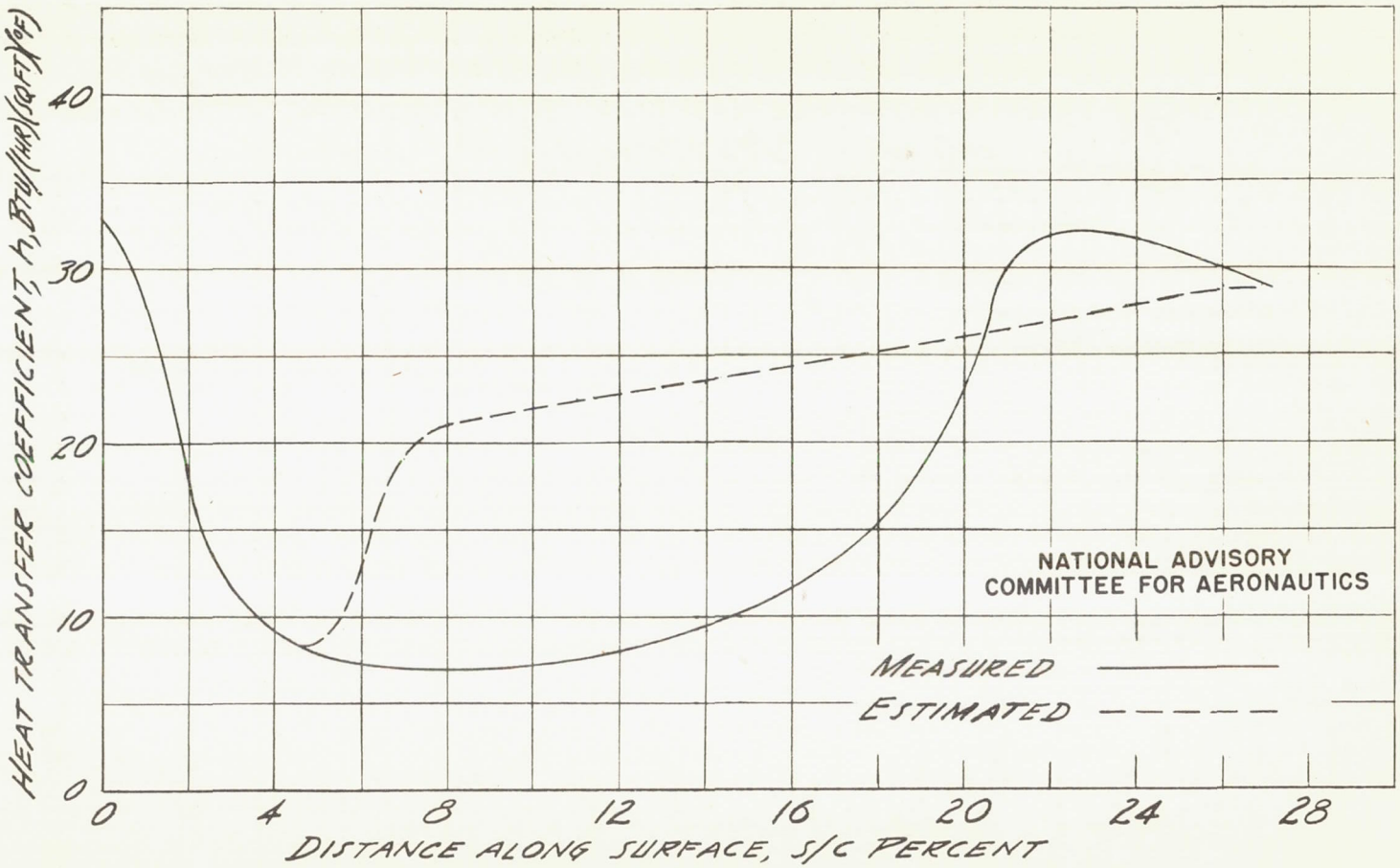

FIGURE 25.-MEASURED CONVECTIVE HEAT-TRANSFER COEFFICIENT AND ESTIMATED TURBULENT COEFFICIENT ASSUMING TRANSITION STARTING AT 5 PERCENT S/C FOR THE NACA 0012 AIRFOIL MODEL. PRESSURE ALTITUDE, 12,000 FT. TRUE AIRSPEED, 170 MPH.

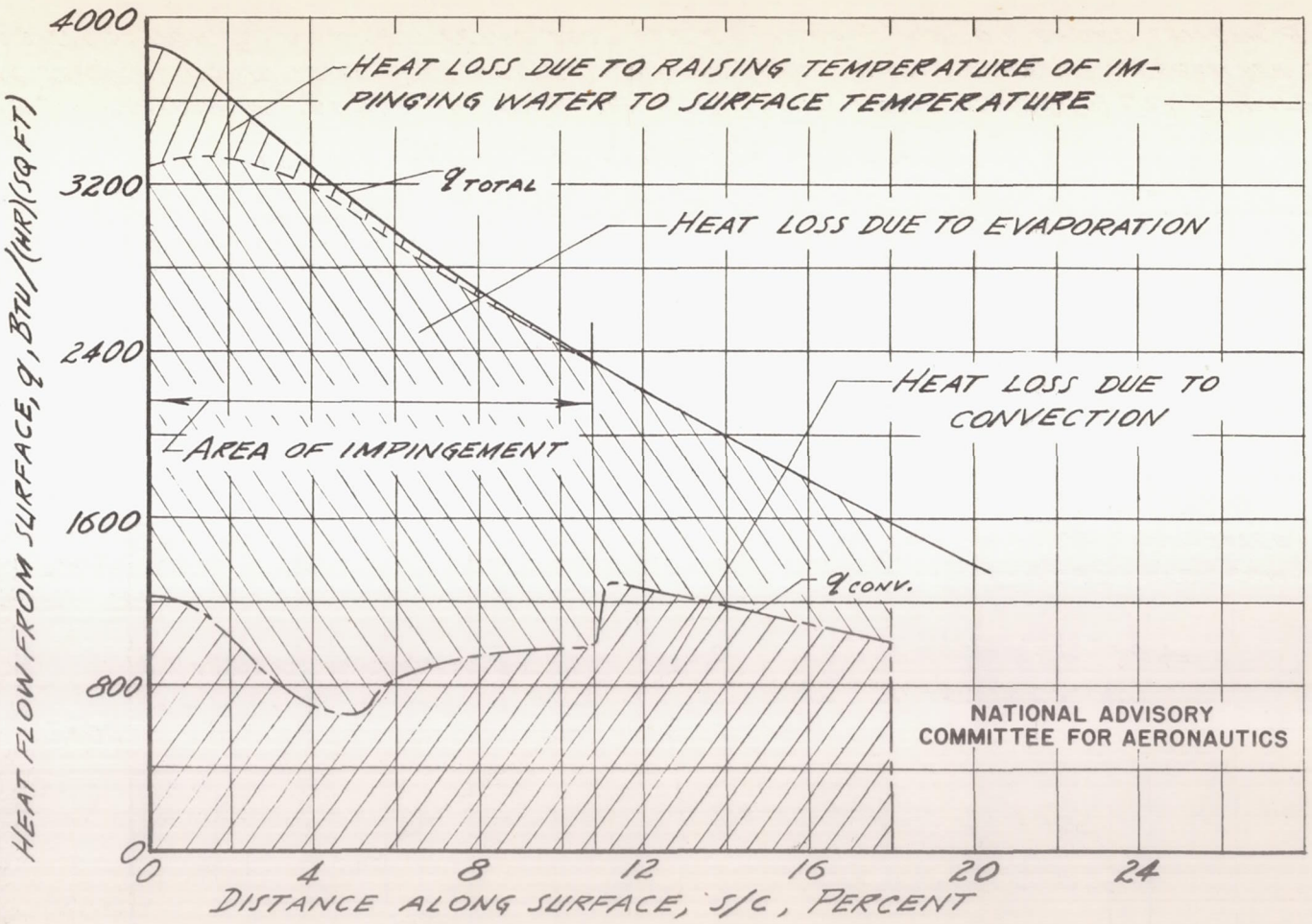

FIGURE 26.- ASSUMED TOTAL HEAT-FLOW DISTRIBUTION AND CALCULATED CONVECTIVE HEAT LOSS FROM AN NACA 0012 HEATED AIRFOIL FOR DETERMINING EXTENT OF HEATED AREA REQUIRED FOR EVAPORATION OF ALL IMPINGING WATER. PRESSURE ALTITUDE, 12,000 FT.; TRUE AIRSPEED, 170 MPH.; LIQUID-WATER CONTENT, 0.5 GRAM PER CUBIC METER; DROP-SIZE DISTRIBUTION, E; MEAN-EFFECTIVE DROP SIZE, 25 MICRONS; FREE-AIR TEMPERATURE, 20°F; AIRFOIL CHORD LENGTH, 8 FT.

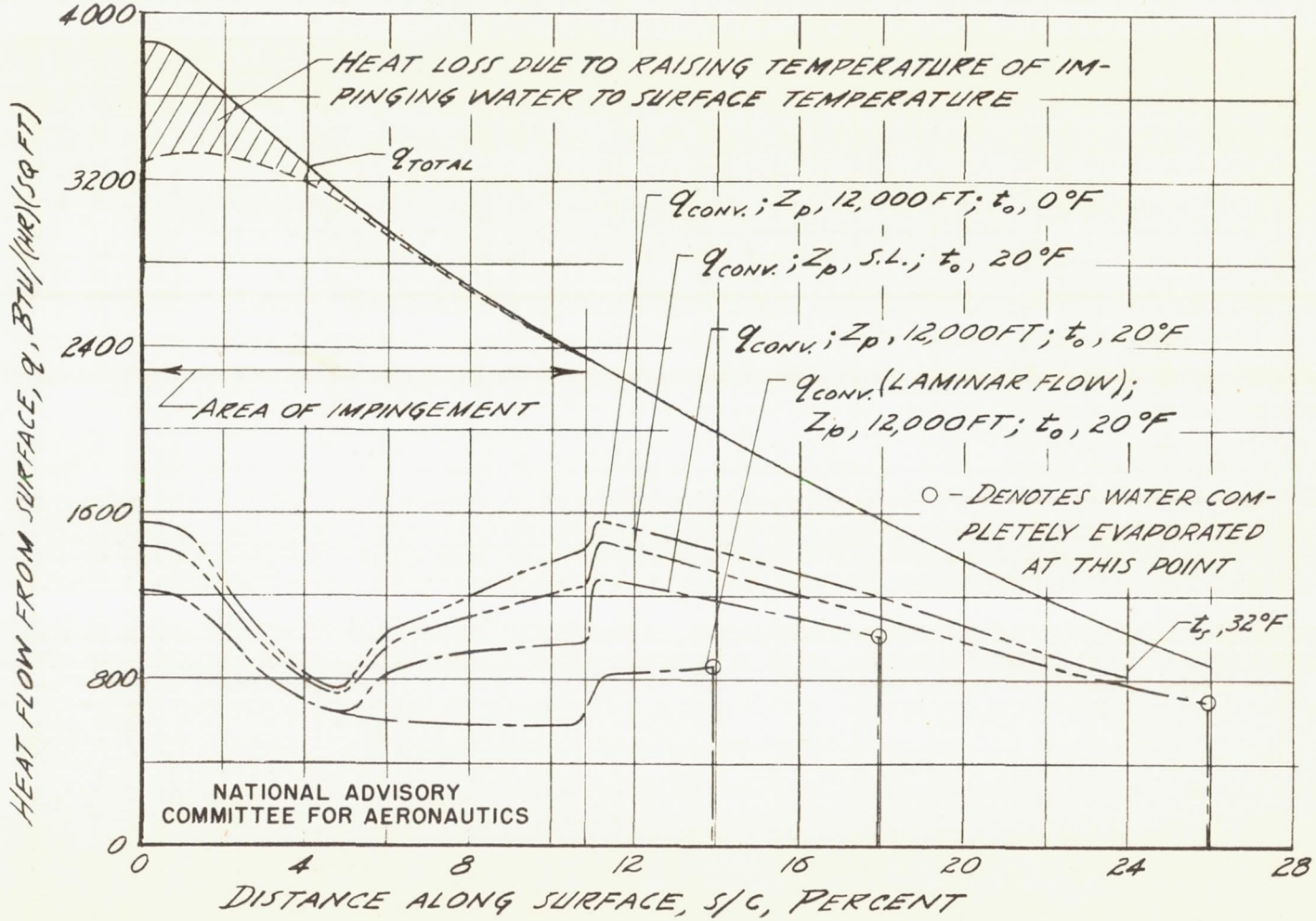

FIGURE 27.- COMPARISON OF CALCULATED CONVECTIVE HEAT LOSSES FROM AN NACA 0012 HEATED AIRFOIL FOR SEVERAL CONDITIONS. TRUE AIRSPEED, 170 MPH; LIQUID-WATER CONTENT, 0.5 GRAM PER CUBIC METER; DROP-SIZE DISTRIBUTION, E; MEAN-EFFECTIVE DROP SIZE, 25 MICRONS; AIRFOIL CHORD LENGTH, 8 FT.

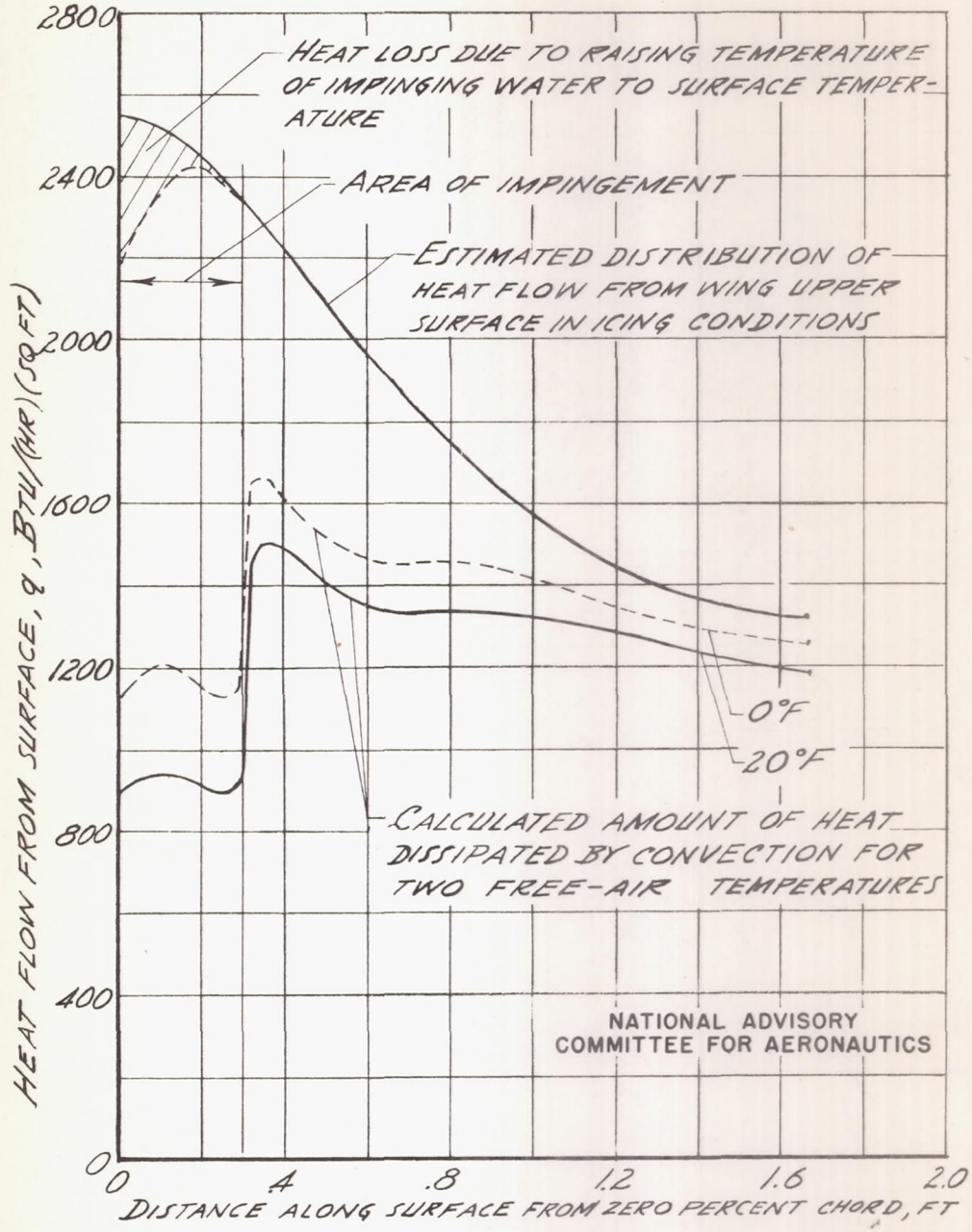

FIGURE 28.- ESTIMATED HEAT FLOW FROM UPPER SURFACE OF C-46 HEATED WING LEADING EDGE AT STATION 157 IN ICING CONDITIONS, AND CALCULATED CONVECTIVE HEAT LOSS, USED IN DETERMINATION OF RATE OF EVAPORATION OF WATER. PRESSURE ALTITUDE, 6,000 FT.; TRUE AIRSPEED, 180 MPH.

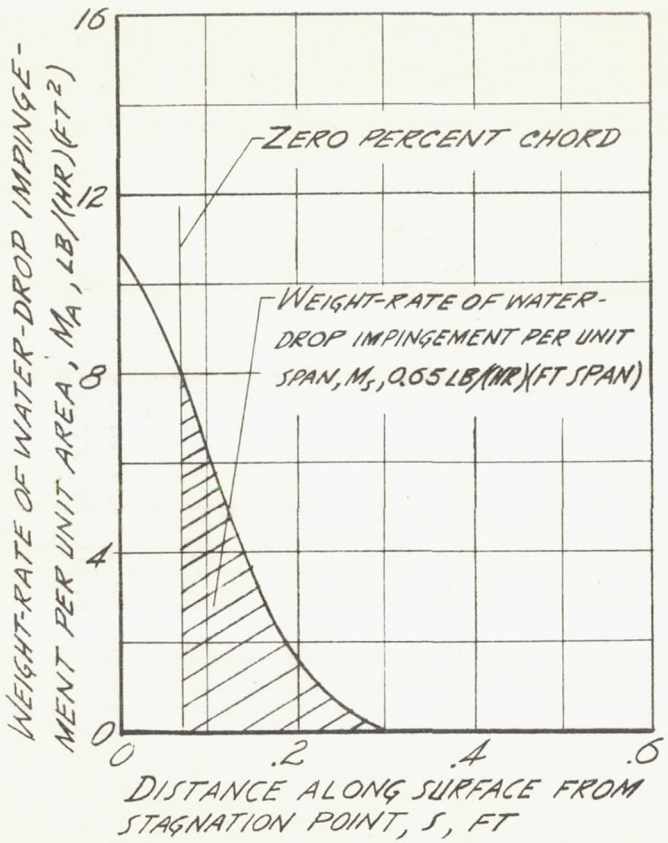

(a) Icing condition A. Liquid-water content, 0.8 gram/cubic meter; mean-effective drop diameter, 15 microns; drop-size distribution, C; free-air temperature, 20°F.

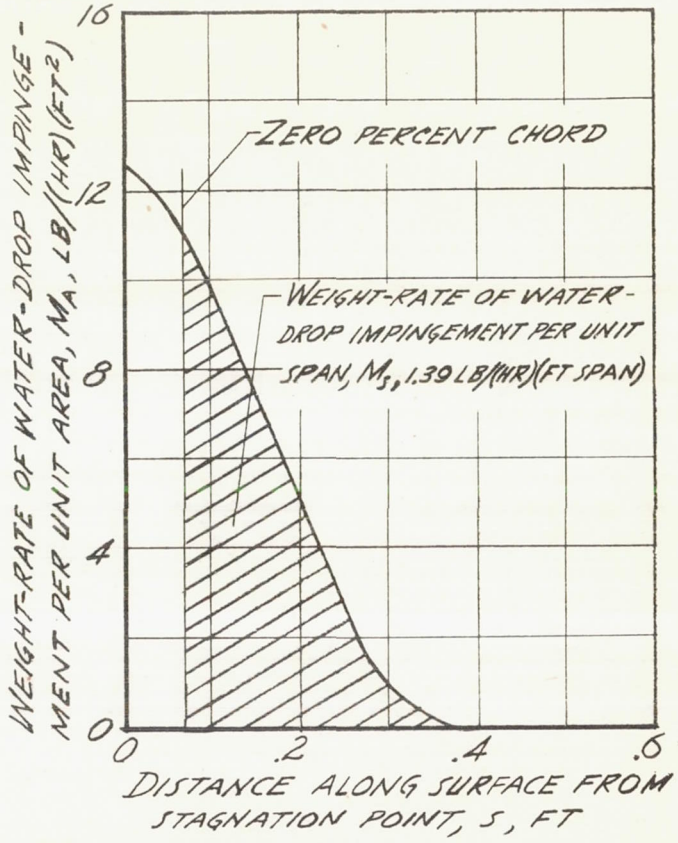

(b) Icing condition B. Liquid-water content, 0.5 gram/cubic meter; mean-effective drop diameter, 25 microns; drop-size distribution, C; free-air temperature, 20°F.

FIGURE 29.- Calculated weight-rate of water-drop impingement on the C-46 airplane left wing upper surface at wing station 157. Pressure altitude, 6,000 ft; true airspeed, 180 mph.

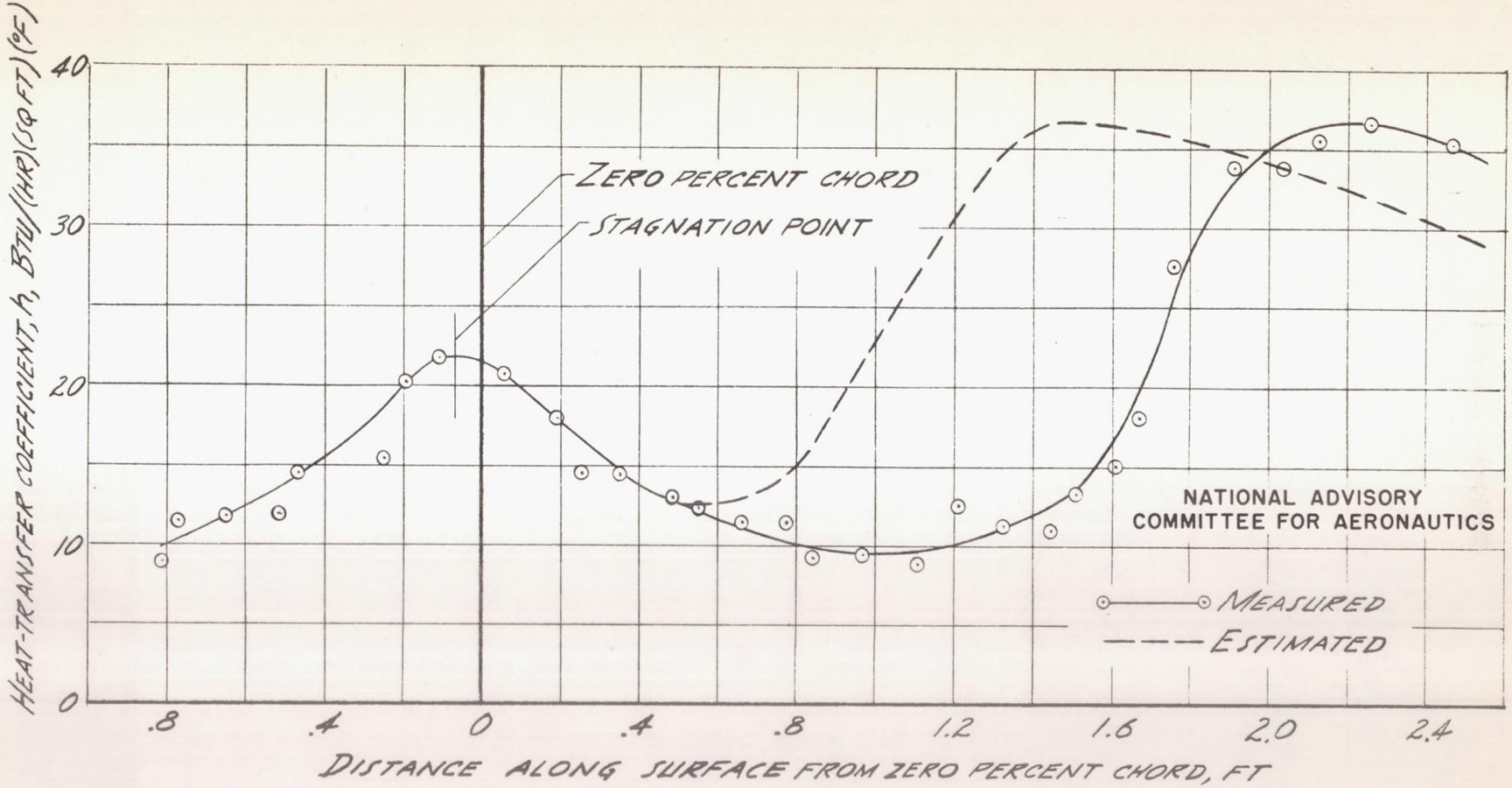

FIGURE 30.- MEASURED AND ESTIMATED CONVECTIVE HEAT-TRANSFER COEFFICIENT ON THE LEFT WING OF THE C-46 AIRPLANE AT STATION 157 FOR TWO POSITIONS OF TRANSITION ON THE WING UPPER SURFACE.